

## **UC Merced**

### **UC Merced Electronic Theses and Dissertations**

#### **Title**

Genetic regulation of sexual biofilm formation in *Candida albicans*

#### **Permalink**

<https://escholarship.org/uc/item/1rg823zw>

#### **Author**

Perry, Austin Michael

#### **Publication Date**

2024

Peer reviewed|Thesis/dissertation

UNIVERSITY OF CALIFORNIA, MERCED

Genetic regulation of sexual biofilm formation in *Candida albicans*

A dissertation submitted in partial satisfaction of the

requirements for the degree of

Doctor of Philosophy

in

Quantitative and Systems Biology

by

Austin Michael Perry

Committee in charge:

Professor Aaron Hernday, Chair of Advisory Committee

Professor Michael Cleary

Professor Chris Amemiya

Professor Clarissa Nobile, Supervisor

2024

Copyright  
Austin Michael Perry, 2024  
All Rights Reserved

The dissertation of Austin Perry, titled, "Genetic regulation of sexual biofilm formation in *Candida albicans*", is approved, and is acceptable in quality and form for publication on microfilm and electronically:

\_\_\_\_\_ Date \_\_\_\_\_

Professor Michael Cleary

\_\_\_\_\_ Date \_\_\_\_\_

Professor Chris Amemiya

Supervisor \_\_\_\_\_ Date \_\_\_\_\_

Professor Clarissa J. Nobile

Chair \_\_\_\_\_ Date \_\_\_\_\_

Professor Aaron Hernday

University of California, Merced

2024

*Dedications*

*This dissertation is dedicated to my family, particularly my loving mother.*

*“All we have to decide is what to do with the time that is given us.”*

*- J. R. R. Tolkien, *The Fellowship of Ring**

## Table of Contents

I. List of Abbreviations.....	vii
II. List of Figures .....	viii
III. List of Tables .....	ix
IV. Acknowledgments .....	x
V. Vita for Austin M. Perry.....	xi
VI. Abstract .....	xiii
Chapter 1 Introduction .....	1
1.1 Abstract.....	1
1.2 Introduction .....	1
1.3 The <i>C. albicans</i> white – opaque switch .....	2
1.4 Pheromone signaling and response in <i>C. albicans</i> .....	5
1.4.1 Mating pheromones.....	5
1.4.2 Pheromones-signaling pathway control .....	6
1.4.3 Differences between the white and opaque cells pheromone response .....	7
1.5 Conventional and sexual <i>C. albicans</i> biofilms.....	8
1.6 Conclusion .....	14
1.7 References .....	14
1.8 Figures.....	22
Chapter 2 Transcriptional analysis of <i>Candida albicans</i> sexual biofilms reveals novel target genes involved in sexual biofilm formation.....	23
2.1 Abstract.....	23
2.2 Introduction .....	23
2.3 Results.....	25
2.3.1 Clinical isolate screen.....	25
2.3.2 Transcriptional profiling of sexual biofilms.....	25
2.3.3 Mixed population sexual biofilms .....	26
2.3.4 Transcriptional profiling of mixed population sexual biofilms.....	27
2.3.5 Identification of functionally relevant genes involved in sexual biofilm formation .....	28
2.4 Discussion and conclusion .....	28
2.5 Materials and methods .....	30
2.5.1 Media .....	30
2.5.2 Pheromone-stimulated biofilm assay and co-culture assays.....	30

2.5.3	<i>Strains and mutant construction</i>	30
2.5.4	<i>RNA-seq cell harvesting and library preparation</i>	31
2.5.5	<i>Differential expression and enrichment analysis</i>	31
2.6	References	32
2.7	Figures	36
Chapter 3	A systematic genetic screen for transcriptional regulators of <i>Candida albicans</i> sexual biofilms	71
3.1	Abstract	71
3.2	Introduction	71
3.3	Results	72
3.3.1	<i>Identification of sexual biofilm regulators in vitro</i>	72
3.3.2	<i>Genome wide differential gene expression patterns of sexual biofilm regulators</i>	73
3.3.3	<i>Gene ontology analyses of transcription factor deletion mutant strains</i>	74
3.4	Discussion	75
3.5	Methods and Materials	76
3.5.1	<i>Strains and media</i>	76
3.5.2	<i>Pheromone-stimulated biofilm assay</i>	76
3.5.3	<i>RNA-seq cell harvesting and library preparation</i>	76
3.5.4	<i>Differential expression and gene enrichment analysis</i>	76
3.6	References	77
3.7	Figures	79
Chapter 4	Conclusion and Future Directions	89
4.1	Conclusions	89
4.2	Future directions	90
4.3	References	92

## I. List of Abbreviations

Abb.	Description
YPD	Yeast Peptone Dextrose Media
dDNA	Donor DNA
gRNA	Guide RNA
NAT	Nourseothricin
TF	Transcription Factor
MTL	Mating type-like [locus]
MAPK	Mitogen-activated protein kinase [pathway]
cAMP	Cyclic Adenosine monophosphate
PKA	Protein kinase A
MF	Mating factor
TFKO	Transcription factor knock out [mutant]
Leu	Leucine
Wh	White [cell type]
GPCR	G-protein coupled receptor
PAMP	Pathogen associated molecular pattern
GSEA	Gene set enrichment analysis
PRY	Pathogen-related yeast [proteins]
NES	Normalized enrichment score
Op	Opaque [cell type]
RNA	Ribonucleic acid
DNA	Deoxyribonucleic acid
ROS	Reactive oxygen species
NETs	Neutrophil extracellular trap



## II. List of Figures

<i>Figure 1.1 Summary of the regulation of conventional (MTL-heterozygous) and sexual (MTL-homozygous) biofilms and their phenotypic characteristics.</i>	22
<i>Figure 2.1 Sexual biofilm formation by clinically isolated strains.</i>	36
<i>Figure 2.2 Transcriptional analysis of clinical isolates responding to synthetic mating pheromone.</i>	37 - 40
<i>Figure 2.3 Sexual biofilms formed by co-cultures of white and opaque cells.</i>	41
<i>Figure 2.4 Transcriptional analysis of sexual biofilms formed by co-cultures of white and opaque cells.</i>	42 - 44
<i>Figure 2.5 Sexual biofilm formation by gene deletion mutant strains.</i>	45
<i>Figure 3.1 Screening and characterization of transcription factors involved in sexual biofilm formation.</i>	79
<i>Figure 3.2 Gene ontology analyses of transcription factor deletion mutant strains forming sexual biofilms.</i>	80 - 83

### III. List of Tables

<i>Supplemental Table 2.1: List of strains.</i>	46
<i>Supplemental Table 2.2: List of significantly upregulated genes in moderate and strong responders.</i>	48 - 55
<i>Supplemental Table 2.3: List of significantly downregulated genes in moderate and strong responders.</i>	56 - 65
<i>Supplemental Table 2.4 List of primers.</i>	66 - 70
<i>Supplemental Table 3.1: List of strains.</i>	84 - 88

#### IV. Acknowledgments

The work presented in this dissertation was made possible through the help and support of many people. I would like to express my eternal gratitude to my advisor and mentor Dr. Clarissa Nobile. I have grown tremendously as a scientist and professional through her guidance and experience. Clarissa first inspired me and interested me in *Candida albicans* as professor of my microbiology and microbial pathogenesis courses during my undergraduate years at UC Merced. Thank you for supporting me, pushing me and educating me all these years.

Next, I would like to thank my thesis committee members: Drs. Aaron Hernday, Mike Cleary, and Chris Amemiya. Your assistance and expertise in each of your specialties provided valuable knowledge and direction to me throughout my graduate career.

I would like to thank my colleagues past and present for their support and feedback throughout my journey at UC Merced. In particular Drs. Megha Gulati, Melanie Ikeh, James Goodwine, Priyanka Bapat, Ashley Valle Arevalo, Craig Ennis, Diana Rodriguez, Akshay Paropkari, Thaddeus Seher, Deepika Gunasekaran, Mohammad Qasim, Morgan Quail; as well as Pegah Mosharaf, Namkha Nguyen, Arefeh Ebadati, Nora Shamoan, Priosmita Biswas, Chantz Williams, and Tahirah Williams. Akshay Paropkari and Deepika Gunasekaran deserve special thanks for their invaluable help as bioinformaticians. I have learned a great deal from each of you and I have enjoyed our fun talks in the lab over the years.

I would like to thank the wonderful friends I made at UC Merced during my stay here. Especially the UCM Grad Bitches, with whom I have spent many nights playing board games and Left 4 Dead. These will be memories I shall cherish for the rest of my life. In addition, I would like to thank the UC Merced softball team, Bad News Bobcats, for being a wonderful source of joy and mirth and an escape from the rigors of academia for many years.

Finally, I'd like to acknowledge the many students whom I mentored during my graduate work. Thank you to Jennifer Otto, Dorian Padillas, Evelyn Kwong, Julieta Muñoz and David Carrasco Reyes, for your many contributions to this and other works. I hope you learned as much from me as I did from all of you.

## V. Vita for Austin M. Perry

### Education:

**Ph.D** University of California, Merced, Quantitative and Systems Biology 2024

**M.S.** University of California, Merced, Quantitative and Systems Biology 2019

**B.S.** University of California, Merced, Microbiology and Immunology 2017

### List of Publications:

1. Gulati, M., Lohse, M.B., Ennis, C.L., Gonzalez, R.E., **Perry, A. M.**, Bapat, P., Valle Arevalo, A., Rodriguez, D.L., Nobile, C.J. *In vitro* culturing and screening of *Candida albicans* biofilms. *Current Protocols in Microbiology*. 2018
2. **Perry, A. M.**; Hernday, A. D.; Nobile, C. J. Unraveling How *Candida albicans* Forms Sexual Biofilms. *Journal of Fungi*. 2020
3. Wooten, D. J.; Zañudo J. G. T.; Murrugarra, D.; **Perry A. M.**; Dongari-Bagtzoglou, A.; Laubenbacher, R.; Nobile C. J.; Albert R. Mathematical modeling of the *Candida albicans* yeast to hyphal transition reveals novel control strategies. *PLoS Computational Biology*. 2021
4. Daneshnia, F.; Junior, J.; Ilkit, M.; Lombardi, L.; **Perry, A. M.**; Gao, M.; Nobile, C.J.; Egger, M.; Perlin, D.S.; Zhai, B.; Hohl, T.M.; Gabaldón, T.; Colombo, A.L.; Hoenigl, M.; Arastehfar, A. Worldwide emergence of fluconazole-resistant *Candida parapsilosis*: current framework and future research roadmap. *The Lancet Microbe*. 2023
5. Li, C.; Tao, L.; Guan, G.; **Perry, A. M.** et al. Atmospheric humidity regulates same-sex mating in *Candida albicans* through the trehalose and osmotic signaling pathways. *Science China Life Science*. 2023
6. Daneshnia, F.; Junior, J.; Ilkit, M.; Lombardi, L.; **Perry, A. M.**; Gao, M.; Nobile, C.J.; Egger, M.; Perlin, D.S.; Zhai, B.; Hohl, T.M.; Gabaldón, T.; Colombo, A.L.; Hoenigl, M.; Arastehfar, A. Evaluation of outbreak persistence caused by multidrug-resistant and echinocandin-resistant *Candida parapsilosis* using multidimensional experimental and epidemiological approaches. *Emerging Microbes and Infections*. 2024
7. Hu, T.; Zheng, Q.; Cao, C.; Guan, Z.; Ji, L.; Bing, J.; **Perry, A. M.**; Nobile, C. J.; Chu, H.; Huang, G. An agricultural triazole induces genomic instability and the formation of haploid cells in *Candida tropicalis*. *In preparation for submission*.
8. Ennis, C. L.; Viramontes, G.; **Perry, A. M.**; Nobile, C. J. Cfl11 is a new mediator of caspofungin-induced flocculation in *Candida albicans*. *In preparation for submission*.

### Oral Presentations:

1. **Perry, A. M.;** Nobile, C. J. Unraveling how *Candida albicans* forms sexual biofilms. September 2020. Molecular and Cell Biology Department, Research in Progress Seminar. University of California, Merced. Merced, California, USA.
2. **Perry, A. M.;** Nobile, C. J. Unraveling how *Candida albicans* forms sexual biofilms. September 2022. Molecular and Cell Biology Department, Research in Progress Seminar. University of California, Merced. Merced, California, USA.
3. **Perry, A. M.;** Nobile, C. J. Unraveling how *Candida albicans forms* sexual biofilms. May 2023. Microbiology Society *Candida* and Candidiasis Conference 2023. Montreal, Quebec, Canada

### Teaching Experiences:

Teaching Assistant – Molecular Basis for Human Health and Disease

University of California, Merced – Fall 2017

Average Course Evaluation: 6.27/7

Teaching Assistant – General Microbiology

University of California, Merced – Spring 2018

Average Course Evaluation: 6.63/7

Teaching Assistant – Molecular Cell Biology

University of California, Merced – Fall 2018

Average Course Evaluation: 6.3/7

Teaching Assistant – Microbial Evolution

University of California, Merced – Spring 2019

Average Course Evaluation: 6.4/7

### Fellowships & Awards:

Natural Sciences Outstanding Undergraduate Award - 2017

QSB Summer Fellowship - 2024

## VI. Abstract

Genetic regulation of sexual biofilm formation in *Candida albicans*

Austin Michael Perry

Doctor of Philosophy

University of California, Merced

2024

Supervisor: Professor Clarissa J. Nobile

Biofilms are structured and densely packed communities of microbial cells attached to surfaces. They are considered the natural growth state for a vast majority of microorganisms. The ability to form biofilms is an important virulence factor for most pathogens, including the opportunistic human fungal pathogen *Candida albicans*. *C. albicans* is one of the most prevalent fungal species of the human microbiota. However, *C. albicans* can also cause severe and life-threatening infections when host conditions permit. Conventional *C. albicans* biofilms are often resistant to antifungal agents and the host immune response and can act as reservoirs of infectious cells, maintaining persistent infections and seeding new infections in a host. The majority of *C. albicans* clinical isolates are heterozygous ( $a/\alpha$ ) at the mating type-like (*MTL*) locus, which defines *Candida* mating types, and can form robust biofilms when cultured *in vitro*. These “conventional” biofilms, formed by *MTL*-heterozygous ( $a/\alpha$ ) cells, have been the primary focus of *C. albicans* biofilm research to date. Recent work in the field has uncovered novel mechanisms through which biofilms are generated by *C. albicans* cells that are homozygous or hemizygous ( $a/a$ ,  $a/\Delta$ ,  $\alpha/\alpha$ , or  $\alpha/\Delta$ ) at the *MTL*-locus. In these studies, the addition of mating pheromone of a particular mating type can induce cells of the other mating type to form specialized “sexual” biofilms. Although sexual biofilms are generally less robust than conventional biofilms, they could serve as a protective niche to promote the parasexual life cycle of mating-competent cells, and thus could be an adaptation which may increase population diversity in dynamic environments.

In this work, we investigate the molecular and genetic mechanisms that enable sexual biofilm formation in *C. albicans* to gain insight into this unique biological process and establish a basis for comparison between sexual and conventional biofilms. Chapter 1 of this dissertation provides a detailed review of sexual biofilm formation in *C. albicans*. Chapter 2 of this dissertation provides detailed analyses and transcriptomics of several clinically isolated strains growing under sexual biofilm inducing conditions as well as co-cultures of white and opaque cells of various mating types. This led to the identification of several downstream genes that are involved in sexual biofilm formation. Chapter 3 of this dissertation identifies several TFs that are involved in regulating sexual biofilms. We find that many regulators of conventional biofilm formation are similarly involved in sexual biofilm formation. Interestingly, some transcription factors appear to switch from positive regulators of one system to negative regulators of the other. In addition, differential gene expression and gene ontology analyses reveal the unique role of these transcription factors in regulating sexual biofilm formation. Finally, Chapter 4 provides a detailed description of the conclusions and future directions for where other researchers can take this project, particularly to build clinical relevance for the sexual biofilm system and to

uncover the transcription network of sexual biofilms and elucidate the evolutionary history of sexual and conventional biofilms.

# Chapter 1

## Introduction

### 1.1 Abstract

Biofilms, structured and densely packed communities of microbial cells attached to surfaces, are the natural growth state for a vast majority of microorganisms. The ability to form biofilms is an important virulence factor for most pathogens, including the opportunistic human fungal pathogen *Candida albicans*. *C. albicans* is one of the most prevalent fungal species of the human microbiota that asymptotically colonizes healthy individuals. However, *C. albicans* can also cause severe and life-threatening infections when host conditions permit (e.g. through alterations in the host immune system, pH, and resident microbiota). Like many other pathogens, this ability to cause infections depends, in part, on the ability to form biofilms. Once formed, *C. albicans* biofilms are often resistant to antifungal agents and the host immune response and can act as reservoirs to maintain persistent infections as well as to seed new infections in a host. The majority of *C. albicans* clinical isolates are heterozygous (**a/α**) at the mating type-like (*MTL*) locus, which defines *Candida* mating types, and can form robust biofilms when cultured *in vitro*. These “conventional” biofilms, formed by *MTL*-heterozygous (**a/α**) cells, have been the primary focus of *C. albicans* biofilm research to date. Recent work in the field, however, has uncovered novel mechanisms through which biofilms are generated by *C. albicans* cells that are homozygous or hemizygous (**a/a**, **a/Δ**, **α/α**, or **α/Δ**) at the *MTL*-locus. In these studies, the addition of pheromones of the opposite mating type can induce the formation of specialized “sexual” biofilms, either through the addition of synthetic peptide pheromones to the culture, or in response to co-culturing of cells of opposite mating types. Although sexual biofilms are generally less robust than conventional biofilms, they could serve as a protective niche to support genetic exchange between mating-competent cells, and thus may represent an adaptive mechanism to increase population diversity in dynamic environments. Although conventional and sexual biofilms appear functionally distinct, both types of biofilms are structurally similar, containing yeast, pseudohyphal and hyphal cells surrounded by an extracellular matrix. Despite their structural similarities, conventional and sexual biofilms appear to be governed by distinct transcriptional networks and signaling pathways, suggesting that they may be adapted for, and responsive to, distinct environmental conditions. Here we review sexual biofilms and compare and contrast them to conventional biofilms of *C. albicans*.

### 1.2 Introduction

Biofilms are communities of microbial cells that are attached to surfaces and encased in a protective substance called the extracellular matrix<sup>1-5</sup>. Biofilms readily form on surfaces that are biotic (e.g. organs, mucosal and epithelial layers, and teeth) and abiotic (e.g. dentures, catheters, and industrial materials)<sup>1-5</sup>. The biofilm growth state provides the microorganisms inside with a sheltered microenvironment that is buffered against fluctuations in the surrounding environment and is protected from predators, environmental stresses, and mechanical forces that microorganisms would normally encounter in the planktonic (or free-living/free-floating) growth state<sup>1-5</sup>. Due to these adaptive benefits, most microorganisms under natural settings have evolved to spend the majority of their existence in the biofilm growth state<sup>1</sup>.



Biofilm formation is a key virulence factor for the majority of pathogens, including *Candida albicans*, which is the most commonly encountered human fungal pathogen in clinical settings<sup>3-7</sup>. *C. albicans* causes a wide variety of infections, ranging from benign mucosal (e.g. yeast infections and thrush) to hematogenously disseminated (bloodstream) candidiasis<sup>6,7</sup>. *Candida* infections are notably serious in immunocompromised individuals, such as AIDS patients, patients undergoing chemotherapy, transplantation patients receiving immunosuppression therapy, and patients with implanted medical devices<sup>8-10</sup>. Although research on *C. albicans* has been ongoing for over 70 years, most work has historically focused on *C. albicans* in its planktonic growth state. Over the last 20 years, however, the biofilm growth state of *C. albicans* has become a major area of research focus. *C. albicans* can form biofilms on abiotic surfaces (e.g. dentures, intravenous catheters, and prosthetic devices), as well as biotic surfaces (e.g. mucosal layers in the oral cavity and genitourinary tract)<sup>3-5</sup>. Once established, the cells within a *C. albicans* biofilm are protected from the host immune response, mechanical perturbations, and chemical stresses, allowing *C. albicans* to persist in the host and potentially cause recalcitrant infections<sup>3-5</sup>. More recently, a specialized “sexual” form of *C. albicans* biofilm has been discovered; although structurally similar to “conventional” biofilms, these “sexual” biofilms have many distinct phenotypic characteristics and generate a unique microenvironment that supports *C. albicans* mating<sup>11,12</sup>.

Best known as the most common cause of life-threatening fungal infections in hospital settings, *C. albicans* is also a normal commensal in the majority of healthy humans. Remarkably, *C. albicans* can asymptotically colonize several diverse regions of the body, including the oral cavity, gastrointestinal tract, skin, and genitourinary tract of humans<sup>13-16</sup>. These niches vary dramatically in terms of pH, nutrient sources and availability, and oxygen content<sup>17-18</sup>. This adaptive plasticity is due, in part, to the ability of *C. albicans* to undergo distinct morphological transitions in response to environmental cues; the best characterized examples include the yeast to hyphal cell transition and the transition between two distinct phenotypic cell types, termed “white” and “opaque”<sup>5,18,19</sup>. We begin by reviewing the white-opaque transition as it is intimately intertwined with the formation of sexual biofilms and mating. Next, we review the pheromone signaling and responses that occur in both white and opaque cell types during sexual biofilm formation and mating. Lastly, we compare and contrast conventional and sexual biofilms and consider the mechanisms through which sexual biofilms may aid in the process of mating.

### 1.3 The *C. albicans* white – opaque switch

White and opaque cell types are heritably maintained for many generations, and reversible switching between the two cell states occurs stochastically under standard laboratory growth conditions<sup>19</sup>. This balance between the white and opaque states is influenced by specific environmental cues that can bias the switch towards one cell type or the other, or even force all of the cells in a population to adopt a particular cell phenotype<sup>18-21</sup>. Approximately 16% of the genome is differentially expressed between the white and opaque cell types, resulting in cells with dramatically different phenotypes and functional attributes<sup>18,22-24</sup>. The morphologies of each cell type are also distinct; white cells are spherical and smooth and give rise to white, dome shaped colonies, whereas opaque cells are oblong and pimpled and form flatter and darker colonies<sup>18-19</sup>. Each state displays distinct metabolic preferences, resulting in striking fitness differences under a variety of environmental conditions<sup>25</sup>. White and opaque cells also respond to environmental conditions in unique ways; for example, opaque cells, but not white cells, can be induced

to form filaments in response to nitrogen or phosphate limitation, while white, but not opaque cells, are induced to form filaments in the presence of serum<sup>26</sup>. The two cell types also display distinct responses to alterations in temperature under standard laboratory growth conditions; white cells are stable at 37°C, while opaque cells revert to the white state *en masse* at 37°C<sup>18</sup>. Opaque cells, however, can be stabilized at 37°C by specific environmental stimuli, such as anaerobic conditions, elevated carbon dioxide levels, presence of *N*-acetylglucosamine, or nutrient limitations<sup>20,21,27-31</sup>. Interestingly, each cell type also interacts with the host immune system in different ways; for example, white cells secrete a macrophage chemoattractant while opaque cells do not, thus increasing the likelihood for opaque cells to escape macrophage engulfment, possibly allowing them to evade this aspect of the host innate immune response<sup>32</sup>.

The ability to undergo the white to opaque transition is controlled by the configuration of a discrete region on chromosome 5 known as the mating type-like (*MTL*) locus<sup>33-35</sup>. The *C. albicans* *MTL*-locus can carry two distinct configurations, **a** and  $\alpha$ , which consist of genes that specify the **a** and  $\alpha$  mating types, respectively<sup>35</sup>. Most *C. albicans* clinical isolates (~97%) are diploid, and exist in the *MTL*-heterozygous (**a**/ $\alpha$ ) configuration, however a few clinical isolates have been found to exist in the *MTL*-homozygous (**a/a** or  $\alpha/\alpha$ ) configuration<sup>33,34</sup>. *MTL*-heterozygous strains express the sex genes *MTLa1* and *MTLa2*, the protein products of which form a heterodimer that directly represses the white to opaque transition by binding to the promoter region of *WOR1*, the master regulator of the opaque cell type, and repressing its transcription<sup>33,36</sup>. *MTL*-homozygous strains contain either *MTLa1* or *MTLa2*, but not both, and thus *WOR1* expression is derepressed and switching to the opaque state occurs stochastically at a rate of approximately once every 10<sup>4</sup> cell divisions<sup>19,33,34,36</sup>. The white state is considered to be the default cell type, and is often referred to as the “ground state” of the white-opaque switch, since it does not require activation of any known white to opaque transition regulators, while the opaque state is referred to as the “excited state” of the switch because it requires expression of *WOR1*, which results in activation of many additional regulatory and non-regulatory genes that are specific to the opaque state<sup>22-37</sup>.

Although the vast majority (~97%) of *C. albicans* clinical isolates are heterozygous at the *MTL* locus, and were previously presumed to be “locked” in the white cell state<sup>33,34</sup>, recent research has shown that the white to opaque switch may be a much more common occurrence *in vivo* than previously thought. For example, it is now appreciated that natural *MTL*-heterozygous isolates can undergo white to opaque switching *in vitro* under elevated levels of CO<sub>2</sub> and in the presence of *N*-acetylglucosamine, conditions that resemble that of the gastrointestinal tract; however, unlike *MTL*-homozygous opaque cells, these *MTL*-heterozygous opaque cells appear unable to mate<sup>21</sup>. In *MTL*-heterozygous cells, *HBR1*, which encodes a transcription factor that mediates the hemoglobin response, promotes expression of genes carried at the *MTLa* locus and thus indirectly reinforces the **a**1/ $\alpha$ 2-mediated repression of *WOR1* and ultimately the repression of white to opaque switching<sup>38,39</sup>. Deletion of one copy of *HBR1* in *MTL*-heterozygous cells results in a substantial reduction in *MTLa1* and *MTLa2* mRNA expression levels and a slight upregulation of *MTLa1* gene expression; the resulting reduction in **a**1/ $\alpha$ 2 heterodimer levels allows these cells to behave like **a** cells in regards to switching and mating<sup>38,39</sup>. In another example, deletion of *OFR1*, which encodes a protein of unknown function, enables *MTL*-heterozygous white cells to switch to the opaque state and express both **a**- and  $\alpha$ -specific pheromones and pheromone receptors, conferring *ofr1* mutants with the unique ability to mate with opaque cells of any *MTL* configuration<sup>40</sup>. In addition, an *MTL*-homozygous clinical isolate strain, P94015, was observed to drift between “white-like” and

“opaque-like” cell states, was found to contain a homozygous nonsense mutation in *EFG1*, which encodes a known repressor of the white to opaque transition<sup>41</sup>. Taken together, physiologically relevant environmental cues, or spontaneously-arising loss-of-function mutations, could enable naturally-occurring strains to undergo white to opaque switching. Lastly, *MTL*-heterozygous cells can become *MTL*-homozygous through loss of heterozygosity on a portion or all of chromosome 5. This can occur through local gene conversion, homozygosis of an entire arm of the chromosome, or through spontaneous loss of one copy of chromosome 5 followed by duplication of the remaining homologous chromosome<sup>42,43</sup>. These loss of heterozygosity events have been shown to occur in response to a wide range of environmental conditions, including exposure to antifungal agents, growth in the presence of sorbose, oxidative stress, and temperature stress<sup>42-46</sup>.

*MTL*-homozygous cells can revert to an *MTL*-heterozygous state through the *C. albicans* parasexual life cycle<sup>47</sup>. During parasex, *MTL*-homozygous opaque cells can become *MTL*-heterozygous by mating with *MTL*-homozygous cells of the opposite mating type; this is termed heterothallic mating<sup>47-49</sup>. Interestingly, opaque cells can also mate with opaque cells of the same mating type, termed homothallic mating, providing a means for genetic exchange within unisexual populations and even between clonal progeny of a single parent cell<sup>50</sup>. Generally, the parasexual life cycle requires that *MTL*-heterozygous white cells undergo loss of heterozygosity at the *MTL*-locus followed by switching to the opaque cell state<sup>33,51-53</sup>. The resulting *MTL*-homozygous opaque cells secrete sex-specific pheromones that can cause opaque cells of the opposite mating type to extend mating projections towards the highest pheromone concentration gradient<sup>53</sup>. Once two mating projections fuse, the resulting conjugation bridge allows for nuclear fusion and the formation of a tetraploid nucleus<sup>53</sup>. This structure is stable for several cell divisions, thereby producing tetraploid progeny<sup>49,53</sup>. Specific environmental cues can cause the tetraploid cells to reduce their ploidy state via concerted chromosome loss, thereby completing the parasexual life cycle by producing diploid cells<sup>48,49,54,55</sup>. This concerted chromosome loss, however, can often result in aneuploidy, which is hypothesized to allow *C. albicans* to rapidly adapt to variable environments and harsh conditions<sup>49,55</sup>. While asexual reproduction (e.g. through budding) can benefit *C. albicans* populations by preserving well-adapted genotypes, parasex can generate novel allelic combinations to allow for rapid evolution in changing environments<sup>48,54,55</sup>, which may contribute to the remarkable ability of *C. albicans* to colonize diverse niches in the body and to its overall success as a commensal and pathogen<sup>49</sup>. Despite these apparent benefits, parasex has thus far been reported to occur at low rates *in vivo*<sup>27,47</sup>. Given that ~97% of the *C. albicans* population *in vivo* is thought to be *MTL*-heterozygous<sup>34</sup>, the probability that two *MTL*-homozygous white cells of opposite mating types undergo the multiple steps required for mating simultaneously, and within close enough proximity to detect mating pheromone, seems exceedingly low. Recent research, however, is beginning to uncover that homothallic mating occurs more frequently under specific *in vitro* environmental conditions, such as glucose starvation and oxidative stress, supporting the idea that homothallic mating may be more common than anticipated *in vivo*<sup>56</sup>. Intriguingly, parasexual mating is hypothesized to occur at high frequencies within sexual biofilms, which are formed by *MTL*-homozygous white cells in response to mating pheromone<sup>11,12</sup>. Like all *C. albicans* biofilms, the multilayer structure of the sexual biofilm is such that its innermost layers are likely to contain lower levels of oxygen and nutrients than the layers closer to its surface, and thus sexual biofilms could be a niche that supports homothallic mating.

Perhaps the most striking difference between the white and opaque cell types is that opaque cells can mate with other opaque cells, but form severely impaired biofilms, while white cells can form robust biofilms, but are unable to mate<sup>51,12,33,47,52,57,58</sup>. Generally, a *C. albicans* biofilm consists of a basal layer of yeast cells with hyphae and pseudohyphae extending away from the substrate to which they are adhered<sup>5,59,60</sup>. In recent years, it has been shown that *MTL*-heterozygous and *MTL*-homozygous white cells form different types of biofilms in response to different stimuli<sup>11,12,57-59</sup>. *MTL*-heterozygous (**a/a**) cells form robust biofilms in response to shear flow forces and various environmental conditions (e.g. temperature, shifts in pH, etc.), and are termed conventional biofilms<sup>5</sup>. Once formed, conventional biofilms are challenging to treat in clinical settings due to their recalcitrance to antifungal agents, mechanical forces, and the host immune response. Alternatively, sexual biofilms formed by *MTL*-homozygous (**a** or  $\alpha$ ) white cells in response to mating pheromone are less robust than conventional biofilms<sup>11,12</sup>, but as discussed above, they may provide an adaptive niche for mating.

## 1.4 Pheromone signaling and response in *C. albicans*

### 1.4.1 Mating pheromones

The **a** and  $\alpha$  pheromones produced by *C. albicans*, encoded by *MFa1* and *MFa1* respectively, play essential roles in the processes of heterothallic and homothallic mating<sup>50,61,62,67</sup>. Opaque  $\alpha$  cells constitutively express high levels of *MFa1*, producing a trimeric pheromone precursor peptide, whereas white  $\alpha$  cells do not<sup>62</sup>. This  $\alpha$ -pheromone precursor peptide is thought to be post-translationally modified by the Kex2 protease and Ste13 dipeptidyl aminopeptidase A, to result in two secreted and identical tridecapeptides with the sequence GFRLTNFGYFEPG and one tetradecapeptide with the sequence GFRLTNFGYFEPGK that represent the mature  $\alpha$  pheromones; both the tridecapeptide and tetradecapeptide are capable of eliciting mating responses<sup>62-67,80</sup>. In contrast, **a** cells only weakly express *MFa1* under standard laboratory conditions<sup>61</sup>. However, when exposed to  $\alpha$ -pheromone, white and opaque **a** cells highly express both *MFa1* and *MFa1*<sup>50,58</sup>. *MFa1* also encodes a precursor peptide which is predicted to be processed similarly to the **a**-pheromone of *Saccharomyces cerevisiae*<sup>61,68,69</sup>. Initial cleavage from the **a**-pheromone precursor peptide is thought to occur via the Ste24 and Axl1 proteases<sup>61,68</sup>. The developing peptide is then further processed by the prenyl-group-adding enzymes Ram1 and Ram2, the prenyl-dependent protease Rce1, and the cysteine-carboxy methyltransferase Ste14<sup>61,68</sup>. The mature **a**-pheromone is a prenylated tetradecapeptide with the sequence AVRSVSTGNCCSTC, and requires Hst6, an ABC transporter, to leave the cell<sup>61,69,70</sup>. Due to the structural simplicity of  $\alpha$ -pheromone and the fact that  $\alpha$ -pheromone can be more easily chemically synthesized relative to **a**-pheromone, most pheromone signaling experiments in the field are carried out using **a** cells and the addition of chemically synthesized  $\alpha$ -pheromone.

Although both *MFa1* and *MFa1* are expressed in **a** cells in response to pheromone,  $\alpha$ -pheromone is typically degraded by Bar1, an aspartyl protease, via a phenomenon known as “barrier activity”<sup>71</sup>. Barrier activity promotes heterothallic mating in ascomycetes by preventing pheromone hyperstimulation and by enabling recovery from cell cycle arrest<sup>71</sup>. It also inhibits the ability of *C. albicans* to undergo auto-pheromone stimulation and thus prevents homothallic mating. Deletion of *BAR1* in *C. albicans* allows for homothallic mating through an autocrine pathway where opaque **a** cells excrete  $\alpha$ -pheromone, which then binds to Ste2, the  $\alpha$ -pheromone receptor, on the same cell, leading to self-activation for mating<sup>50</sup>. In addition, glucose starvation and

oxidative stress enable unisexual populations of opaque **a** cells to undergo homothallic mating despite high *BAR1* expression levels<sup>56</sup>, resulting in auto-activated opaque cells that can mate with other opaque cells of the same mating type<sup>50,56</sup>. These findings suggest that certain strain backgrounds as well as specific niches in the human body can override the phenomenon of barrier activity, allowing for unisexual populations to become activated by pheromone<sup>50,56</sup>. This has important consequences for the parasexual lifecycle of *C. albicans* as homothallism allows for same-sex mating to occur within cell mixtures of the same mating types and between certain strains that are incompatible for heterothallic mating<sup>50</sup>. Given that this mechanism results in pheromone stimulation and mating for unisexual populations of opaque cells, a similar scenario could be envisioned within a sexual biofilm. The biofilm environment may even enhance the rate of homothallic mating by sequestering pheromone and possibly protecting pheromone from degradation within the biofilm structure<sup>11,12</sup>. In addition, within a biofilm, recently divided opaque cells would be held in close proximity to each other, increasing the likelihood of finding a mate nearby and thus the frequency of mating between progeny of a single opaque cell. Given that *C. albicans* relies on generating aneuploid progeny for genetic diversity, rather than recombination during meiosis, homothallic mating between clones in this capacity could rapidly and efficiently introduce genetic diversity into a population<sup>50,54,55</sup>.

#### 1.4.2 Pheromones-signaling pathway control

*C. albicans* employs a conserved Mitogen-Activated Protein Kinase (MAPK) signaling pathway to transduce pheromone signals and alter gene expression<sup>72,73</sup>. This pathway begins with the conserved mating type-specific G-protein coupled receptors (GPCRs), Ste2, expressed on **a** cells to recognize  $\alpha$ -pheromone, and Ste3, expressed on  $\alpha$  cells to recognize **a**-pheromone<sup>72-74</sup>. Activation of either GPCR results in the dissociation of the G $\alpha$  subunit (Cag1) from the G $\beta$  subunit (Ste4), and the G $\gamma$  subunit (Ste18) of a heterotrimeric G-protein<sup>72-75</sup>. The G-protein subunits then activate Cst20, a kinase that activates the downstream MAPK cascade, consisting of Ste11, Hst7, and Cek1/Cek2<sup>72-74</sup>. All kinases in this pathway, with the exception of Cst20, are held together in close proximity by the scaffolding protein Cst5<sup>72-74,76</sup>. Cek1 and Cek2 then activate the transcription factor Cph1 in both white and opaque cells, resulting in the differential expression of white and opaque state-specific genes<sup>58,72</sup>. The activities of Cek1 and Cek2 are regulated by Cpp1, a MAP kinase phosphatase<sup>77</sup>. Interestingly, *STE4*, *CST5*, *CEK1* and *CEK2* are expressed at lower levels in white cells than opaque cells<sup>78</sup>, and their repression contributes to the sterility of white cells as white cells engineered to express *STE4*, *CST5* and *CEK2* (*CEK1* was not tested) at levels similar to opaque cells have been shown to undergo mating at frequencies approaching that of opaque cells<sup>78</sup>. It is also interesting to note that Cek1 (rather than Cek2) appears to play a major role in opaque cell mating; opaque *cek1*  $\Delta/\Delta$  deletion mutants mate at much lower frequencies than opaque *cek2*  $\Delta/\Delta$  deletion mutants<sup>77</sup>. The precise contributions of Cek1 and Cek2 to the pheromone response in white and opaque cells is complex and an intriguing research area for future study. Nonetheless, we do know that G-protein signaling pathways, such as this one, are highly conserved among fungal pathogens and are involved in controlling several important developmental processes, including mating, filamentation, and virulence<sup>79</sup>.

### 1.4.3 Differences between the white and opaque cells pheromone response

When opaque cells sense pheromone of the opposite mating type, they become activated for mating via the MAPK signaling pathway (described above). This pheromone stimulation can occur under a variety of different environmental conditions, including planktonic and biofilm conditions<sup>58,61,62,80</sup>. Interestingly, opaque cells have been observed to respond more efficiently to pheromone in media containing alternative carbon sources (e.g. Spider media)<sup>80</sup>. Additionally, the opaque cell pheromone response can be enhanced under a variety of environmental conditions by deletion of *GPA2*, which encodes a G-protein  $\alpha$ -subunit that functions at the beginning of the cyclic AMP-protein kinase A (cAMP-PKA) pathway<sup>80</sup>. This finding suggests that mating may occur more frequently within certain (e.g. specific nutrient limiting) host niches and that there is likely crosstalk between the signaling pathways regulating pheromone (i.e. MAPK) and nutrient sensing (i.e. cAMP-PKA) responses.

The opaque cell pheromone response in *C. albicans* is mediated by the transcription factor Cph1, a homolog of the transcription factor Ste12 in *S. cerevisiae* that is activated by a MAPK signaling pathway and controls genes involved in mating<sup>58,69,72,73,81-83</sup>. In opaque cells responding to pheromone, Cph1 initiates a transcriptional response that results in an upregulation of genes involved in filamentation (e.g. *FGR23*), cell fusion (e.g. *FUS1*, *FIG1*), karyogamy (e.g. *KAR4*), MAPK signaling (e.g. *CEK1/2*), and adhesion and virulence (e.g. *HWP1/2*, *ECE1*, *SAP4/5/6*, *RBT1/4*)<sup>52,53,58,62,80</sup>. Interestingly, although opaque cells generally grow slower than white cells, genes involved in DNA replication and the cell cycle (e.g. *MCM6*, *MCM7*, *PRI2*, and *POL5a*) are specifically repressed in opaque cells responding to pheromone, suggesting that exposure to pheromone further slows progression out of the G1 phase of the cell cycle<sup>52,53,58,62,80,84</sup>. In opaque **a** cells, *STE2* is upregulated, and the  $\alpha$ -pheromone receptor Ste2 becomes localized to the tip of growing cellular extensions known as mating projections or conjugation tubes<sup>11,52,53,58,62</sup>; mating projections are phenotypically similar to hyphae, but lack septa<sup>52,53</sup>. Not surprisingly, transcriptional profiling data revealed that opaque cells forming mating projections in response to pheromone upregulate a subset of the genes associated with filamentation and virulence that are upregulated by white cells forming hyphae in response to serum<sup>62,85</sup>. These findings indicate that there is overlap among genes expressed during hyphal formation and pheromone treatment, but that there are also several genes that are distinctly expressed in each process<sup>62</sup>.

Although *C. albicans* white cells are unable to mate, **a** and  $\alpha$  white cells still express pheromone receptors and are thought to respond to pheromone in a Cph1-dependent manner<sup>11,58</sup>, albeit at a much slower rate than opaque cells<sup>58</sup>. For example, under standard sexual biofilm conditions, the transcriptional response of opaque cells four hours after pheromone exposure is comparable to that of white cells 24 hours after pheromone exposure<sup>58</sup>. Interestingly, the pheromone response in white cells appears to occur primarily under sexual biofilm conditions; in fact, much of the response is lost when white cells are subjected to pheromone under planktonic conditions<sup>52,80</sup>. It is also interesting to note that similar to the pheromone response in opaque cells, sexual biofilm formation is highly dependent on nutrient levels<sup>57,80,87</sup>, suggestive again of cross-talk between the pheromone response and nutrient sensing signaling pathways. Despite white cells being unable to mate, many genes involved in MAPK signaling and mating are upregulated in white cells responding to pheromone (e.g. *STE2*, *HST6*, *FIG1*, *FUS1*, *KAR4*), which may be an artefact derived from the co-option of Cph1 by white cells for biofilm formation<sup>58</sup>. In addition, many of the adhesion-, biofilm- and other virulence-associated genes

upregulated in opaque cells responding to pheromone are similarly upregulated by white cells responding to pheromone in biofilms (e.g. *RBT1*, *HWP1/2*, *ECE1*, *PGA23/50*, *SAP5/6*)<sup>58</sup>. However, unlike opaque cells, white cells do not experience a halt in their cell cycle upon exposure to  $\alpha$ -pheromone<sup>11,52</sup>. Overall, in synthetic pheromone-stimulated biofilms, 116 genes are differentially expressed in both white and opaque cells, white cells uniquely differentially express 147 genes, and opaque cells uniquely differentially express 190 genes<sup>58</sup>. Given that Cph1 is believed to mediate both sexual biofilm formation in white cells and mating in opaque cells in response to pheromone, Cph1 may be involved in mediating a core pheromone response involving filamentation and adhesion that can be modified depending on the epigenetic state of the cell<sup>58,72</sup>. Over the course of evolutionary time, it appears that *C. albicans* has rewired aspects of cell-cell communication to be used for host-pathogen interactions, which may provide insight into the unique history of this opportunistic pathogen. Additional work on the regulatory controls of white and opaque cells may improve our understanding of how transcription factors drift to regulate novel functions.

## 1.5 Conventional and sexual *C. albicans* biofilms

### 1.5.1 Comparison of the properties of sexual and conventional biofilms

Conventional and sexual biofilms formed by *C. albicans* are both composed of yeast-form, pseudohyphal, and hyphal cells<sup>5,12,60,87</sup>. The *C. albicans* biofilm life cycle typically begins when planktonic yeast-form cells adhere to a substrate in response to specific environmental stimuli<sup>4,5</sup>. These yeast-form cells proliferate, resulting in a dense mat that is tightly anchored to its substrate. Hyphae and pseudohyphae then begin to grow and extend away from the substrate, providing architectural support for the biofilm. As the growing *C. albicans* biofilm matures, the cells within the biofilm produce extracellular matrix material, composed predominantly of proteins, polysaccharides, and DNA that surrounds all cells within the biofilm<sup>4,5</sup>. Once a mature biofilm is formed, daughter yeast-form cells disperse from the biofilm and revert to the planktonic growth state or form new biofilms elsewhere<sup>4,5,88</sup>. Although this generalized biofilm life cycle is common across all *C. albicans* biofilms, the configuration of the *MTL*-locus and the phenotypic state of the cells play important roles in determining the environmental stimuli that induce biofilm formation as well as certain unique physical characteristics of the biofilms formed. *MTL*-heterozygous white cells form thick and resilient conventional biofilms in response to specific environmental stimuli, such as shear flow rate and host factors, whereas *MTL*-homozygous white cells form thinner and weaker sexual biofilms in response to mating pheromone<sup>11,12,57,58</sup>.

Generally, microorganisms that exist in biofilms are protected from environmental stresses relative to microorganisms that exist planktonically<sup>1</sup>. The extracellular matrix surrounding both *C. albicans* conventional and sexual biofilms acts as a physical barrier inhibiting many compounds, such as antimicrobial agents, from penetrating into the deeper layers of the biofilm<sup>3-5</sup>. Mature conventional biofilms, in particular, are highly resilient to most forms of environmental stress, such as treatment with antifungal agents, exposure to mechanical forces, and attack by the host immune system<sup>4,5</sup>. In addition to the physical barrier provided by the matrix, the resilience of conventional biofilms to antifungal agents is also due to the fact that cells within conventional, but not sexual, biofilms upregulate drug efflux pumps (e.g. *Cdr1/2*, *Mdr1*), thereby prohibiting antifungal drugs from reaching lethal concentrations within the biofilm<sup>58,60</sup>. Consistent with this finding, sexual biofilms are much more easily permeated by a variety of compounds than

conventional biofilms<sup>12,59</sup>. Interestingly, this phenotype can be partially rescued by the overexpression of *BCR1*<sup>12,59</sup>, which encodes the biofilm master regulator of several downstream adhesins, suggesting that cell-cell and/or cell-substrate adherence may also contribute to the recalcitrance of conventional biofilms to antimicrobial compounds. Cells within conventional biofilms are also more tightly adhered to each other and their substrates compared to sexual biofilms<sup>12,58,59</sup>. These differences in adherence are likely due to the upregulation of genes involved in adhesion (e.g. *ALS3*) in conventional biofilms, which are less (if at all) upregulated in sexual biofilms<sup>3-5,58,60</sup>. Additional factors contributing to the drug resistance of conventional biofilms include variation in cell membrane sterol composition and the presence of metabolically dormant persister cells, which can display extreme tolerance to most classes of antifungal drugs<sup>3,4,13,89,90</sup>. We note that these two factors have only been studied in conventional biofilms, and thus whether or not they also are present in sexual biofilms is unknown, and an intriguing area of interest for future studies.

If sexual biofilms do not provide the same protective environment as conventional biofilms, why does *C. albicans* bother to form sexual biofilms in the first place? Given that ~97% of the *C. albicans* population in nature is thought to be *MTL*-heterozygous, the chance that two *MTL*-homozygous white cells of opposite mating types will exist in close enough proximity to undergo the complex steps involved to mate is seemingly unlikely<sup>34</sup>. Even if two opaque cells were in close enough proximity to one another, ambient forces would likely disrupt the pheromone concentration gradient before the cells could find one another and fuse. Since sexual biofilms are not nearly as thick or dense as conventional biofilms, these properties could enable opaque cells to extend mating projections through the biofilm towards other opaque cells, while still being sufficiently dense to maintain pheromone gradients and provide some stability against external forces<sup>11,12</sup>. Consistent with the idea that sexual biofilms provide an optimal environment for mating, white cells produce their own pheromone when responding to  $\alpha$ -pheromone, which promotes both homothallic and heterothallic mating<sup>91</sup>. In terms of the host response, white cells are preferentially phagocytosed by macrophages as compared to opaque cells and only white cells secrete a leukocyte chemoattractant<sup>32,92</sup>. Thus white cells may protect mating opaque cells by acting as decoys to sequester infiltrating host cells<sup>32</sup>. Overall, by stabilizing pheromone gradients and providing an optimal environment for opaque cells to undergo mating, sexual biofilms may promote mating in specialized niches of the body that support white-opaque switching (e.g. the skin).

Cell heterogeneity resulting from the various microenvironments present throughout conventional biofilms is also likely to contribute to biofilm resilience<sup>3</sup>. These microenvironment differences lead to specific gene expression changes within cells in discrete environmental niches of the biofilm, resulting in widespread cellular heterogeneity throughout the biofilm architecture<sup>93</sup>. For example, the innermost regions of conventional biofilms are hypoxic and contain less nutrients and more waste products compared to the outermost regions of the biofilm<sup>94</sup>. These unique microenvironments also enable *C. albicans* to coexist and interact with specific microbial species. For example, the hypoxic inner regions of conventional *C. albicans* biofilms support the growth of obligate anaerobic bacteria, such as *Bacteroides fragilis* and *Clostridium perfringens*<sup>3,94</sup>. Although the microenvironments present in sexual biofilms have not been studied to date, because sexual biofilms are much thinner than conventional biofilms<sup>12,59</sup>, there are likely to be fewer opportunities for microenvironments to form. Nonetheless, given their phenotypic differences, the microenvironments of conventional and sexual biofilms are certainly distinct.



Interspecies interactions within polymicrobial biofilms between *C. albicans* and other species (mostly bacteria) have only been studied to date within the context of conventional *C. albicans* biofilms. These interactions can be beneficial or antagonistic in nature. A large proportion of research to date has focused on the beneficial interactions between *C. albicans* and *Staphylococcus* species, such as *Staphylococcus aureus*; these two species are often co-isolated from biofilm infections with high mortality rates in clinical settings<sup>95</sup>. Although these two species can form biofilms independently, initial attachment of *C. albicans* cells to surfaces is enhanced when *C. albicans* is co-inoculated with *S. aureus*<sup>86</sup>. In mature polymicrobial biofilms of *S. aureus* and *C. albicans*, *S. aureus* cells can be found adhered to *C. albicans* hyphae and are present throughout the biofilm structure<sup>86,96,97</sup>. *S. aureus* is, in fact, known to specifically recognize and bind to the adhesin Als3 on the cell surface of *C. albicans* hyphae, and consistent with this, cells of *C. albicans als3* mutants have been found to interact with significantly fewer *S. aureus* cells than wild-type *C. albicans* cells<sup>96</sup>. Interestingly, *ALS3* expression is reduced in sexual biofilms compared to conventional biofilms<sup>58,60</sup>, and thus one may hypothesize that *S. aureus* and *C. albicans* are less likely to co-localize in the context of sexual biofilms. Other structural components of *C. albicans* biofilms are also known to play roles in mixed-species interactions. For example,  $\beta$ -glucans present in the extracellular matrix of *C. albicans* biofilms were found to aid methicillin-resistant *S. aureus* (MRSA) strains in surviving vancomycin, one of the few antibiotics effective against MRSA<sup>3,98</sup>. In terms of antagonistic interactions, *Enterococcus faecalis* can secrete EntV, a bacteriocin that inhibits conventional *C. albicans* biofilm formation<sup>3,99</sup>. In another example, *Pseudomonas aeruginosa* can secrete a 12-carbon acyl homoserine lactone that hinders *C. albicans* filamentation and conventional biofilm formation by mimicking farnesol, a quorum sensing molecule produced by *C. albicans* that modulates filamentation<sup>100,101</sup>. *P. aeruginosa* can also release phenazines that specifically inhibit *C. albicans* filamentation and conventional biofilm formation<sup>102</sup>. Overall, given that sexual and conventional biofilms have different physical and biochemical properties, the interactions of these two biofilm systems with other microorganisms are likely to differ considerably.

Conventional and sexual biofilms also differ in their interactions with the host immune response. Neutrophils and mononuclear leukocytes are important host players against fungal infections<sup>103,104</sup>. When neutrophils recognize *C. albicans* cells, they activate a number of antimicrobial defenses, including phagocytosis, degranulation, the release of reactive oxygen species (ROS), and the release of web-like neutrophil extracellular traps (NETs)<sup>103</sup>. In general, neutrophils are very effective at killing planktonic *C. albicans* yeast and hyphal cells<sup>105</sup>, where these antimicrobial mechanisms work efficiently. When it comes to *C. albicans* conventional biofilms, however, neutrophils are generally unable to penetrate beyond the outermost regions of the biofilm, ROS are not produced, and neutrophil extracellular traps (NETs) are not released<sup>3,4,59,106,107</sup>. This biofilm-specific recalcitrance to neutrophils is largely due to the presence of the extracellular matrix, as physical disruption of the matrix in conventional biofilms restores the ability of neutrophils to release NETs<sup>106</sup>. Consistently, neutrophils are able to release NETs and kill *C. albicans* cells within a biofilm formed by the *C. albicans pmr1* mutant, which is unable to produce matrix mannan<sup>106</sup>. Interestingly, in the presence of a sexual biofilm, neutrophils can penetrate into the innermost layers of the biofilm<sup>59</sup>, although whether NETs are released and fungal cells are killed is unknown. Based on this information, one would hypothesize that sexual biofilms are more susceptible to clearance by neutrophils than conventional biofilms.

In terms of mononuclear leukocytes, these host cells typically respond to *C. albicans* infection by phagocytosing invading cells and releasing cytokines<sup>108</sup>. *C. albicans* cells in conventional biofilms are two to three times more resistant to killing by mononuclear leukocytes than cells growing planktonically<sup>103,108</sup>. In addition, *C. albicans* cells growing in conventional biofilms are capable of altering the cytokine profile of attacking mononuclear cells<sup>108</sup>. For example, the presence of a conventional biofilm leads to the downregulation of TNF- $\alpha$ , a pro-inflammatory cytokine produced by mononuclear leukocytes that would normally suppress biofilm formation<sup>103,108,109</sup>. Intriguingly, conventional biofilms that are grown in the presence of mononuclear leukocytes form thicker biofilms, a phenomenon that is thought to be mediated by an unknown soluble factor that is present when the two are co-cultured<sup>108</sup>. Whether or not this process also occurs with sexual biofilms in the presence of mononuclear cells is unknown, but provides an interesting area for future exploration.

The host response to *C. albicans* infection is typically initiated by the interaction of host pattern recognition receptors and pathogen-associated molecular patterns (PAMPs) and involves secretion of a variety of antimicrobial compounds. Interestingly, several characteristics of conventional and sexual biofilms inhibit the recognition of PAMPs. For example, hyphal cells, a major component of both conventional and sexual biofilms, are able to 'mask' the  $\beta$ -glucan in their cell walls, blocking a key PAMP recognized by many host immune cell types<sup>4,110,111</sup>. In addition, several cell surface and secreted proteins are capable of sequestering and inactivating host complement proteins and other secreted anti-immune proteins are expressed at higher levels in conventional biofilms than planktonic cells<sup>3,4,60</sup>. Although studies to date have only examined conventional biofilms, it seems likely that sexual biofilms would also retain some of these host response characteristics. In fact, we know that some cell surface and secreted proteins involved in inactivating the host immune response (e.g. *SAP4*, *MSB2*) are also upregulated in sexual biofilms<sup>58</sup>. Nonetheless, how sexual biofilms interact with the immune system and how they compare to conventional biofilms in this regard has not been investigated to date.

### 1.5.2 Genetic regulation of sexual and conventional biofilms

Our current knowledge of the regulation of conventional and sexual biofilms is summarized in Figure 1. Given that there are many phenotypic differences between conventional and sexual biofilms, it seems likely that the genetic regulation and transcriptional profiles of these two systems should differ as well. As discussed above, the signaling pathway that triggers the formation of sexual biofilms is a MAPK cascade initiated by the pheromone receptors Ste2 or Ste3<sup>72-74</sup>. This pathway is unique to sexual biofilms, as a Ras1/cAMP pathway that includes Cdc35 and Tpk2 and an unknown receptor have been shown to trigger conventional biofilm formation<sup>59,112,113</sup>. In the conventional biofilm pathway, Ras1 activation results in cAMP production. Increased concentrations of cAMP activates PKA to initiate the complex transcriptional network controlling conventional biofilm formation<sup>59,112,113</sup>. When comparing the transcriptional profiles of *MTL*-heterozygous white cells grown planktonically versus in conventional biofilm conditions and white *a* cells grown in sexual biofilm conditions with and without the presence of  $\alpha$ -pheromone, there are 662 genes that are induced twofold or more in conventional biofilms, 486 genes that are induced twofold or more in sexual biofilms, and 128 genes similarly induced twofold or more in both systems (e.g. *HWP1*, *SAP4*, *SAP5*, *ALS1*)<sup>58,60</sup>. In addition, 187 genes are repressed at least twofold in conventional biofilms, 355 genes are repressed at least twofold in sexual biofilms, and only 19 genes are similarly repressed at least twofold in

both systems<sup>58,60</sup>. The dramatic differences in transcriptomic profiles between sexual and conventional biofilms strongly supports the idea that distinct transcriptional networks regulate the formation of these two structures.

The core transcriptional network controlling conventional biofilm formation consists of nine transcription factors: Tec1, Ndt80, Rob1, Brg1, Bcr1, Efg1, Flo8, Gal4 and Rfx2<sup>60,114</sup>. By screening a mutant library containing 165 strains with homozygous deletions of genes encoding DNA-binding proteins, a transcriptional network of six transcription factors was identified (Tec1, Ndt80, Rob1, Brg1, Bcr1, Efg1), whose deletion hindered conventional biofilm formation *in vitro* and *in vivo*<sup>60</sup>. Interestingly, two of these transcription factor mutants were defective in one *in vivo* model of biofilm formation but not in another (e.g. the *bcr1* mutant was severely defective in the rat catheter model, but formed a decent biofilm in the rat denture model, while the *brg1* mutant formed normal biofilms in the catheter model, but was severely defective in the denture model)<sup>60</sup>. These findings suggest that the genetic regulation of conventional biofilms may be different depending on the environment<sup>60</sup>. Further investigation into the transcriptional regulators of conventional biofilm formation in a temporal biofilm study revealed three additional core regulators: Flo8, Gal4 and Rfx2<sup>114</sup>. Interestingly, deletion of *GAL4* and *RFX2* resulted in generally enhanced conventional biofilms relative to wildtype, indicating that they may serve as negative regulators of the network<sup>114</sup>. In order to understand how these transcription factors regulate conventional biofilm formation, genome-wide chromatin immunoprecipitation and microarray experiments were performed on each transcription factor and transcription factor mutant, respectively. These experiments revealed that, in addition to regulating about 1,000 downstream “target” genes, each of the nine transcription factors occupies the promoter regions of and activates at least three of the other transcription factors, in addition to their own promoter regions, forming a complex network of positive feedback loops<sup>60,114,115</sup>. Overall, the majority of TFs involved in the conventional biofilm network act as both positive and negative regulators of various downstream target genes, with the exception of Tec1, which seems to act primarily as an activator<sup>60</sup>. Although the core transcriptional network regulating conventional biofilm formation has been identified, many additional transcription factors have been found to regulate certain aspects of conventional biofilm formation. For example, Rlm1 and Zap1 are both involved in the regulation of the extracellular matrix<sup>116-118</sup>. As we continue research on biofilms into the future, there will certainly be additional regulators identified to play important roles in different aspects of conventional biofilm formation, as well as an increase in our knowledge of the core regulators of sexual biofilm formation.

Sexual biofilms are currently known to rely on four of the nine core transcription factors involved in the conventional biofilm network: Bcr1, Rob1, Brg1, and Tec1<sup>58</sup>. Deletion of any of these four transcription factors results in a significant decrease in sexual biofilm thickness relative to wildtype<sup>58</sup>. Deletion of *EFG1* does not hinder sexual biofilm formation<sup>58</sup>; rather, the *efg1* mutant appears to form equally thick sexual biofilms relative to wildtype, indicating that *EFG1* is not required for sexual biofilm formation<sup>58</sup>. Interestingly, the *ndt80* mutant forms thicker sexual biofilms than wildtype, although this may not be due to Ndt80 acting as a negative regulator of sexual biofilm formation since deletion of *NDT80* leads to the misregulation of cell separation genes, specifically *SUN41* and *CHT3*<sup>58</sup>. This could consequently result in thicker sexual biofilms as an artifact of enhanced cell clumping and/or reduced cell dispersion during sexual biofilm formation. The fact that this does not occur in conventional biofilms, and that Ndt80 is in fact required for conventional biofilm formation, is an intriguing area for future research. The roles of the other three core transcription factors involved in regulating conventional biofilm

formation – Flo8, Gal4 and Rfx2 – have not yet been explored at all in terms of sexual biofilms and is another area of interest for future research. Finally, the transcription factor Cph1, which is not required for conventional biofilm formation, plays a central role in the regulation of sexual biofilm formation<sup>58,60</sup>. Deletion of *CPH1* results in the complete obliteration of sexual biofilm formation, and it has been hypothesized that Cph1 is the terminal transcription factor activated by the MAPK cascade in both white and opaque cells responding to pheromone<sup>58</sup>. These ideas have been challenged, where another group found that although the same GPCR (Ste2/3), MAPK cascade (Ste11, Hst7, Cek1/2) and scaffolding protein (Cst5) are used in both white and opaque cell pheromone responses, there are cell type differences in the terminal transcription factors that are activated by pheromone<sup>73</sup>. In opaque cells, their findings suggests that Cph1 is activated for mating, while in white cells, Tec1 is activated for sexual biofilm formation<sup>73,119,120</sup>. The discrepancies between these two findings may be partially explained by differences in growth conditions utilized by the two groups<sup>11,12,58,73,87</sup>. In fact, the different conditions lead to the formation of sexual biofilms with distinct structural features, and one possibility is that different transcription networks may be involved in the two conditions that depend on environmental cues. Given this information, the terminal transcription factor(s) activated by pheromone-stimulated MAPK signaling in white cells remain to be conclusively determined.

The transcriptional network regulating conventional biofilms has been shown to have evolved fairly recently<sup>60</sup>. By determining the master regulators of sexual biofilm formation and its accompanying transcriptional network, we will be able to explore how two seemingly unrelated transcriptional networks and signaling pathways have evolved to interact with one another. If Cph1 is the terminal transcription factor of the pheromone response in white cells, this would indicate that a conserved signaling cascade and its transcriptional regulator evolved to control a novel set of genes during pheromone activation. We can envision two scenarios where this could occur. First, genes associated with biofilm formation may have come under the direct control of Cph1 by the addition of Cph1 recognition sequences to their promoters. Alternatively, one or several regulators of biofilm formation may have come under the control of Cph1<sup>115</sup>. In the latter scenario, deemed the “regulator-first” model of the evolution of transcription networks<sup>115</sup>, Cph1 would have been directly inserted into the older conventional biofilm network, gaining control of several downstream genes associated with biofilm formation, while adding many of the genes that it previously regulated to the network. This model could account for the large size of transcriptional networks (e.g. the conventional biofilm network comprises approximately 20% of the genome), and the reason why complex transcriptional networks include such large numbers of seemingly extraneous target genes<sup>58,60,115</sup>. Since white cells are unable to mate, their main purpose is to form biofilms in response to pheromone, thus reason dictates that they have no need to express genes involved in mating when stimulated by pheromone. Yet, the expression of mating genes has been observed in white cells responding to mating pheromone, where there is a clear induction of genes involved in cell fusion, karyogamy and other aspects of mating (e.g. *FUS1* and *KAR4*)<sup>58</sup>. This regulator-first model is consistent with the hypothesis that Cph1 is the terminal transcription factor activated by the MAPK cascade in both white and opaque cells responding to pheromone. In the alternative hypothesis, Tec1, whose expression is only induced in conventional biofilms via Efg1, may have come under direct control of a novel signaling pathway, namely the pheromone response MAPK cascade. In this scenario, Tec1 would still regulate many of the genes it traditionally regulated and the transcriptional profile of the white cell pheromone response would look similar to conventional biofilm

formation. Given that we see a dramatic change in transcriptional profiles between the two biofilm systems and the activation of so many extraneous genes involved in mating in white cells responding to pheromone, we favor the regulator-first model for the evolution of the sexual biofilm transcriptional network.

## 1.6 Conclusion

Sexual biofilms represent a specialized kind of biofilm formed by *MTL*-homozygous cells responding to mating pheromone. The physical characteristics of sexual biofilms differ dramatically from conventional biofilms; indeed they appear to lack the major characteristics that contribute to the highly pathogenic nature of conventional biofilms. The molecular differences that result in such distinct phenotypes between the two systems remain to be determined. The significance of the unusual characteristics of sexual biofilms and their roles in the lifecycle of *C. albicans* is also not clearly understood. The low frequency of *MTL*-homozygous strains observed in nature and the apparent lack of opaque-specific niches outside of the laboratory led to questions about the existence of a parasexual lifecycle in *C. albicans* in nature. However, it is now appreciated that sexual biofilms may serve as a permeable and penetrable, yet protective, microenvironment that promotes mating in *C. albicans*. Although no *in vivo* model has been established to investigate the relevance of sexual biofilms in the host, the apparent disadvantageous properties of sexual biofilms for survival in the host may be outweighed by their ability to promote parasexual mating. Future work on the genetic regulation and molecular mechanisms of sexual biofilm formation will improve our understanding of the significance of sexual biofilms as well as the relevance of phenotypic switching and parasexual mating in the lifecycle of *C. albicans* in nature. Overall, the molecular and genetic regulation of conventional and sexual biofilm formation is quite different between the two systems. Conventional biofilms are modulated by the Ras1/cAMP signaling pathway, whereas sexual biofilms are modulated by a MAP kinase pathway; each activating a largely distinct set of transcription factors and likely different transcriptional networks. Understanding how these two transcriptional networks regulate their target genes to give rise to similar yet distinct phenotypes will also provide a basis for studies on the evolution of biofilm formation. Current and future research into sexual biofilms should provide a wealth of knowledge into the molecular genetics, pathogenesis, and evolutionary history of one of the most pervasive fungal pathogens of humans.

## 1.7 References

1. Hall-Stoodley, L.; Costerton, J.W.; Stoodley, P. Bacterial biofilms: From the natural environment to infectious diseases. *Nat. Rev. Microbiol.* **2004**, *2*, 95–108.
2. Kolter, R.; Greenberg, E.P. Microbial sciences: The superficial life of microbes. *Nature* **2006**, *441*, 300–302.
3. Lohse, M.B.; Gulati, M.; Johnson, A.D.; Nobile, C.J. Development and regulation of single-and multi-species *Candida albicans* biofilms. *Nat. Rev. Microbiol.* **2018**, *16*, 19–31.
4. Gulati, M.; Nobile, C.J. *Candida albicans* biofilms: development, regulation, and molecular mechanisms. *Microbes Infect.* **2016**, *18*, 310–321.
5. Nobile, C.J.; Johnson, A.D. *Candida albicans* biofilms and human disease. *Annu. Rev. Microbiol.* **2015**, *69*, 71–92.
6. Wenzel, R.P. Nosocomial Candidemia : Risk Factors and Attributable Mortality. *Clin. Infect. Dis.* **1995**, *20*, 1531–1534.

7. Rex, J.H.; Walsh, T.J.; Sobel, J.D.; Filler, S.G.; Pappas, P.G.; Dismukes, W.E.; Edwards, J.E. Practice Guidelines for the treatment of candidiasis. *Clin. Infect. Dis.* **2000**, *30*, 662–678.
8. Calderone, R.A.; Fonzi, W.A. Virulence factors of *Candida albicans*. *Trends Microbiol.* **2001**, *9*, 327–335.
9. Kullber, B.J.; Oude Lashof, A.M. Epidemiology of opportunistic invasive mycoses. *Eur. J. Med. Res.* **2002**, *7*, 183–191.
10. Weig, M.; Gross, U.; Mühlshlegel, F. Clinical aspects and pathogenesis of *Candida* infection. *Trends Microbiol.* **1998**, *6*, 468–470.
11. Daniels, K.J.; Srikantha, T.; Lockhart, S.R.; Pujol, C.; Soll, D.R. Opaque cells signal white cells to form biofilms in *Candida albicans*. *EMBO J.* **2006**, *25*, 2240–2252.
12. Park, Y.N.; Daniels, K.J.; Pujol, C.; Srikantha, T.; Soll, D.R. *Candida albicans* forms a specialized “sexual” as well as “pathogenic” biofilm. *Eukaryot. Cell* **2013**, *12*, 1120–1131.
13. Ganguly, S.; Mitchell, A.P. Mucosal biofilms of *Candida albicans*. *Curr. Opin. Microbiol.* **2011**, *14*, 380–385.
14. Kumamoto, C.A. *Candida* biofilms. *Curr. Opin. Microbiol.* **2002**, *5*, 608–611.
15. Kumamoto, C.A. Inflammation and gastrointestinal *Candida* colonization. *Curr. Opin. Microbiol.* **2011**, *14*, 386–391.
16. Kennedy, M.J.; Volz, P.A. Ecology of *Candida albicans* gut colonization: Inhibition of *Candida* adhesion, colonization, and dissemination from the gastrointestinal tract by bacterial antagonism. *Infect. Immun.* **1985**, *49*, 654–663.
17. Köhler, J.R.; Casadevall, A.; Perfect, J. The Spectrum of Fungi That Infects Humans. *Cold Spring Harb. Perspect. Med.* **2014**, *5*, a019273.
18. Lohse, M.B.; Johnson, A.D. White-opaque switching in *Candida albicans*. *Curr. Opin. Microbiol.* **2009**, *12*, 650–654.
19. Slutsky, B.; Staebell, M.; Anderson, J.; Risen, L.; Pfaller, M.; Soll, D.R. “White-opaque transition”: A second high-frequency switching system in *Candida albicans*. *J. Bacteriol.* **1987**, *169*, 189–197.
20. Huang, G.; Yi, S.; Sahni, N.; Daniels, K.J.; Srikantha, T.; Soll, D.R. N-acetylglucosamine induces white to opaque switching, a mating prerequisite in *Candida albicans*. *PLoS Pathog.* **2010**, *6*, e1000806.
21. Xie, J.; Tao, L.; Nobile, C.J.; Tong, Y.; Guan, G.; Sun, Y.; Cao, C.; Hernday, A.D.; Johnson, A.D.; Zhang, L.; Bai, F.Y.; Huang, G. White-Opaque Switching in Natural *MTLa/α* Isolates of *Candida albicans*: Evolutionary Implications for Roles in Host Adaptation, Pathogenesis, and Sex. *PLoS Biol.* **2013**, *11*, e1001525.
22. Tuch, B.B.; Mitrovich, Q.M.; Homann, O.R.; Hernday, A.D.; Monighetti, C.K.; de La Vega, F.M.; Johnson, A.D. The transcriptomes of two heritable cell types illuminate the circuit governing their differentiation. *PLoS Genet.* **2010**, *6*, e1001070.
23. Lan, C.Y.; Newport, G.; Murillo, L.A.; Jones, T.; Scherer, S.; Davis, R.W.; Agabian, N. Metabolic specialization associated with phenotypic switching in *Candida albicans*. *Proc. Natl. Acad. Sci. USA* **2002**, *99*, 14907–14912.
24. Tsong, A.E.; Miller, M.G.; Raisner, R.M.; Johnson, A.D. Evolution of a Combinatorial Transcriptional Circuit: A Case Study in Yeasts. *Cell* **2003**, *115*, 389–399.
25. Ene, I. V.; Lohse, M.B.; Vladu, A. V.; Morschhäuser, J.; Johnson, A.D.; Bennett, R.J. Phenotypic profiling reveals that *Candida albicans* opaque cells represent a metabolically specialized cell state compared to default white cells. *MBio* **2016**, *7*, e01269-16.

26. Si, H.; Hernday, A.D.; Hirakawa, M.P.; Johnson, A.D.; Bennett, R.J. *Candida albicans* White and Opaque Cells Undergo Distinct Programs of Filamentous Growth. *PLoS Pathog.* **2013**, *9*, e1003210.
27. Dumitru, R.; Navarathna, D.H.M.L.P.; Semighini, C.P.; Elowsky, C.G.; Dumitru, R. V.; Dignard, D.; Whiteway, M.; Atkin, A.L.; Nickerson, K.W. *In vivo* and *in vitro* anaerobic mating in *Candida albicans*. *Eukaryot. Cell* **2007**, *6*, 465–472.
28. Huang, G. Regulation of phenotypic transitions in the fungal pathogen *Candida albicans*. *Virulence* **2012**, *3*, 251–261.
29. Ramírez-Zavala, B.; Reuß, O.; Park, Y.; Ohlsen, K.; Morschhäuser, J. Environmental Induction of White–Opaque Switching in *Candida albicans*. *PLoS Pathog.* **2008**, *4*, e1000089.
30. Huang, G.; Srikantha, T.; Sahni, N.; Yi, S.; Soll, D.R. Report CO(2) Regulates White-to-Opaque Switching in *Candida albicans*. *Curr. Biol.* **2009**, *19*, 330–334.
31. Alby, K.; Bennett, R.J. Stress-Induced Phenotypic Switching in *Candida albicans*. *Mol. Biol. Cell* **2009**, *20*, 3178–3191.
32. Geiger, J.; Wessels, D.; Lockhart, S.R.; Soll, D.R. Release of a Potent Polymorphonuclear Leukocyte Chemoattractant Is Regulated by White-Opaque Switching in *Candida albicans*. *Infect. Immun.* **2004**, *72*, 667–677.
33. Miller, M.G.; Johnson, A.D. White-opaque switching in *Candida albicans* is controlled by mating-type locus homeodomain proteins and allows efficient mating. *Cell* **2002**, *110*, 293–302.
34. Lockhart, S.R.; Pujol, C.; Daniels, K.J.; Miller, M.G.; Johnson, A.D.; Pfaller, M.A.; Soll, D.R. In *Candida albicans*, white-opaque switchers are homozygous for mating type. *Genetics* **2002**, *162*, 737–745.
35. Hull, C.M.; Johnson, A.D. Identification of a Mating Type–Like Locus in the Asexual Pathogenic Yeast *Candida albicans*. *Science* **1999**, *285*, 1271–1275.
36. Huang, G.; Wang, H.; Chou, S.; Nie, X.; Chen, J.; Liu, H. Bistable expression of WOR1, a master regulator of white-opaque switching in *Candida albicans*. *Proc. Natl. Acad. Sci. USA* **2006**, *103*, 12813–12818.
37. Hernday, A.D.; Lohse, M.B.; Fordyce, P.M.; Nobile, C.J.; DeRisi, J.L.; Johnson, A.D. Structure of the transcriptional network controlling white-opaque switching in *Candida albicans*. *Mol. Microbiol.* **2013**, *90*, 22–35.
38. Pendrak, M.L.; Yan, S.S.; Roberts, D.D. Hemoglobin regulates expression of an activator of mating-type locus  $\alpha$  genes in *Candida albicans*. *Eukaryot. Cell* **2004**, *3*, 764–775.
39. Pendrak, M.L.; Yan, S.S.; Roberts, D.D. Sensing the host environment: Recognition of hemoglobin by the pathogenic yeast *Candida albicans*. *Arch. Biochem. Biophys.* **2004**, *426*, 148–156.
40. Sun, Y.; Gadoury, C.; Hirakawa, M.P.; Bennett, R.J.; H Marcus, D.; Marcil, A. Deletion of a Yci1 Domain Protein of *Candida albicans* Allows Homothallic Mating in *MTL*-heterozygous Cells. *MBio* **2016**, *7*, e00465-16.
41. Hirakawa, M.P.; Martinez, D.A.; Sakthikumar, S.; Anderson, M.Z.; Berlin, A.; Gujja, S.; Zeng, Q.; Zisson, E.; Wang, J.M.; Greenberg, J.M.; Berman, J.; Bennett, R.J.; Cuomo, C.A. Genetic and phenotypic intra-species variation in *Candida albicans*. *Genome Res.* **2015**, *25*, 413–425.
42. Magee, B.B.; Magee, P.T. Induction of mating in *Candida albicans* by construction of *MTL $\alpha$*  and *MTL $\alpha$*  strains. *Science* **2000**, *289*, 310–313

43. Forche, A.; Abbey, D.; Pisithkul, T.; Weinzierl, M.A.; Ringstrom, T.; Bruck, D.; Petersen, K.; Berman, J. Stress alters rates and types of loss of heterozygosity in *Candida albicans*. *MBio* **2011**, *2*, e00129-11.
44. Ou, T.Y.; Chang, F.M.; Cheng, W.N.; Lara, A.; Chou, M.L.; Lee, W.F.; Lee, K.C.; Lin, C.T.; Lee, W.S.; Yu, F.L.; Su, C.H. Fluconazole induces rapid high-frequency *MTL*-homozygosity with microbiological polymorphism in *Candida albicans*. *J. Microbiol. Immunol. Infect.* **2017**, *50*, 899–904.
45. Hilton, C.; Markie, D.; Corner, B.; Rikkerink, E.; Poulter, R. Heat shock induces chromosome loss in the yeast *Candida albicans*. *Mol. Gen Genet.* **1985**, *200* 162.
46. Berman, J.; Hadany, L. Does stress induce (para)sex? Implications for *Candida albicans* evolution. *Trends Genet.* **2012**, *28*, 197–203.
47. Hull, C.M. Evidence for Mating of the “Asexual” Yeast *Candida albicans* in a Mammalian Host. *Science* **2000**, *289*, 307–310.
48. Bennett, R.J.; Johnson, A.D. Completion of a parasexual cycle in *Candida albicans* by induced chromosome loss in tetraploid strains. *EMBO J.* **2003**, *22*, 2505–2515.
49. Bennett, R.J. The parasexual lifestyle of *Candida albicans*. *Curr. Opin. Microbiol.* **2015**, *28*, 10–17.
50. Alby, K.; Schaefer, D.; Bennett, R.J. Homothallic and heterothallic mating in the opportunistic pathogen *Candida albicans*. *Nature* **2009**, *460*, 890–893.
51. Soll, D.R.; Lockhart, S.R.; Zhao, R. Relationship between switching and mating in *Candida albicans*. *Eukaryot. Cell* **2003**, *2*, 390–397.
52. Lockhart, S.R.; Zhao, R.; Daniels, K.J.; Soll, D.R.  $\alpha$ -pheromone-induced “shmooing” and gene regulation require white-opaque switching during *Candida albicans* mating. *Eukaryot. Cell* **2003**, *2*, 847–855.
53. Lockhart, S.R.; Daniels, K.J.; Zhao, R.; Wessels, D.; Soll, D.R. Cell Biology of Mating in *Candida albicans*. *Eukaryot. Cell* **2003**, *2*, 49–61.
54. Forche, A.; Alby, K.; Schaefer, D.; Johnson, A.D.; Berman, J.; Bennett, R.J. The parasexual cycle in *Candida albicans* provides an alternative pathway to meiosis for the formation of recombinant strains. *PLoS Biol.* **2008**, *6*, e110.
55. Hickman, M.A.; Paulson, C.; Dudley, A.; Berman, J. Parasexual ploidy reduction drives population heterogeneity through random and transient aneuploidy in *Candida albicans*. *Genetics* **2015**, *200*, 781–794.
56. Guan, G.; Tao, L.; Yue, H.; Liang, W.; Gong, J.; Bing, J.; Zheng, Q.; Veri, A.O.; Fan, S.; Robbins, N.; Cowen, L.E.; Huang, G. Environment-induced same-sex mating in the yeast *Candida albicans* through the Hsf1 – Hsp90 pathway. *PLoS Biol.* **2019**, *17*, e2006966.
57. Sahni, N.; Yi, S.; Pujol, C.; Soll, D.R. The white cell response to pheromone is a general characteristic of *Candida albicans* strains. *Eukaryot. Cell* **2009**, *8*, 251–256.
58. Lin, C.H.; Kabrawala, S.; Fox, E.P.; Nobile, C.J.; Johnson, A.D.; Bennett, R.J. Genetic Control of Conventional and Pheromone-Stimulated Biofilm Formation in *Candida albicans*. *PLoS Pathog.* **2013**, *9*, e1003305.
59. Yi, S.; Sahni, N.; Daniels, K.J.; Lu, K.L.; Srikantha, T.; Huang, G.; Garnaas, A.M.; Soll, D.R. Alternative mating type configurations ( $\mathbf{a/a}$  versus  $\mathbf{a/a}$  or  $\mathbf{\alpha/\alpha}$ ) of *Candida albicans* result in alternative biofilms regulated by different pathways. *PLoS Biol.* **2011**, *9*, e1001117.
60. Nobile, C.J.; Fox, E.P.; Nett, J.E.; Sorrells, T.R.; Mitrovich, Q.M.; Hernday, A.D.; Tuch, B.B.; Andes, D.R.; Johnson, A.D. A recently evolved transcriptional network controls biofilm development in *Candida albicans*. *Cell* **2012**, *148*, 126–138.



61. Dignard, D.; El-Naggar, A.L.; Logue, M.E.; Butler, G.; Whiteway, M. Identification and characterization of MFAl, the gene encoding *Candida albicans* a-factor pheromone. *Eukaryot. Cell* **2007**, *6*, 487–494.
62. Bennett, R.; Uhl, M.A.; Miller, M.G.; Johnson, A. Identification and characterization of a *Candida albicans* mating pheromone. *Mol. Cell. Biol.* **2003**, *23*, 8189–8201.
63. Julius, D.; Brake, A.; Blair, L.; Kunisawa, R.; Thorner, J. Isolation of the putative structural gene for the lysine-arginine-cleaving endopeptidase required for processing of yeast prepro- $\alpha$ -factor. *Cell* **1984**, *37*, 1075–1089.
64. Newport, G.; Agabian, N. KEX2 influences *Candida albicans* proteinase secretion and hyphal formation. *J. Biol. Chem.* **1997**, *272*, 28954–28961.
65. Julius, D.; Blair, L.; Brake, A.; Sprague, G.; Thorner, J. Yeast  $\alpha$  factor is processed from a larger precursor polypeptide: The essential role of a membrane-bound dipeptidyl aminopeptidase. *Cell* **1983**, *32*, 839–852.
66. Bautista-Muñoz, C.; Hernández-Rodríguez, C.; Villa-Tanaca, L. Analysis and expression of STE13ca gene encoding a putative X-prolyl dipeptidyl aminopeptidase from *Candida albicans*. *FEMS Immunol. Med. Microbiol.* **2005**, *45*, 459–469.
67. Panwar, S.L.; Legrand, M.; Dignard, D.; Whiteway, M.; Magee, P.T. MF $\alpha$ 1, the Gene Encoding the  $\alpha$  Mating Pheromone of *Candida albicans*. *Eukaryot. Cell.* **2003**, *2*, 1350–1360.
68. Chen, P.; Sapperstein, S.K.; Choi, J.D.; Michaelis, S. Biogenesis of the *Saccharomyces cerevisiae* Mating Pheromone a-Factor. **1997**, *136*, 251–269.
69. Magee, B.B.; Legrand, M.; Alarco, A.M.; Raymond, M.; Magee, P.T. Many of the genes required for mating in *Saccharomyces cerevisiae* are also required for mating in *Candida albicans*. *Mol. Microbiol.* **2002**, *46*, 1345–1351.
70. Raymond, M.; Dignard, D.; Alarco, A.M.; Mainville, N.; Magee, B.B.; Thomas, D.Y. A Ste6p/P-glycoprotein homologue from the asexual yeast *Candida albicans* transports the a-factor mating pheromone in *Saccharomyces cerevisiae*. *Mol. Microbiol.* **2002**, *27*, 587–598.
71. Schaefer, D.; Côte, P.; Whiteway, M.; Bennett, R.J. Barrier activity in *Candida albicans* mediates pheromone degradation and promotes mating. *Eukaryot. Cell* **2007**, *6*, 907–918.
72. Chen, J.; Chen, J.; Lane, S.; Liu, H. A conserved mitogen-activated protein kinase pathway is required for mating in *Candida albicans*. *Mol. Microbiol.* **2002**, *46*, 1335–1344.
73. Yi, S.; Sahni, N.; Daniels, K.J.; Pujol, C.; Srikantha, T.; Soll, D.R. The Same Receptor, G Protein, and Mitogen-activated Protein Kinase Pathway Activate Different Downstream Regulators in the Alternative White and Opaque Pheromone Responses of *Candida albicans*. *Mol. Biol. Cell* **2008**, *19*, 957–970.
74. Lin, C.H.; Choi, A.; Bennett, R.J. Defining pheromone-receptor signaling in *Candida albicans* and related asexual *Candida* species. *Mol. Biol. Cell* **2011**, *22*, 4918–4930.
75. Dignard, D.; André, D.; Whiteway, M. Heterotrimeric G-protein subunit function in *Candida albicans*: Both the  $\alpha$  and  $\beta$  subunits of the pheromone response G protein are required for mating. *Eukaryot. Cell* **2008**, *7*, 1591–1599.
76. Yi, S.; Sahni, N.; Daniels, K.J.; Lu, K.L.; Huang, G.; Garnaas, A.M.; Pujol, C.; Srikantha, T.; Soll, D.R. Utilization of the Mating Scaffold Protein in the Evolution of a New Signal Transduction Pathway for Biofilm Development. *MBio* **2011**, *2*, e00237-10.

77. Rastghalam, G.; Omran, R.P.; Alizadeh, M.; Fulton, D.; Mallick, J.; Whiteway, M. MAP Kinase Regulation of the *Candida albicans* Pheromone Pathway. *mSphere* **2019**, *4*, e00598-18.
78. Scaduto, C.M.; Kabrawala, S.; Thomson, G.J.; Scheving, W.; Ly, A.; Anderson, M.Z.; Whiteway, M.; Bennett, R.J. Epigenetic control of pheromone MAPK signaling determines sexual fecundity in *Candida albicans*. *Proc. Natl. Acad. Sci. USA* **2017**, *114*, 13780-13785.
79. Dohlman, H.G.; Song, J.; Apanovitch, D.M.; DiBello, P.R.; Gillen, K.M. Regulation of G protein signalling in yeast. *Semin. Cell Dev. Biol.* **1998**, *9*, 135–141.
80. Bennett, R.J.; Johnson, A.D. The role of nutrient regulation and the Gpa2 protein in the mating pheromone response of *Candida albicans*. *Mol. Microbiol.* **2006**, *62*, 100–119.
81. Ramírez-Zavala, B.; Weyler, M.; Gildor, T.; Schmauch, C.; Kornitzer, D.; Arkowitz, R.; Morschhäuser, J. Activation of the Cph1-Dependent MAP Kinase Signaling Pathway Induces White-Opaque Switching in *Candida albicans*. *PLoS Pathog.* **2013**, *9*, e1003696.
82. Roberts, R.L.; Fink, G.R. Elements of a single map kinase cascade in *Saccharomyces cerevisiae* mediate two developmental programs in the same cell type: Mating and invasive growth. *Genes Dev.* **1994**, *8*, 2974–2985.
83. Herskowitz, I. MAP Kinase Pathways in Yeast: For Mating and More. *Cell* **1995**, *80*, 187-197.
84. Hartwell, L.H. Synchronization of haploid yeast cell cycles, a prelude to conjugation. *Exp. Cell Res.* **1973**, *76*, 111–117.
85. Nantel, A.; Dignard, D.; Bachewich, C.; Marcus, D.; Marcil, A.; Bouin, A.P.; Sensen, C.W.; Hogues, H.; van het Hoog, M.; Gordon, P.; Rigby, T.; Benoit, F.; Tessier, D.C.; Thomas, D.Y.; Whiteway, M. Transcription Profiling of *Candida albicans* Cells Undergoing Yeast-to-Hyphal Transition. *Mol. Biol. Cell* **2002**, *13*, 3452–3465.
86. Lin, Y.J.; Alsad, L.; Vogel, F.; Koppar, S.; Nevarez, L.; Auguste, F.; Seymour, J.; Syed, A.; Christoph, K.; Loomis, J.S. Interactions between *Candida albicans* and *Staphylococcus aureus* within mixed species biofilms. *Bios* **2013**, *84*, 30–39.
87. Daniels, K.J.; Park, Y.N.; Srikantha, T.; Pujol, C.; Soll, D.R. Impact of Environmental Conditions on the Form and Function of *Candida albicans* Biofilms. *Eukaryot. Cell* **2013**, *12*, 1389–1402.
88. Uppuluri, P.; Chaturvedi, A.K.; Srinivasan, A.; Banerjee, M.; Ramasubramanian, A.; Köehler, J.; Kadosh, D.; Lopez-ribot, J.L. Dispersion as an Important Step in the *Candida albicans* Biofilm Developmental Cycle. *PLoS Pathog.* **2010**, *6*, e1000828.
89. Mukherjee, P.K.; Chandra, J.; Kuhn, D.M.; Ghannoum, M.A. Mechanism of Fluconazole Resistance in *Candida albicans* Biofilms: Phase-Specific Role of Efflux Pumps and Membrane Sterols. *Infect. Immun.* **2003**, *71*, 4333–4340.
90. LaFleur, M.D.; Kumamoto, C.A.; Lewis, K. *Candida albicans* biofilms produce antifungal-tolerant persister cells. *Antimicrob. Agents Chemother.* **2006**, *50*, 3839–3846.
91. Tao, L.; Cao, C.; Liang, W.; Guan, G.; Zhang, Q.; Nobile, C.J.; Huang, G. White Cells Facilitate Opposite- and Same-Sex Mating of Opaque Cells in *Candida albicans*. *PLoS Genet.* **2014**, *10*, e1004737.
92. Lohse, M.B.; Johnson, A.D. Differential phagocytosis of white versus opaque *Candida albicans* by *Drosophila* and mouse phagocytes. *PLoS One* **2008**, *3*, e0001473.

93. Kean, R.; Delaney, C.; Rajendran, R.; Sherry, L.; Metcalfe, R.; Thomas, R.; Mclean, W.; Williams, C.; Ramage, G. Gaining Insights from *Candida* Biofilm Heterogeneity: One Size Does Not Fit All. *J. Fungi* **2018**, *4*, 12.
94. Fox, E.P.; Cowley, E.S.; Nobile, C.J.; Hartooni, N.; Newman, D.K.; Johnson, A.D. Anaerobic bacteria grow within *Candida albicans* biofilms and induce biofilm formation in suspension cultures. *Curr. Biol.* **2014**, *24*, 2411–2416.
95. Tsui, C.; Kong, E.F.; Jabra-Rizk, M.A. Pathogenesis of *Candida albicans* biofilm. *Pathog. Dis.* **2016**, *74*, ftw018.
96. Peters, B.M.; Ovchinnikova, E.S.; Krom, B.P.; Schlecht, L.M.; Zhou, H.; Hoyer, L.L.; Busscher, H.J.; van der Mei, H.C.; Jabra-Rizk, M.A.; Shirtliff, M.E. *Staphylococcus aureus* adherence to *Candida albicans* hyphae is mediated by the hyphal adhesin Als3p. *Microbiol.* **2012**, *158*, 2975–2986.
97. Peters, B.M.; Jabra-Rizk, M.A.; Scheper, M.A.; Leid, J.G.; Costerton, J.W.; Shirtliff, M.E. Microbial interactions and differential protein expression in *Staphylococcus aureus*-*Candida albicans* dual-species biofilms. *FEMS Immunol. Med. Microbiol.* **2010**, *59*, 493–503.
98. Kong, E.F.; Tsui, C.; Kucharíková, S.; Andes, D.; van Dijck, P.; Jabra-Rizk, M.A. Commensal Protection of *Staphylococcus aureus* against Antimicrobials by *Candida albicans* Biofilm Matrix. *MBio* **2016**, *7*, e01365-16.
99. Graham, C.E.; Cruz, M.R.; Garsin, D.A.; Lorenz, M.C. *Enterococcus faecalis* bacteriocin EntV inhibits hyphal morphogenesis, biofilm formation, and virulence of *Candida albicans*. *Proc. Natl. Acad. Sci. USA* **2017**, *114*, 4507–4512.
100. Lindsay, A.K.; Hogan, D.A. *Candida albicans*: Molecular interactions with *Pseudomonas aeruginosa* and *Staphylococcus aureus*. *Fungal Biol. Rev.* **2014**, *28*, 85–96.
101. Ramage, G.; Saville, S.P.; Wickes, B.L.; López-ribot, J.L. Inhibition of *Candida albicans* Biofilm Formation by Farnesol, a Quorum-Sensing Molecule. *Appl. Environ. Microbiol.* **2002**, *68*, 5459–5463.
102. Morales, D.K.; Grahl, N.; Okegbe, C.; Dietrich, L.E.P.; Jacobs, N.J.; Hogan, A. Control of *Candida albicans* Metabolism and Biofilm Formation by *Pseudomonas aeruginosa* Phenazines. *MBio*. **2013**, *4*, e00526-12.
103. Kernien, J.F.; Snarr, B.D.; Sheppard, D.C.; Nett, J.E. The interface between Fungal Biofilms and Innate Immunity. *Front Immunol.* **2018**, *8*, 1968.
104. Brown, G.D. Innate Antifungal Immunity: The Key Role of Phagocytes. *Annu. Rev. Immunol.* **2011**, *29*, 1–21.
105. Urban, C.F.; Reichard, U.; Brinkmann, V.; Zychlinsky, A. Neutrophil extracellular traps capture and kill *Candida albicans* and hyphal forms. *Cell. Microbiol.* **2006**, *8*, 668–676.
106. Johnson, C.J.; Cabezas-Olcoz, J.; Kernien, J.F.; Wang, S.X.; Beebe, D.J.; Huttenlocher, A.; Ansari, H.; Nett, J.E. The Extracellular Matrix of *Candida albicans* Biofilms Impairs Formation of Neutrophil Extracellular Traps. *PLoS Pathog.* **2016**, *12*, e1005884.
107. Xie, Z.; Thompson, A.; Sobue, T.; Kashleva, H.; Xu, H.; Vasilakos, J.; Dongari-Bagtzoglou, A. *Candida albicans* biofilms do not trigger reactive oxygen species and evade neutrophil killing. *J. Infect. Dis.* **2012**, *206*, 1936–1945.
108. Chandra, J.; McCormick, T.S.; Imamura, Y.; Mukherjee, P.K.; Ghannoum, M.A. Interaction of *Candida albicans* with adherent human peripheral blood mononuclear cells increases *C. albicans* biofilm formation and results in differential

- expression of pro- and anti-inflammatory cytokines. *Infect. Immun.* **2007**, *75*, 2612–2620.
109. Rocha, F.A.C.; Alves, A.M.C.V.; Rocha, M.F.G.; Cordeiro, R.D.A.; Brilhante, R.S.N.; Pinto, A.C.M.D.; Nunes, R.D.M.; Girão, V.C.C.; Sidrim, J.J.C. Tumor necrosis factor prevents *Candida albicans* biofilm formation. *Sci. Rep.* **2017**, *7*, 1206.
  110. Gantner, B.N.; Simmons, R.M.; Underhill, D.M. Dectin-1 mediates macrophage recognition of *Candida albicans* yeast but not filaments. *EMBO* **2005**, *24*, 1277–1286.
  111. Chen, T.; Wagner, A.S.; Tams, R.N.; Eyer, J.E.; Kauffman, S.J.; Gann, E.R.; Fernandez, E.J.; Reynolds, T.B. Lrg1 Regulates  $\beta$  (1,3)-Glucan Masking in *Candida albicans* through the Cek1 MAP Kinase Pathway. *MBio* **2019**, *10*, e01767-19.
  112. Inglis, D.O.; Sherlock, G. Ras signaling gets fine-tuned: Regulation of multiple pathogenic traits of *Candida albicans*. *Eukaryot. Cell* **2013**, *12*, 1316–1325.
  113. Huang, G.; Huang, Q.; Wei, Y.; Wang, Y.; Du, H. Multiple roles and diverse regulation of the Ras/cAMP/protein kinase A pathway in *Candida albicans*. *Mol. Microbiol.* **2019**, *111*, 6–16.
  114. Fox, E.P.; Bui, C.K.; Nett, J.E.; Hartooni, N.; Mui, M.C.; Andes, D.R.; Nobile, C.J.; Johnson, A.D. An expanded regulatory network temporally controls *Candida albicans* biofilm formation. *Mol. Microbiol.* **2015**, *96*, 1226–1239.
  115. Sorrells, T.R.; Johnson, A.D. Making sense of transcription networks. *Cell* **2015**, *161*, 714–723.
  116. Nobile, C.J.; Nett, J.E.; Hernday, A.D.; Homann, O.R.; Deneault, J.; Nantel, A.; Andes, D.R.; Johnson, A.D.; Mitchell, A.P. Biofilm Matrix Regulation by *Candida albicans* Zap1. *PLoS Biol.* **2009**, *7*, e1000133.
  117. Nett, J.E.; Sanchez, H.; Cain, M.T.; Ross, K.M.; Andes, D.R. Interface of *Candida albicans* Biofilm Matrix-Associated Drug Resistance and Cell Wall Integrity Regulation. *Eukaryot. Cell* **2011**, *10*, 1660–1669.
  118. Nett, J.E.; Sanchez, H.; Cain, M.T.; Andes, D.R. Genetic Basis of *Candida Biofilm* Resistance Due to Drug-Sequestering Matrix Glucan. *J. Infect. Dis.* **2010**, *202*, 171–175.
  119. Daniels, K.J.; Srikantha, T.; Pujol, C.; Park, Y.N.; Soll, D.R. Role of Tec1 in the development, architecture, and integrity of sexual biofilms of *Candida albicans*. *Eukaryot. Cell* **2015**, *14*, 228–240.
  120. Sahni, N.; Yi, S.; Daniels, K.J.; Huang, G.; Srikantha, T.; Soll, D.R. Tec1 mediates the pheromone response of the white phenotype of *Candida albicans*: Insights into the evolution of new signal transduction pathways. *PLoS Biol.* **2010**, *8*, e1000363.

## 1.8 Figures

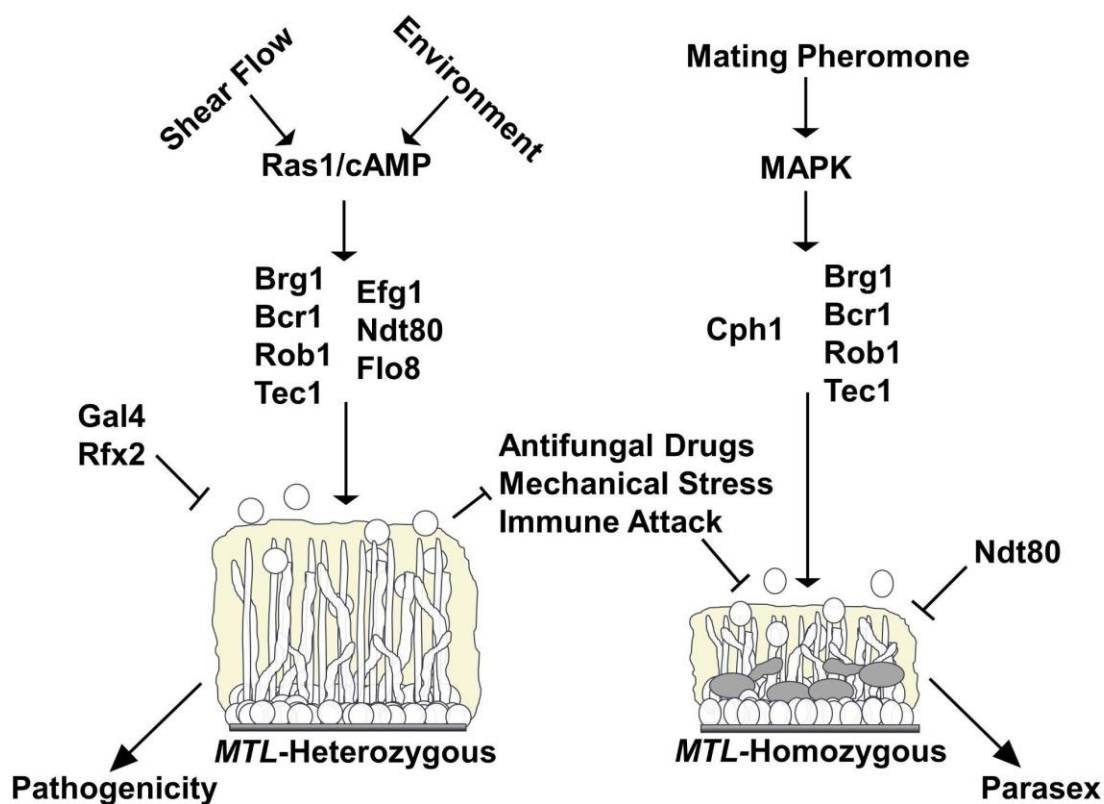


**Figure 1.1 Summary of the regulation of conventional (*MTL*-heterozygous) and sexual (*MTL*-homozygous) biofilms and their phenotypic characteristics.** Arrows with smaller heads indicate activation (e.g. shear flow and environmental conditions activate the Ras1/cAMP pathway). Arrows with large heads indicate the lifestyle each biofilm type facilitates (e.g. *MTL*-heterozygous biofilms facilitate a pathogenic lifestyle). T-bars indicate inhibitory relationships (e.g. Gal4 and Rfx2 inhibit conventional biofilm formation and conventional biofilms inhibit the deleterious effects of antifungal drugs, mechanical stress and immune attack).

## Chapter 2

### Transcriptional analysis of *Candida albicans* sexual biofilms reveals novel target genes involved in sexual biofilm formation

Austin M. Perry, Deepika Gunasekaran, Clarissa J. Nobile  
In preparation for submission

#### 2.1 Abstract

Nearly every microbe on the planet can proliferate as structured communities of cells called biofilms. The commensal and opportunistic pathogen, *Candida albicans*, can form two different kinds of biofilms depending on its genetic background and environmental conditions: “conventional” and “sexual”. *C. albicans* sexual biofilms present a fascinating system to study for many reasons. They represent the cross-section between three major areas of *C. albicans* research: mating, biofilm formation, and white-opaque switching. They serve as an important, protective niche in which we can examine the interactions of white and opaque *C. albicans* cells as they undergo epigenetic switching and cell-cell communication. In addition, sexual biofilms can be studied as a relevant niche which promotes mating behavior between many *Candida* species; a phenomenon known to contribute to antifungal resistance. In this work, we analyze the transcriptomes of a library of clinically isolated strains as they form sexual biofilms in response to a synthetic pheromone. We also observe *C. albicans* in a more natural setting by mixing white and opaque cells together, relying on naturally produced pheromone and possibly other factors to stimulate sexual biofilm formation. Finally, we use these analyses to generate a list of genes that are highly expressed in the sexual biofilm condition to delete and assay the resulting mutants for alterations in their ability to form sexual biofilms.

#### 2.2 Introduction

Biofilms are considered to be the predominant growth state of microorganisms in the environment and are a leading cause of persistent human infection<sup>1-5</sup>. They are organized communities of surface-associated microorganisms embedded in an extracellular matrix composed of DNA, proteins, and carbohydrates<sup>1-5</sup>. By creating a dense three-dimensional structure, microorganisms within biofilms are generally protected from a variety of environmental stresses that could harm them in the planktonic growth state (e.g. mechanical, chemical, immune)<sup>1-5</sup>. As such, biofilm formation is considered to be a major virulence factor in many pathogens, including *Candida albicans* – one of the most predominant human pathogens<sup>5,6</sup>.

*Candida albicans* is a commensal fungus found in the microbiota of over 90% of adults around the world, but it is also among the most prevalent human fungal pathogens; costing the United States billions every year<sup>3-5,7,8</sup>. *C. albicans* can reside as a harmless commensal on the skin, and in the mouth, gastrointestinal tract or genitourinary tract of healthy humans for years<sup>9-12</sup>. However, in individuals experiencing weakened immune systems (e.g. chemotherapy), disruptions to their microbiome (e.g. antibiotic usage), or fluctuations to internal pH levels can induce this normally harmless fungus to cause disease<sup>5</sup>. This dynamic lifestyle can be attributed in part to *C. albicans* natural ability to adopt a wide range of cell morphologies. Among these are filamentous morphotypes (i.e. hyphae and pseudohyphae) which can come together to form biofilms, and the epigenetic switch between white and opaque cell types<sup>5,13-16</sup>.

*C. albicans* can form various types of biofilms depending on the genotype of the cells within<sup>17,18</sup>. Of particular interest are those known as “conventional” biofilms; the predominant focus of the field to date. This is for good reason as conventional biofilms are formed by the vast majority (~97%) of *C. albicans* clinical isolates due to their genetic status as mating type-like heterozygotes (**a/a**)<sup>19,20</sup>. These biofilms are particularly robust and are known to cause major problems in the clinic due to their resistance to immune attacks and medical treatment<sup>5</sup>. In addition, *C. albicans* **a/a** cells form conventional biofilms in response to a variety of environmental conditions (e.g. elevated temperatures, mechanical agitation, alterations in pH, overgrowth, etc.)<sup>3-5,21,22</sup>. Alternatively, *MTL*-homozygous or –hemizygous cells (**a/a**, **a/Δ**, **α/α**, or **α/Δ**) only make up a small subset of the global population (~3%)<sup>20</sup>. These cells form a unique and specialized “sexual” biofilm, generally requiring mixed populations of **a** and **α** cells to do so<sup>17,23-27</sup>. This is because white cells of a particular mating type require the mating-pheromone from the opposite mating type in order to form a sexual biofilm<sup>25-27</sup>.

Sexual biofilms generally lack all the resistance characteristics of canonical biofilms (i.e. increased antifungal resistance, resilience to mechanical disruption and attacks from the immune system), yet *C. albicans* has still maintained this costly developmental program over the course of evolution<sup>17</sup>. It could be that the very characteristics that weaken the sexual biofilm to hazardous environmental pressures simultaneously enables *C. albicans* opaque cells to mate at higher frequencies. Indeed, sexual biofilms are much less dense than conventional biofilms, which enables antifungal drugs, immune cells and other molecules to penetrate to their very core<sup>17</sup>. Yet this tenuity, as compared to conventional biofilms, enables opaque cells to extend mating projections towards other opaque cells along mating-pheromone concentration gradients maintained by the little structure sexual biofilms do possess<sup>26</sup>. In addition, white cells themselves produce pheromone upon stimulation, promoting both homothallic and heterothallic mating of nearby opaque cells<sup>28</sup>. If sexual biofilms were as dense as conventional biofilms, mating-pheromones would not be able to disperse very far and opaque cells would find it more difficult to extend mating-projections through such a dense structure. These findings have led researchers to speculate that sexual biofilms provide a protective niche in environments that are conducive to white-opaque switching (e.g. gastrointestinal tract), as a mechanism to facilitate the cryptic process of parasexual mating in *C. albicans*.

While much is known about the molecular mechanisms behind conventional biofilm formation in *C. albicans*, very little is known about sexual biofilms. Previous research has shown, through microarray studies, that the transcriptional profile of *C. albicans* forming sexual biofilms displays a curious crossover between genes involved in both conventional biofilm formation and mating<sup>24</sup>. In this work, we demonstrate that sexual biofilm formation is a conserved phenotype in *C. albicans* by screening a library of clinically isolated strains for their ability to form sexual biofilms. To begin investigating the molecular mechanisms underlying sexual biofilm formation, we present the first full transcriptomic profile of *C. albicans* strains forming sexual biofilms by performing RNA-sequencing on this library of clinical isolates. Using a comparative analysis between the transcriptional profiles of the clinical isolates, we generate a list of significantly differentially expressed genes. A subset of genes we target for deletion using a CRISPR/Cas9 system to determine their role in sexual biofilm formation. In addition, we find a sex-specific effect on sexual biofilm thickness when white and opaque cells are cultured together. These findings further our mechanistic understanding of how *C. albicans* forms sexual biofilms.

## 2.3 Results

### 2.3.1 Clinical isolate screen

Treatment of settled *C. albicans* white *MTL*-homozygous or *MTL*-hemizygous cells with mating pheromone of the opposite mating type is known to induce sexual biofilm formation<sup>23,26,27</sup>. This generally involves an increase in the adhesive properties of the cells and induces filamentation. However, not all *C. albicans* strains behave the exact same way to a given environmental stimulus<sup>29</sup>. In order to understand how individual strains form sexual biofilms and find commonalities between them, we screened 12 clinically isolated strains of various *MTL*-configurations for their ability to form sexual biofilms in response to a synthetic alpha-pheromone ( $\alpha$ -factor). These strains were taken from different regions of the body and from both diseased and healthy individuals (Supplemental Table 1). The isolates form a range of different sexual biofilm thicknesses (Figure 2.1). There was no correlation between disease status of the patient or location of the body from which the isolate was taken and thickness of sexual biofilm the isolate formed. We classified P37037, P78042 and P94015 as “weak” sexual biofilm formers as there appeared to be little response to stimulation with  $\alpha$ -factor. There was a high degree of similarity between sexual biofilms formed by P37005, P60002, P87, P75063 and P37039; these were classified as “strong” sexual biofilm formers. We classified L26 and 12C as “moderate” sexual biofilm formers because their response was in between that of the strong and weak formers.

### 2.3.2 Transcriptional profiling of sexual biofilms

The *C. albicans* genome contains approximately 6,000 protein-coding genes; nearly 20% being unique to this species<sup>30</sup>. To identify the core set of genes required for efficient sexual biofilm formation, we performed single-end 3'Tag-sequencing, a recently developed version of RNA-sequencing, on all ten *MTL-a* clinical isolates as they were treated with synthetic  $\alpha$ -factor or the DMSO vehicle<sup>31</sup>. This analysis also allowed us to probe the cause of the differences between the thickness of the sexual biofilm formed by each strain. We found that the weak strains did not have many significantly differentially expressed genes and we excluded them from further analysis. By comparing the differentially expressed genes from sexual biofilms treated with  $\alpha$ -factor and vehicle-treated samples of the moderate and strong formers, we identified several commonly differentially expressed genes between the groups and a few genes that were unique to each grouping. Grouped analysis of RNA-seq data from different strains in this fashion enables one to narrow their focus on functionally relevant differentially expressed genes, rather than strain-specific differentially expressed genes<sup>29</sup>. Using a threshold of  $\log_2 \geq 0.58$  and  $\log_2 \leq -0.58$  p-adj. value of  $\leq 0.05$ , we found 180 upregulated genes and 122 downregulated genes in the strong responders (Figure 2.2A, Supplemental Table 2). We found 161 upregulated genes and 214 downregulated genes in the moderate responders (Figure 2.2B, Supplemental Table 3). Of these genes, only 48 were commonly upregulated between moderate and strong responders; only 40 genes were commonly downregulated between the moderate and strong responders (Figure 2.2D). Among the genes that were similarly upregulated between moderate and strong responders, we see many amino acid permeases (e.g. *AAP1*, *AGP2*, *CYS3*, *GAP2*, etc.), some genes involved in mating (e.g. *FAV1*, *RAM2*, *MFA1*), and some transcription factors (e.g. *GRF10*, *TEC1*) (Supplemental Tables 2 and 3). In addition, when analyzing a combination of all moderate and strong transcriptomic profiles under  $\alpha$ -factor stimulation versus vehicle-treated conditions, we find many genes



involved in adhesion and filamentation upregulated as well (e.g. *ALS1*, *ORF19.7167*, *IHD1*, *HWP1*). Interestingly, we find *ALS1* but not *ALS3* to be upregulated.

We performed Gene Set Enrichment Analysis (GSEA) on the 3' Tag-sequencing data from an analysis combining all data from moderate and strong strains under vehicle- and pheromone-treated conditions to identify the functionally enriched pathways in sexual biofilm formation. We found many biological processes to be enriched, including but not limited to “cell adhesion” (p-adj.= .0084), “single-species biofilm formation on inanimate substrates” (p-adj. = .032), “glucose transmembrane transportation” (p-adj. = .029) and “cytogamy” (p-adj. = .018) (Figure 2.2).

In an attempt to understand the transcriptional differences between moderate and strong formers, we looked at the sets of genes that were uniquely differentially expressed between the two states. Strong responders upregulated sets of chitin synthase genes (i.e. *CHS1*, *CHS2*, *CHS8*, *CHT2*), sugar transporters (i.e. *HGT12*, *HGT13*, *HGT20*) and several ferro-reductase genes (i.e. *FRP1*, *FRP2*, *FRP3*) not found in moderate responders (Supplemental Tables 2 and 3). Together, upregulation of these genes may provide developing sexual biofilms with additional metabolic energy and construction materials for cell walls. Other genes are uniquely found to be upregulated in either moderate or strong responders that may have additional impacts on the robustness of sexual biofilm each strain was able to form. Some of these are other cell wall proteins, such as *RBT1* and *RBT5*, that may also result in a greater ability to extend hyphal cells and form more robust sexual biofilms.

### 2.3.3 Mixed population sexual biofilms

Most experiments in the field, and this dissertation, are done using pure cultures of a cells treated with synthetic  $\alpha$ -factor. This experimental scheme is due to the difficulty of working with and synthesizing **a**-factor, which is prenylated and hydrophobic. However, this does not exactly mimic the phenomenon in nature where opaque cells may be engaged in other interactions with white cells while inducing them to form sexual biofilms beyond simple pheromone stimulation. In order to probe this aspect of sexual biofilms, we mixed **a** and  $\alpha$  white and opaque cells together at equal ratios and individually. We saw that culturing any particular cell type or mating type independently failed to form a sexual biofilm (Figure 2.3A). Interestingly, mixing white cells of opposite phenotypes also failed to form a thick sexual biofilm. This is likely due to the lack of initial pheromone stimulation by opaque  $\alpha$  cells. Indeed, only  $\alpha$  opaque cells constitutively express their pheromone<sup>32</sup>. All other cell types and mating configurations require stimulation before they express their own pheromone<sup>33</sup>. Mixing opaque cells of opposite mating types appeared to result in some kind of sexual biofilm. This is likely explained by the known upregulation of adhesion genes as part of the opaque cell mating program<sup>25,34,35</sup>. Finally, we observed a mating-type dependent effect upon white and opaque cells of opposite mating-types; white **a** cells were able to form a more robust sexual biofilm when mixed with opaque  $\alpha$  cells than those formed by white  $\alpha$  cells mixed with opaque **a** cells (Figure 2.3A). This could be due in part to the hydrophobic nature of **a**-factor and an inability to disperse readily in a static assay. In addition, it could be due to the fact that **a** cells generally release very low levels of **a**-factor and require stimulation by  $\alpha$ -factor in order to release greater amounts of **a**-factor. This may result in a temporal shift in sexual biofilm initiation; a white  $\alpha$  cell would have to spontaneously switch to the opaque state where it could begin constitutive expression of  $\alpha$ -factor to stimulate white and opaque **a** cells to begin to release **a**-factor which in turn would finally stimulate the remaining white  $\alpha$  cells to form a sexual biofilm. There could

also simply be a difference in the sexual biofilm forming capabilities of white **a** cells and white  $\alpha$  cells due to some inherent difference between mating types that is yet to be revealed.

#### 2.3.4 Transcriptional profiling of mixed population sexual biofilms

Previous transcriptomics in this work were performed on pure populations of white **a** cells treated with a synthetic  $\alpha$ -factor. In addition, the co-cultures presented in Section 1.3.3 were performed at 1:1 ratios of white and opaque cells. However, in nature *C. albicans* cells are thought to predominantly exist in the white state, with the occasional opaque cell appearing unless in very precise environmental conditions. We wanted to see what the minimum percentage of a population had to be opaque in order to stimulate the majority white cells to form a sexual biofilm. This also prepared us for performing RNA-sequencing across this panel of crosses, where we want to minimize the number of opaque cells contaminating white transcriptomic profiles. When mixing white **a** cells and opaque  $\alpha$  cells, biofilm thickness seemed to decrease to an unidentifiable level when 5% or less of the population was opaque. The same effect holds for mixtures of white  $\alpha$  cells and opaque **a** cells (Figure 2.4B and 2.4C). On each cross shown in Figure 2.3A, using a population consisting of 95% the first labeled cell type crossed with 5% of the following cell type (e.g. alpha\_wh\_x\_alpha\_op; white  $\alpha$  cells would make up 95% of the population while opaque  $\alpha$  cells would make up only 5%), we performed 3' Tag-sequencing<sup>31</sup>.

We started by focusing our differential gene expression analysis between white populations crossed with opaque populations of the same and opposite mating type. Using a threshold of  $\log_2 \geq 0.58$  and  $\log_2 \leq -0.58$  p-adj. value of  $\leq 0.05$ , we found that 58 genes are upregulated and only 15 genes were downregulated when comparing the transcriptional profiles of a population of white  $\alpha$  cells mixed with opaque  $\alpha$  cells versus a population of white  $\alpha$  cells mixed with opaque **a** cells. We performed Gene Set Enrichment Analysis (GSEA) on this cross to identify the functionally enriched pathways in mixed population sexual biofilms. We found similar biological processes to be enriched in mixed populations as compared to those in clinical isolates; including but not limited to “adhesion of symbiont to host” (p-adj. = 0.01), “positive regulation of cell adhesion involved in single-species biofilm formation” (p-adj. = 0.0011), “single-species biofilm formation on inanimate substrates” (p-adj. = 0.001227), “transmembrane transport” (p-adj. = 0.000311), “proteolysis” (p-adj. = .01), and “filamentous growth of a population of unicellular organisms in response to chemical stimulus” (p-adj. = 0.023) (Figure 2.4).

Many of the differentially expressed genes identified in the clinical isolates that responded to pheromone were similarly differentially expressed in the co-culture setting (e.g. *IHD1*, *ASG7*, *ORF19.7167*, *PHR1*, *HWP1*). Interestingly, some genes were found to be specific to each setting. Notably, one such gene, *ECE1*, was found to only be upregulated in the co-cultures. *ECE1* is always an intriguing gene to identify as it is a major virulence factor of *C. albicans*<sup>36</sup>. Although this could be an artifact caused by the difference in strain backgrounds between the clinical isolates and QMY23, the co-culture base strain; this finding may also indicate that interactions between white cells and opaque cells of opposite mating types results in further differential gene expression in white cells than treatment with mating pheromone alone. Other virulence-related genes were also upregulated in this environment, such as *SAP4*, *PRA1*, *CSH1*. The upregulation of *ECE1* and other genes associated with virulence in this setting may have implications for the pathogenic capabilities of sexual biofilms *in vivo*.

### 2.3.5 Identification of functionally relevant genes involved in sexual biofilm formation

From our analyses on the 3' Tag-sequencing data of sexual biofilms formed by clinical isolates and co-cultures of white and opaque cells, we generated a list of candidate genes that we target for deletion with a markerless CRISPR/Cas9 system<sup>37</sup>. Based on their upregulation in both moderate and strong responders, we decided to delete eight target genes: *ASG7*, *IHD1*, *PTP3*, *ORF19.1725*, *ORF19.1779*, *ORF19.3932.1*, *ORF19.6200* and *ORF19.7167*. To generate a base strain in which we could generate deletion mutant strains, I deleted *MTL- $\alpha$*  from SN250 transforming it into **a/ $\Delta$** , creating APY001. All subsequent mutants were created in the APY001 background. By passaging the deletion mutant strains through our pheromone-stimulated biofilm assay, we determined that homozygous deletion of *ORF19.1725*, *ORF19.3932.1*, *ORF19.6200*, *ORF19.7167*, *ASG7*, *IHD1*, *PTP3*, resulted in an inability to produce a significant pheromone response (Figure 2.5). These results indicate that each of these genes has some function in the formation of sexual biofilms.

## 2.4 Discussion and conclusion

When looking at the transcriptional profiles of *C. albicans* clinical isolates growing under the same environmental conditions, researchers can see significant variation between the sets of genes each strain expresses. This has only recently been identified through the advancement of sequencing technologies, allowing next-generation sequencing to be done in less costly ways that enable higher throughput. Many studies to date have focused their analyses on single “reference” strains. In the case of *C. albicans*, most studies focus solely on the clinically isolated strain, SC5314, and its derivatives. Although this provides an effective way of normalizing assays across laboratories, not all strains of a given species employ the same differentially expressed genes to generate a given phenotype. Strains from the environment will generally have a unique set of point mutations dispersed throughout their genomes. If these variations happen to fall in a transcription factor’s DNA recognition sequence, it can result in dramatically different binding patterns of transcription factors along the genome; resulting in different regulons. While this variation can be difficult to interpret, by comparing transcriptional profiles across multiple strains for the same phenotype, we can determine which genes are consistently expressed across all or most strains. These are likely genes that are important to the phenotype in question. In this work, we saw that our library of clinical isolates formed sexual biofilms of varying robustness; some strains formed robust sexual biofilms, whereas others had almost no response. When comparing the transcriptomes of these strains as they respond to  $\alpha$ -factor, we saw dramatically varying differential expression patterns. We excluded the transcriptomes of the “weak” sexual biofilm formers as they had very few differentially expressed genes. However, by comparing the transcriptional profiles of the “moderate” and “strong” responders, we saw that out of the nearly 200 genes differentially expressed in each group, only 48 were differentially expressed in both groups (Figure 2.2D). These genes included an interesting mix of genes known to be involved in mating (e.g. *FAV1*, *RAM2*, *MFA1*) as well as conventional biofilm formation (e.g. *IHD1*, *XOG1*, *TEC1*)<sup>38,39</sup>. However, they lacked key members of each gene set as well.

We began identifying the contribution of each of these genes to sexual biofilm formation by individually deleting a subset of those 46 shared genes and determining the mutant’s subsequent sexual biofilm forming capability. By generating these mutants and determining their sexual biofilm forming capabilities, we can determine which genes are functionally relevant to sexual biofilms. Indeed, we identified 7 genes involved in sexual

biofilm formation: *IHD1*, *PTP3*, *ASG7*, *ORF19.1725*, *ORF19.3932.1*, *ORF19.6200*, *ORF19.7167*. *ORF19.1725* is a putative adhesin that has previously identified relevance to sexual biofilm formation<sup>40</sup> and served as a useful internal control.

*IHD1* is an uncharacterized protein that is a GPI-anchored protein whose expression is induced during hyphal development<sup>41</sup>. This gene is widely cited and is part of the core filamentation response network in *C. albicans*<sup>39,42–44</sup>. Interestingly it is not known to interfere with filamentation or adhesion upon deletion, however we are showing that it disrupts sexual biofilm formation<sup>42</sup>. GPI-anchored proteins can act as adhesins or other cell wall proteins. Perhaps we have uncovered the niche in which deletion of *ihd1* becomes functionally important for *C. albicans*. Interestingly, homologues of this protein can be found in *Candida dubliniensis* and *Candida tropicalis*<sup>41</sup> which are also capable of forming sexual biofilms in response to mating pheromone<sup>45,46</sup>.

*PTP3* is a putative tyrosine phosphatase whose expression is known to be induced in hyphal cells<sup>39,41,44,47</sup>. Previous research has shown that Ptp3, and its homologue Ptp2, are involved in hyphal development by dephosphorylating Hog1, inactivating it<sup>47</sup>. Inactive Hog1 is unable to keep the repressor, Sko1, on the promoter of *BRG1*; thus enabling Brg1 to activate its downstream regulon of filamentous genes<sup>47</sup>. Both of these transcription factors (*SKO1* and *BRG1*) are implicated in the regulation of sexual biofilms (See Chapter 3.) Our finding that deletion of *PTP3* inhibits sexual biofilm formation may indicate that Hog1 and Tor1 signaling may be involved in the regulation of sexual biofilms.

*ORF19.6200* is an uncharacterized protein that is a member of the “Pathogen-Related Yeast” (PRY) family of proteins. These are secreted sterol-binding proteins originally identified in *Saccharomyces cerevisiae*<sup>48</sup>. Interestingly, several of these proteins have been identified in *C. albicans* earning the title: CaPRY family of proteins<sup>49</sup>. Of the five identified CaPRY members, *ORF19.6200*, *ORF19.2787*, *ORF19.2336*, *RBE1* and *RBT4*, only *ORF19.6200* and *RBT4* were upregulated in both moderate and strong responders. Interestingly, both *ORF19.6200* and *RBT4* are upregulated in white cells compared to opaque cells<sup>48</sup> and we have shown that they become more dramatically upregulated upon pheromone stimulation. Previous research has shown that *rbt4*  $\Delta/\Delta$  deletion mutant strains experience significantly reduced virulence<sup>50</sup> and that a *rbe1*  $\Delta/\Delta$  / *rbt4*  $\Delta/\Delta$  deletion mutant strain shows increased sensitivity to clearance by polymorphonuclear leukocytes<sup>48</sup>. Given the high degree of homology between CaPRY genes<sup>48</sup>, a similar mode of action may exist for their corresponding gene products and *ORF19.6200* may serve in additional roles for *C. albicans* biology beyond its involvement in sexual biofilm formation.

Very little is known about *ORF19.3932.1* beyond that it has predicted nucleic acid binding activity and it has never been referenced beyond its initial annotation on the *Candida* genome database<sup>41</sup>. Another gene we targeted, *ASG7*, also has little known about it beyond its structure containing two transmembrane domains. Its expression is specific to a cells and is known to be upregulated in response to  $\alpha$ -factor<sup>41</sup>. Future research into the structure and function of this gene with regards to sexual biofilm formation could yield helpful insights into the mechanisms underlying this complex biological process and inform us on the machinery *C. albicans* employs to form sexual biofilms.

Interestingly, *ORF19.7167* encodes a predicted adhesin-like protein<sup>51</sup> and was previously shown to not impact sexual biofilm thickness upon deletion<sup>24</sup>. Our results contradict this finding as we show that deletion of *ORF19.7167* resulted in no significant pheromone response. Although this discrepancy may be simply explained by difference in strain backgrounds, P370005<sup>24,40</sup> rather than the SN250 a/ $\Delta$  used in this work, further work will need to be done to clarify this discrepancy and the role of *ORF19.7167* in *C. albicans* sexual biofilm formation. As one of the many adhesins that the *C. albicans*

genome encodes, it may be that P370005 has additional adhesins, not expressed in SN250 that compensates for the deletion of *ORF19.7167*.

All together, our findings uncover many interesting aspects of sexual biofilm formation in *C. albicans*. Using transcriptional analyses of various clinical isolates and co-cultures of white and opaque cells we identified many genes and biological pathways that are involved in the formation of sexual biofilms. From these data we learned what kinds of factors and genes bolster *C. albicans* to form more robust sexual biofilms and generated a list of genes that may be involved in sexual biofilm formation based on their degree of differential expression or common upregulation among our datasets. By deleting these genes in a pheromone-responsive, CRISPR-competent strain of our own construction and assaying them for sexual biofilm formation, we identified several genes that appear to be important for sexual biofilm formation.

## 2.5 Materials and methods

### 2.5.1 Media

*C. albicans* strains were cultured at 25°C in YPD (2% Bacto peptone, 2% dextrose, 1% yeast extract, pH 6.8). Nourseothricin-resistant mutants were selected on YPD + NAT200 (2% Bacto peptone, 2% dextrose, 1% yeast extract, and 200 µg/ml nourseothricin (GoldBio, N-500-5)) and later grown on SD media (2% Dextrose, 6.7% YNB with ammonium sulfate, and auxotrophic supplements) without leucine to remove the NAT marker and the Cas9 and gRNA cassettes. Nourseothricin-sensitive isolates were patched on YPD and YPD + NAT400 plates (2% Bacto peptone, 2% dextrose, 1% yeast extract, supplemented with 400 µg/ml nourseothricin) as previously reported<sup>37</sup>. Sexual biofilms were grown in Lee's Medium supplemented with 1.25% glucose.

### 2.5.2 Pheromone-stimulated biofilm assay and co-culture assays

The sexual biofilm assay was performed as previously described<sup>24,51</sup>. Briefly, each well of a 12-well plate was inoculated with  $5 \times 10^7$  cells ( $OD_{600} = 2.5$ ) of an overnight culture grown in Spider to 1,000 µL of Lee's media. Synthetic *C. albicans*  $\alpha$ -factor (GFRLTNFGYFEPG; Lifetein Product) -- diluted in pure DMSO to 100 mg/mL and subsequently diluted to 10 mg/mL in sterile water before addition to wells -- was added to each well at a final concentration of 10 µg/ml (6.6 µM). Control wells were treated with .01% DMSO. Biofilms were incubated at 25°C in Elmi plate incubators for 24 hours without mechanical perturbation. Spent media was aspirated and biofilms were washed with 1,000 µL of 1xPBS. After removal of the 1xPBS wash and unadhered cells, biofilm thickness was quantified via  $OD_{600}$  using a BioTek Epoch 2 plate reader. Co-culturing experiments were performed in the same manner, but did not include  $\alpha$ -factor or the vehicle.

### 2.5.3 Strains and mutant construction

The clinical isolate library used in this work was originally published in Hirakawa et al.<sup>53</sup>. Many of these strains were naturally *a/a*. *MTL- $\alpha$*  was deleted in those clinical isolates listed as *a/Δ* in Table 1 using pJD1. QMY23 was originally published in Mitrovich et al.<sup>54</sup>. Briefly, QMY23 was generated by integration of the HIS1 and LEU2 markers at the endogenous LEU2 locus of SN87. This strain was subsequently grown on sorbose-medium to produce mating competent *a/a* and *a/α* strains<sup>55</sup>.

In order to obtain a CRISPR-competent *a/Δ* strain, I obtained SN250 which is a *LEU2 +/Δ*, *arg4 Δ/Δ* *a/α* base strain. I deleted the entire *MTL- $\alpha$*  locus using pJD1, a plasmid

that was designed to target either *MTL*-locus indiscriminately as described in Lohse et al. 2016<sup>56</sup>. I confirmed the deletion of the *MTL- $\alpha$*  locus using colony PCR and several pairs of primers targeting key genes within the *MTL- $\alpha$*  locus. Primers are listed in Supplemental Table 4. This strain, SN250  $\alpha/\Delta$ , became my base strain (APY001) for CRISPR deletions. All strains used in this study are listed in Supplemental Table 1.

Of the 48 high priority genes of interest, we constructed eight deletion mutant strains using the recently developed CRISPR method described previously<sup>37</sup>. In brief, the CRISPR/Cas9 method employs a *C. albicans* LEU2 heterozygous base strain (APY001) disrupted by the integration of a fragment that contains the Cas9 expression cassette, a nourseothricin-resistance marker (NAT), and a gRNA construct. Transformants were selected on Yeast Peptone Dextrose (YPD) plates containing nourseothricin, and the CRISPR components were removed by streaking the transformed colonies on SD lacking leucine<sup>37</sup>. Target gene deletions were verified by colony PCR using a pair of primers to confirm the integration of the donor DNA in place of the target gene and another pair of primers to confirm the absence of the gene of interest. Gel electrophoresis was performed to verify the size of the amplicons. All primers are listed in Supplemental Table 4.

#### 2.5.4 RNA-seq cell harvesting and library preparation

Growth of pheromone-stimulated biofilms was performed as described above. However, after the 1xPBS wash and removal of unadhered cells, a fresh aliquot of 1000  $\mu$ L of 1xPBS is used to resuspend the remaining adherent cells. Each sample was pooled from 5 wells of a 12-well plate into a 50 mL Falcon centrifuge tube. Two biological replicates were collected for each strain and condition. Samples were centrifuged at 4000 rpm for 5 minutes at ambient temperature. The supernatant was decanted under sterile conditions and the pellets were frozen in a -80°C freezer until their RNA was extracted. RNA was extracted using the RiboPure RNA Purification Kit for yeast (Invitrogen, Cat #AM1926). Briefly, the harvest cells were lysed in a lysis buffer on an Omni Bead beater for 5 cycles (30s on, 2 min off), >90% cell lysis was checked under the light microscope and the aqueous phase was applied to filter cartridges. Sequential washing steps and DNase treatment were carried out as per the instruction manual. Purified RNA was assessed for purity and yield using a Take3 plate in the Epoch 2 Microplate reader and stored at -80°C until further use. 500 ng total RNA was prepared for mature poly(A) RNA selection for 100 bp single-end sequencing using QuantSeq 3' mRNA-seq Library Prep Kit FWD (Lexogen, Cat #192). Samples were sequenced on an Illumina NextSeq 500 by the UC Davis Genome Center.

#### 2.5.5 Differential expression and enrichment analysis

Libraries were sequenced using Illumina NextSeq platforms. The data was mapped to *Candida albicans* SC5314 reference genome and transcript abundance was retrieved for the *C. albicans* genes using the computational workflow published by Paropkari et al., 2023<sup>57</sup>. Briefly, single-end reads were trimmed using BBDuk (BBMap version 38.18)<sup>58</sup>, aligned to the reference genome and transcript abundance was estimated using STAR (version 2.7.10a)<sup>59</sup> as mentioned in Paropkari et al., 2023<sup>57</sup>. *C. albicans* SC5314 reference genome, coding sequence annotations and Gene Ontology (GO) annotations were retrieved from the *Candida*

Genome Database (CGD)<sup>41</sup>. All statistical analyses such as identifying differentially expressed genes, estimating log<sub>2</sub> fold change values, adjusting p-values for multiple hypothesis testing and functional enrichment analysis and plots were generated using custom scripts in R (version 4.1.2). Differentially expressed genes were identified using DESeq2<sup>60</sup> and log<sub>2</sub> fold change values were estimated using the Approximate Posterior Estimation for the GLM (apeglm) method<sup>61</sup>. Statistical significance of the log<sub>2</sub> fold change of genes between conditions was estimated by adjusting p-values for multiple hypothesis testing using Independent Hypothesis Weighting (IHW)<sup>62</sup>. Genes were considered significantly differentially expressed if the IHW adjusted p-value is less than 0.05 and absolute log<sub>2</sub> fold change is greater than 0.58. Gene Set Enrichment Analysis (GSEA) was used to identify significantly differentially expressed GO functional categories<sup>63</sup>.

## 2.6 References

1. Hall-Stoodley, L., Costerton, J. W. & Stoodley, P. Bacterial biofilms: from the Natural environment to infectious diseases. *Nat. Rev. Microbiol.* **2**, 95–108 (2004).
2. Kolter, R. & Greenberg, E. P. The superficial life of microbes. *Nature* **441**, 300–302 (2006).
3. Lohse, M. B., Gulati, M., Johnson, A. D. & Nobile, C. J. Development and regulation of single- and multi-species *Candida albicans* biofilms. *Nat. Rev. Microbiol.* **16**, 19–31 (2018).
4. Gulati, M. & Nobile, C. J. *Candida albicans* biofilms: development, regulation, and molecular mechanisms. *Microbes Infect.* **18**, 310–321 (2016).
5. Nobile, C. J. & Johnson, A. D. *Candida albicans* Biofilms and Human Disease. *Annu. Rev. Microbiol.* **69**, 71–92 (2015).
6. Köhler, J. R., Casadevall, A. & Perfect, J. The Spectrum of Fungi That Infects Humans. *Cold Spring Harb. Perspect. Med.* **5**, a019273 (2015).
7. Wenzel, R. P. Nosocomial Candidemia: Risk Factors and Attributable Mortality. *Clin. Infect. Dis.* **20**, 1531–1534 (1995).
8. Rex, J. H. *et al.* Practice Guidelines for the Treatment of Candidiasis. *Clin. Infect. Dis.* **30**, 662–678 (2000).
9. Ganguly, S. & Mitchell, A. P. Mucosal biofilms of *Candida albicans*. *Curr. Opin. Microbiol.* **14**, 380–385 (2011).
10. Kumamoto, C. A. *Candida* biofilms. *Curr. Opin. Microbiol.* **5**, 608–611 (2002).
11. Kumamoto, C. A. Inflammation and gastrointestinal *Candida* colonization. *Curr. Opin. Microbiol.* **14**, 386–391 (2011).
12. Kennedy, M. J. & Volz, P. A. Ecology of *Candida albicans* gut colonization: inhibition of *Candida* adhesion, colonization, and dissemination from the gastrointestinal tract by bacterial antagonism. *Infect. Immun.* **49**, 654–663 (1985).
13. Calderone, R. A. & Fonzi, W. A. Virulence factors of *Candida albicans*. *Trends Microbiol.* **9**, 327–335 (2001).
14. Lohse, M. B. & Johnson, A. D. White-opaque switching in *Candida albicans*. *Curr. Opin. Microbiol.* **12**, 650–654 (2009).
15. Slutsky, B. *et al.* 'White-opaque transition': a second high-frequency switching system in *Candida albicans*. *J. Bacteriol.* **169**, 189–197 (1987).
16. Soll, D. R. White-opaque switching in *Candida albicans*: cell biology, regulation, and function. *Microbiol. Mol. Biol. Rev.* **0**, e00043-22 (2024).
17. Yi, S. *et al.* Alternative Mating Type Configurations (a/a versus a/a or a/a) of *Candida*

- albicans* Result in Alternative Biofilms Regulated by Different Pathways. *PLOS Biol.* **9**, e1001117 (2011).
18. Park, Y.-N., Daniels, K. J., Pujol, C., Srikantha, T. & Soll, D. R. *Candida albicans* Forms a Specialized “Sexual” as Well as “Pathogenic” Biofilm. *Eukaryot. Cell* **12**, 1120–1131 (2013).
  19. Miller, M. G. & Johnson, A. D. White-opaque switching in *Candida albicans* is controlled by mating-type locus homeodomain proteins and allows efficient mating. *Cell* **110**, 293–302 (2002).
  20. Lockhart, S. R. *et al.* In *Candida albicans*, White-Opaque Switchers Are Homozygous for Mating Type. *Genetics* **162**, 737–745 (2002).
  21. Inglis, D. O. & Sherlock, G. Ras Signaling Gets Fine-Tuned: Regulation of Multiple Pathogenic Traits of *Candida albicans*. *Eukaryot. Cell* **12**, 1316–1325 (2013).
  22. Huang, G., Huang, Q., Wei, Y., Wang, Y. & Du, H. Multiple roles and diverse regulation of the Ras/cAMP/protein kinase A pathway in *Candida albicans*. *Mol. Microbiol.* **111**, 6–16 (2019).
  23. Perry, A. M., Hernday, A. D. & Nobile, C. J. Unraveling How *Candida albicans* Forms Sexual Biofilms. *J. Fungi* **6**, 14 (2020).
  24. Lin, C.-H. *et al.* Genetic Control of Conventional and Pheromone-Stimulated Biofilm Formation in *Candida albicans*. *PLOS Pathog.* **9**, e1003305 (2013).
  25. Lockhart, S. R., Zhao, R., Daniels, K. J. & Soll, D. R.  $\alpha$ -Pheromone-Induced “Shmooing” and Gene Regulation Require White-Opaque Switching during *Candida albicans* Mating. *Eukaryot. Cell* **2**, 847–855 (2003).
  26. Daniels, K. J., Srikantha, T., Lockhart, S. R., Pujol, C. & Soll, D. R. Opaque cells signal white cells to form biofilms in *Candida albicans*. *EMBO J.* **25**, 2240–2252 (2006).
  27. Sahni, N., Yi, S., Pujol, C. & Soll, D. R. The White Cell Response to Pheromone Is a General Characteristic of *Candida albicans* Strains. *Eukaryot. Cell* **8**, 251–256 (2009).
  28. Tao, L. *et al.* White Cells Facilitate Opposite- and Same-Sex Mating of Opaque Cells in *Candida albicans*. *PLOS Genet.* **10**, e1004737 (2014).
  29. Cravener, M. V. *et al.* Reinforcement amid genetic diversity in the *Candida albicans* biofilm regulatory network. *PLOS Pathog.* **19**, e1011109 (2023).
  30. Braun, B. R. *et al.* A Human-Curated Annotation of the *Candida albicans* Genome. *PLOS Genet.* **1**, e1 (2005).
  31. Lohman, B. K., Weber, J. N. & Bolnick, D. I. Evaluation of TagSeq, a reliable low-cost alternative for RNAseq. *Mol. Ecol. Resour.* **16**, 1315–1321 (2016).
  32. Dignard, D., El-Naggar, A. L., Logue, M. E., Butler, G. & Whiteway, M. Identification and Characterization of *MFA1*, the Gene Encoding *Candida albicans*  $\alpha$ -Factor Pheromone. *Eukaryot. Cell* **6**, 487–494 (2007).
  33. Panwar, S. L., Legrand, M., Dignard, D., Whiteway, M. & Magee, Paul. T. *MFA1*, the Gene Encoding the  $\alpha$  Mating Pheromone of *Candida albicans*. *Eukaryot. Cell* **2**, 1350–1360 (2003).
  34. Costa, A. C. B. P., Omeran, R. P., Law, C., Dumeaux, V. & Whiteway, M. Signal-mediated localization of *Candida albicans* pheromone response pathway components. *G3 Genes Genomes Genetics* **11**, jkaa033 (2020).
  35. Zhao, R. *et al.* Unique Aspects of Gene Expression during *Candida albicans* Mating and Possible G1 Dependency. *Eukaryot. Cell* **4**, 1175–1190 (2005).
  36. Candidalysin: Connecting the pore forming mechanism of this virulence factor to its immunostimulatory properties - ScienceDirect. <https://www.sciencedirect.com/science/article/pii/S0021925822012728>.

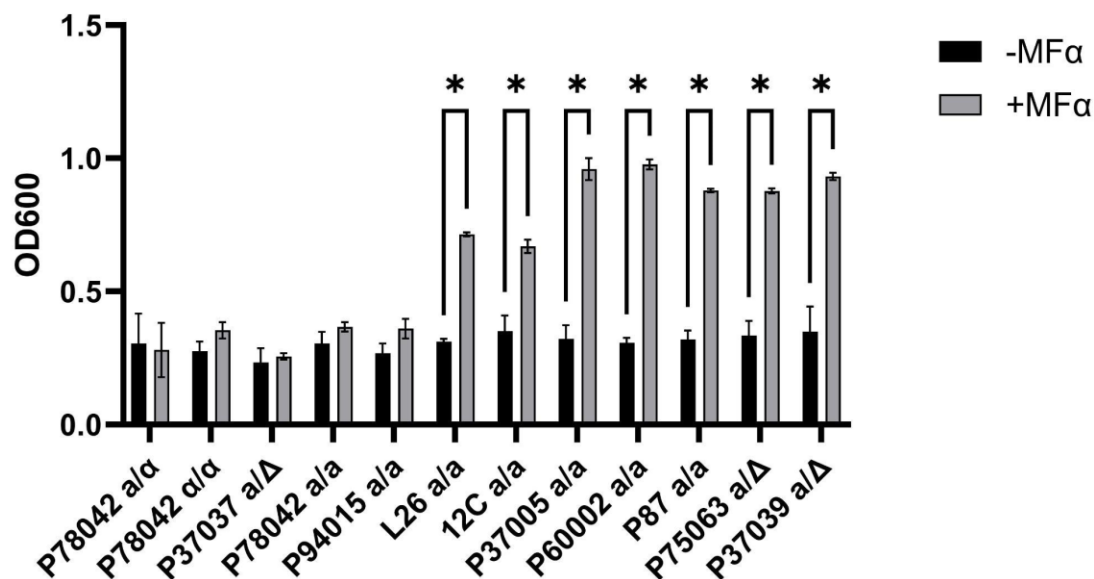


37. Nguyen, N., Quail, M. M. F. & Hernday, A. D. An Efficient, Rapid, and Recyclable System for CRISPR-Mediated Genome Editing in *Candida albicans*. *mSphere* **2**, 10.1128/mspheredirect.00149-17 (2017).
38. Bennett, R. J., Uhl, M. A., Miller, M. G. & Johnson, A. D. Identification and Characterization of a *Candida albicans* Mating Pheromone. *Mol. Cell. Biol.* **23**, 8189–8201 (2003).
39. Nobile, C. J. *et al.* A Recently Evolved Transcriptional Network Controls Biofilm Development in *Candida albicans*. *Cell* **148**, 126–138 (2012).
40. Deng, F.-S. & Lin, C.-H. Identification and characterization of *ORF19.1725*, a novel gene contributing to the white cell pheromone response and virulence-associated functions in *Candida albicans*. *Virulence* **9**, 866–878 (2018).
41. Skrzypek, M. S. *et al.* The *Candida* Genome Database (CGD): incorporation of Assembly 22, systematic identifiers and visualization of high throughput sequencing data. *Nucleic Acids Res.* **45**, D592–D596 (2017).
42. Martin, R. *et al.* A Core Filamentation Response Network in *Candida albicans* Is Restricted to Eight Genes. *PLoS ONE* **8**, e58613 (2013).
43. Kadosh, D. & Johnson, A. D. Induction of the *Candida albicans* Filamentous Growth Program by Relief of Transcriptional Repression: A Genome-wide Analysis. *Mol. Biol. Cell* **16**, 2903–2912 (2005).
44. Nantel, A. *et al.* Transcription Profiling of *Candida albicans* Cells Undergoing the Yeast-to-Hyphal Transition. *Mol. Biol. Cell* **13**, 3452–3465 (2002).
45. de Souza, C. M., dos Santos, M. M., Furlaneto-Maia, L. & Furlaneto, M. C. Adhesion and biofilm formation by the opportunistic pathogen *Candida tropicalis*: what do we know? *Can. J. Microbiol.* **69**, 207–218 (2023).
46. Alby, K., Bennett, R. Interspecies pheromone signaling promotes biofilm formation and same-sex mating in *Candida albicans*. <https://www.pnas.org/doi/epdf/10.1073/pnas.1017234108>.
47. Su, C., Lu, Y. & Liu, H. Reduced TOR signaling sustains hyphal development in *Candida albicans* by lowering Hog1 basal activity. *Mol. Biol. Cell* **24**, 385–397 (2013).
48. Choudhary, V. & Schneider, R. Pathogen-Related Yeast (PRY) proteins and members of the CAP superfamily are secreted sterol-binding proteins. *Proc. Natl. Acad. Sci. U. S. A.* **109**, 16882–16887 (2012).
49. Röhm, M. *et al.* A family of secreted pathogenesis-related proteins in *Candida albicans*. *Mol. Microbiol.* **87**, 132–151 (2013).
50. Braun, B. R., Head, W. S., Wang, M. X. & Johnson, A. D. Identification and characterization of TUP1-regulated genes in *Candida albicans*. *Genetics* **156**, 31–44 (2000).
51. Chaudhuri, R., Ansari, F. A., Raghunandan, M. V. & Ramachandran, S. FungalRV: adhesin prediction and immunoinformatics portal for human fungal pathogens. *BMC Genomics* **12**, 192 (2011).
52. Gulati, M. *et al.* *In vitro* Culturing and Screening of *Candida albicans* Biofilms. *Curr. Protoc. Microbiol.* **50**, e60 (2018).
53. Hirakawa, M. P. *et al.* Genetic and phenotypic intra-species variation in *Candida albicans*. *Genome Res.* **25**, 413–425 (2015).
54. Mitrovich, Q. M., Tuch, B. B., Guthrie, C. & Johnson, A. D. Computational and experimental approaches double the number of known introns in the pathogenic yeast *Candida albicans*. *Genome Res.* **17**, 492–502 (2007).
55. Magee, B. B. & Magee, P. T. Induction of Mating in *Candida albicans* by Construction

- of MTL $\alpha$  and MTL $\beta$  Strains. *Science* **289**, 310–313 (2000).
56. Lohse, M. B. *et al.* Systematic Genetic Screen for Transcriptional Regulators of the *Candida albicans* White-Opaque Switch. *Genetics* **203**, 1679–1692 (2016).
  57. Paropkari, A. D., Bapat, P. S., Sindi, S. S. & Nobile, C. J. A Computational Workflow for Analysis of 3' Tag-Seq Data. *Curr. Protoc.* **3**, e664 (2023).
  58. Bushnell, B. *BBMap: A Fast, Accurate, Splice-Aware Aligner*. <https://www.osti.gov/biblio/1241166> (2014).
  59. Dobin, A. *et al.* STAR: ultrafast universal RNA-seq aligner. *Bioinformatics* **29**, 15–21 (2013).
  60. Love, M. I., Huber, W. & Anders, S. Moderated estimation of fold change and dispersion for RNA-seq data with DESeq2. *Genome Biol.* **15**, 550 (2014).
  61. Zhu, A., Ibrahim, J. G. & Love, M. I. Heavy-tailed prior distributions for sequence count data: removing the noise and preserving large differences. *Bioinformatics* **35**, 2084–2092 (2019).
  62. Ignatiadis, N., Klaus, B., Zaugg, J. B. & Huber, W. Data-driven hypothesis weighting increases detection power in genome-scale multiple testing. *Nat. Methods* **13**, 577–580 (2016).
  63. Subramanian, A. *et al.* Gene set enrichment analysis: A knowledge-based approach for interpreting genome-wide expression profiles. *Proc. Natl. Acad. Sci.* **102**, 15545–15550 (2005).

## 2.7 Figures

A.



B.

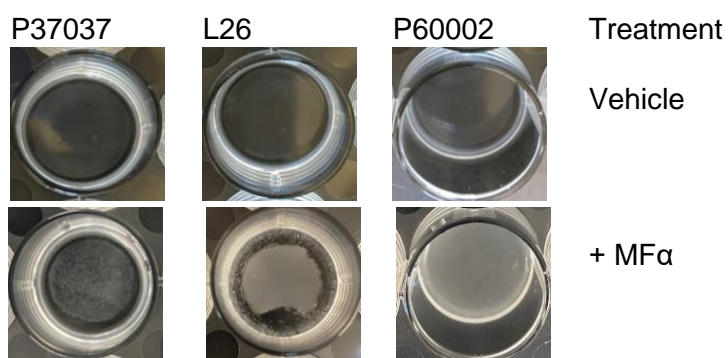
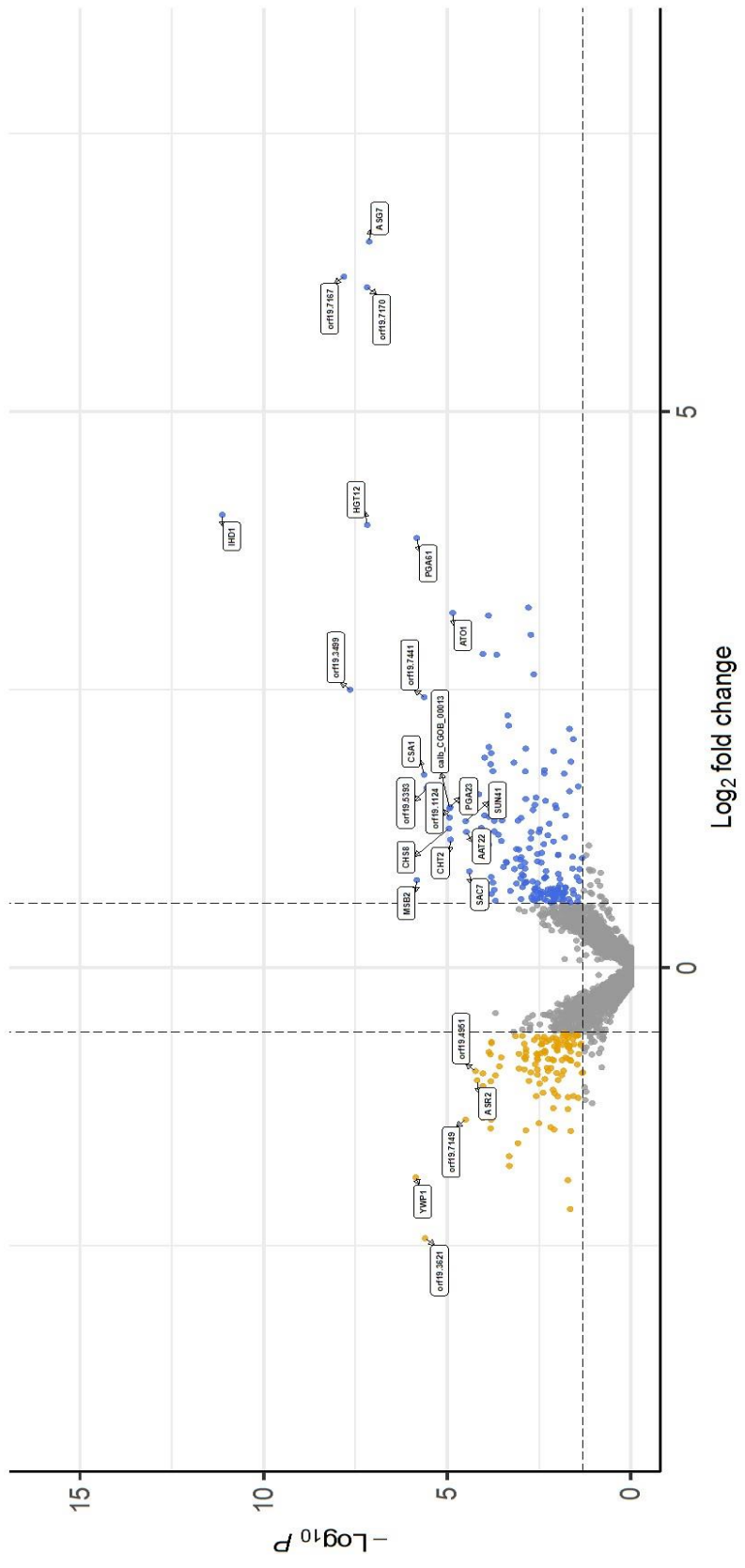


**Figure 2.1 Sexual biofilm formation by clinically isolated strains.** Sexual biofilm thickness, as determined by optical density using 600nm light, of clinically isolated strains in Lee's + glucose alone and in the presence of 10  $\mu\text{g/ml}$   $\alpha$ -pheromone. Averages and standard deviations are taken from one biological replicate and three technical replicates. Significance comparisons are relative to untreated control samples and were determined using student's paired one-tailed t-tests assuming unequal variance in GraphPad, for  $p \leq$

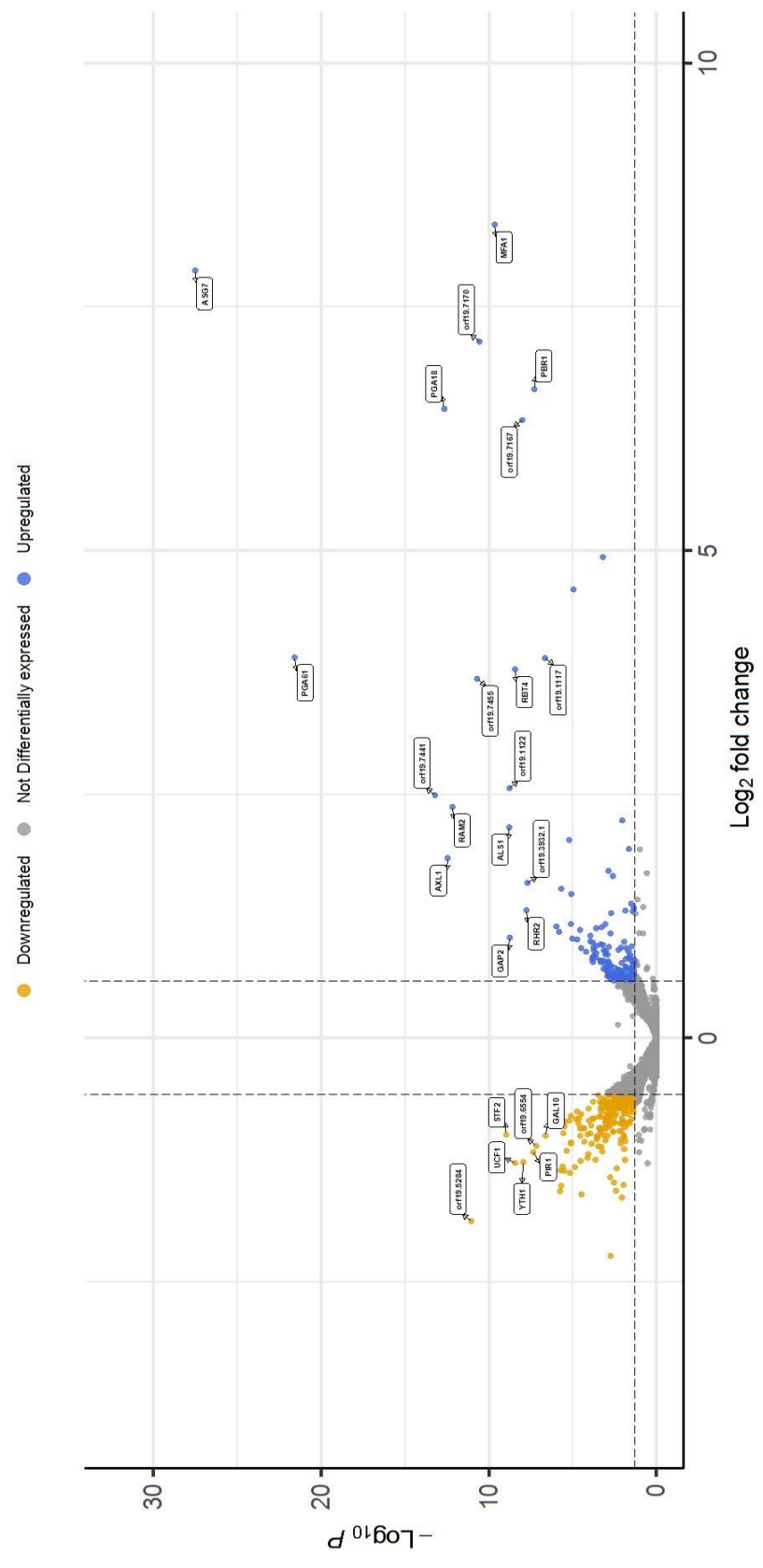
.001 (\*).

A.

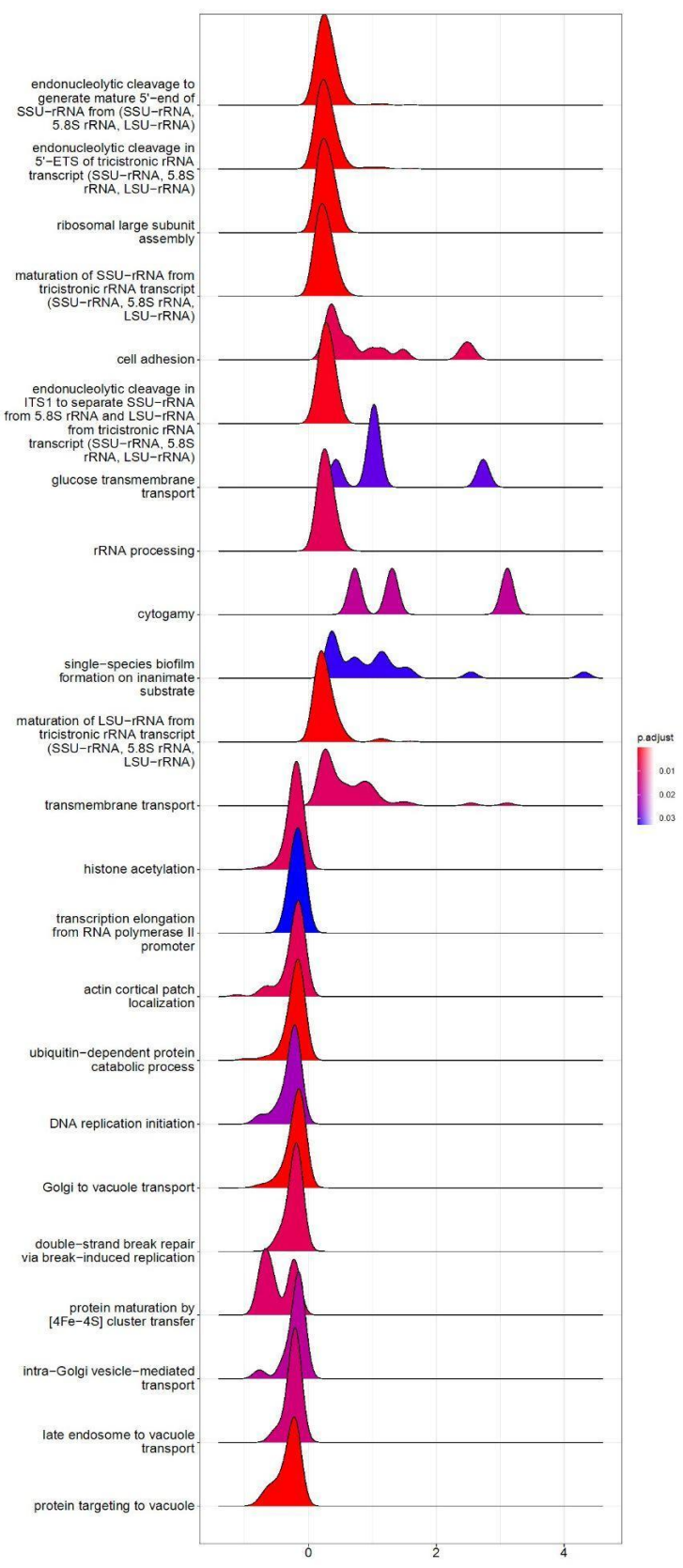
● Downregulated ● Not Differentially expressed ● Upregulated



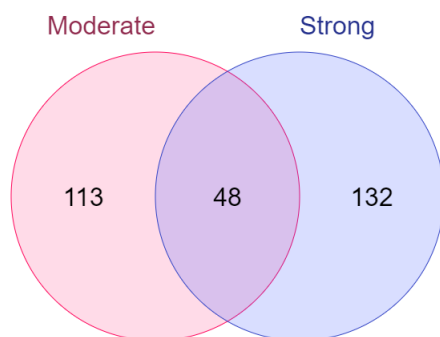
B.



C.



D.



E.

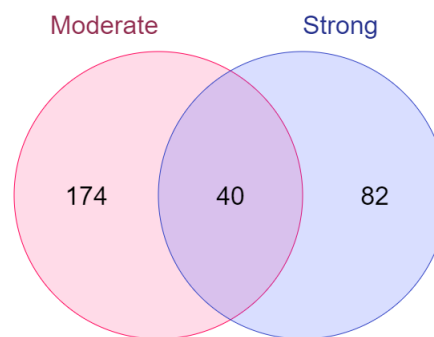
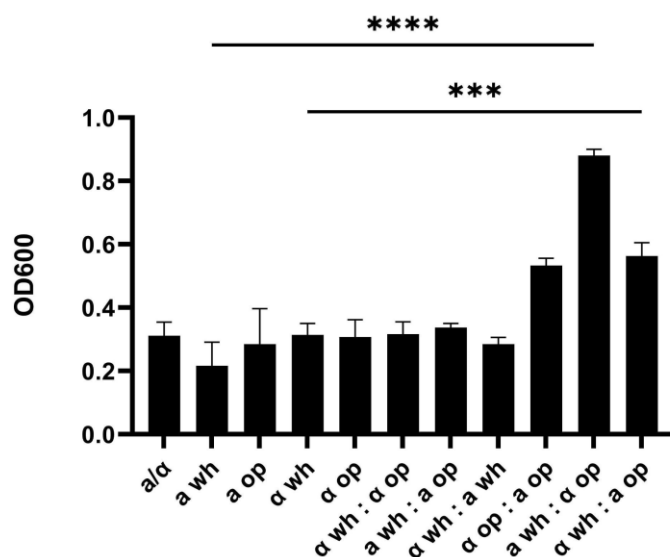
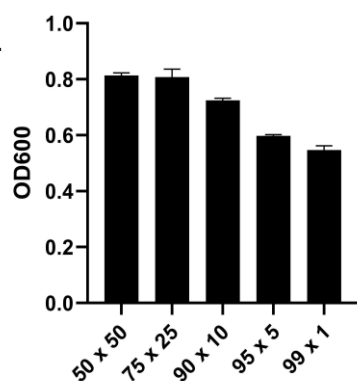


**Figure 2.2 Transcriptional analysis of clinical isolates responding to synthetic mating pheromone.** (A) Volcano plot depicting significantly differentially expressed genes in clinical isolates categorized as “strong” responders. (B) Volcano plot depicting significantly differentially expressed genes in clinical isolates categorized as “moderate” responders. (C) Gene ontology analysis presented as a ridgeplot. Data was taken from both “moderate” and “strong” responders. Distance along the x-axis of a curve represents the degree of differential expression. Height of each curve represents the number of genes of a given gene ontology annotation at a particular differential expression level. (D) Venn diagram of significantly upregulated genes between moderate and strong responders. Threshold of  $\log_2 \geq 0.58$ , p-adj. value of  $\leq 0.05$ . (E) Venn diagram of significantly downregulated genes between moderate and strong responders. Threshold of  $\log_2 \text{FC} \leq -0.58$ , p-adj. value of  $\leq 0.05$ .

A.



B.



C.

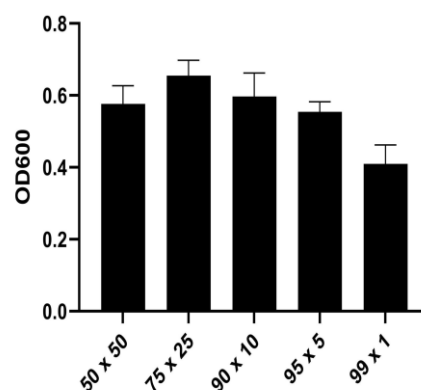
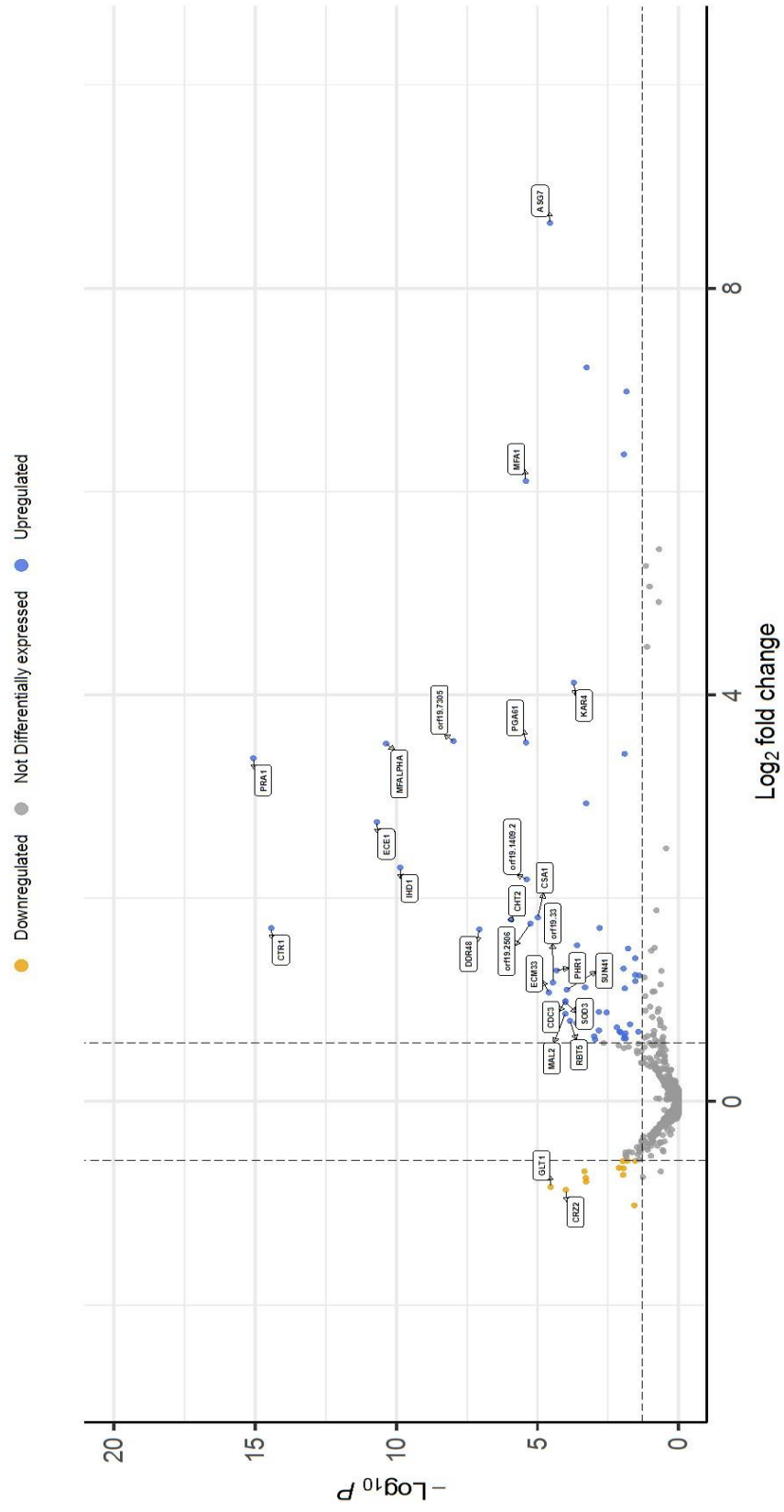


**Figure 2.3 Sexual biofilms formed by co-cultures of white and opaque cells.** (A) Thickness of sexual biofilms, as measured by optical density with 600nm light, of co-cultures of white and opaque cells of each mating type as they grow together in 1:1 ratios, or independently. Significance comparisons are relative to white strains alone and were determined using one-way ANOVA statistics in GraphPad, for  $p \leq .001$  (\*\*\*) and  $p \leq .0001$  (\*\*\*\*) (B) Thickness of sexual biofilms composed of white a cells mixed with opaque  $\alpha$  cells at defined ratios as measured by optical density with 600nm light. (C) Thickness of sexual biofilms composed of white  $\alpha$  cells mixed with opaque a cells at defined ratios as measured by optical density with 600nm light.



A.



B.

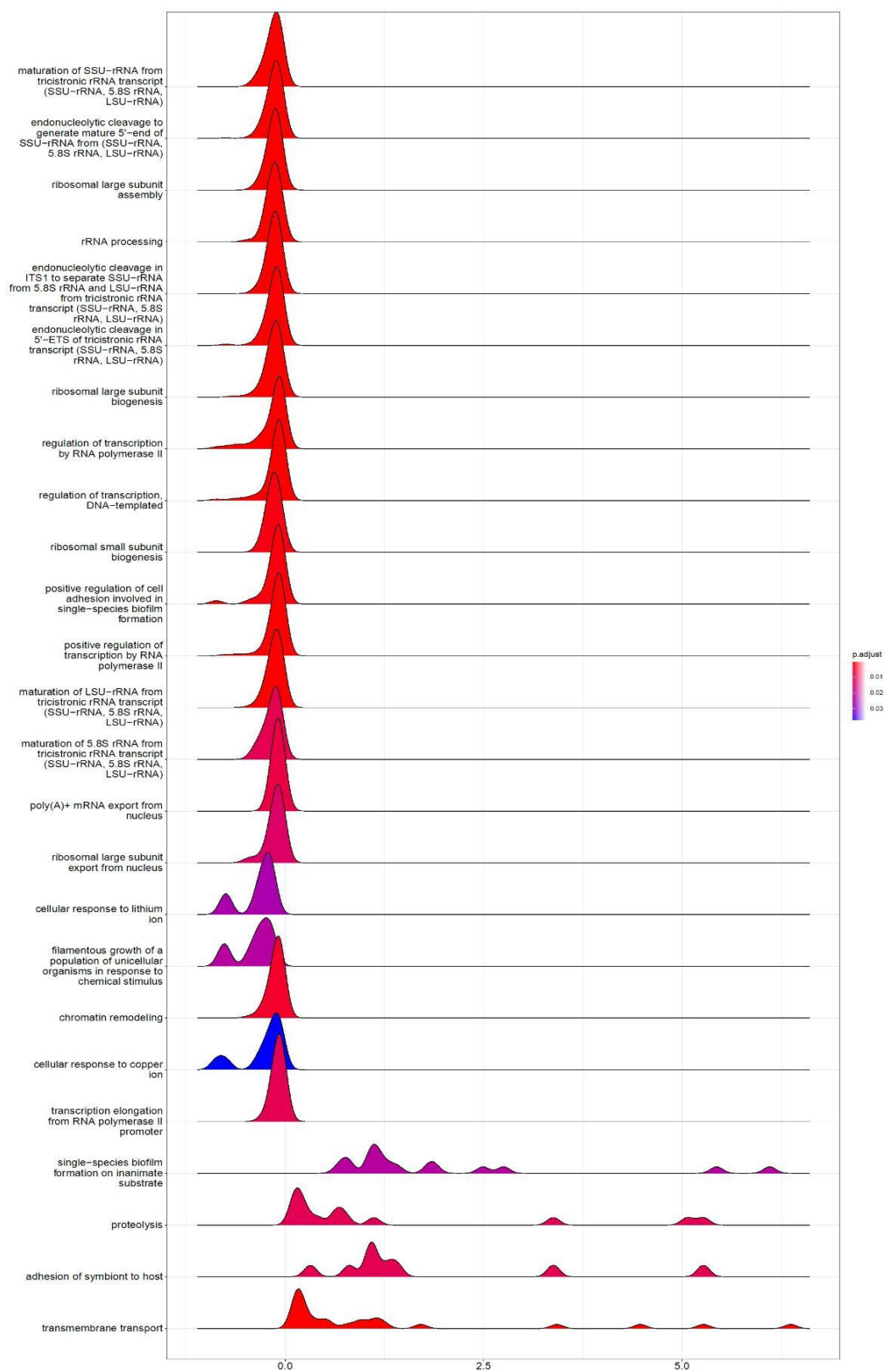


**Figure 2.4 Transcriptional analysis of sexual biofilms formed by co-cultures of white and opaque cells.** (A) Volcano plot depicting significantly differentially expressed genes in co-cultures of alpha white cells and a opaque cells compared to co-cultures of.alpha white cells and alpha opaque cells. (B) Gene ontology analysis presented as a ridgeplot. Distance along the x-axis of a curve represents the degree of differential expression. Height of each curve represents the number of genes of a given gene ontology annotation at a particular differential expression level.

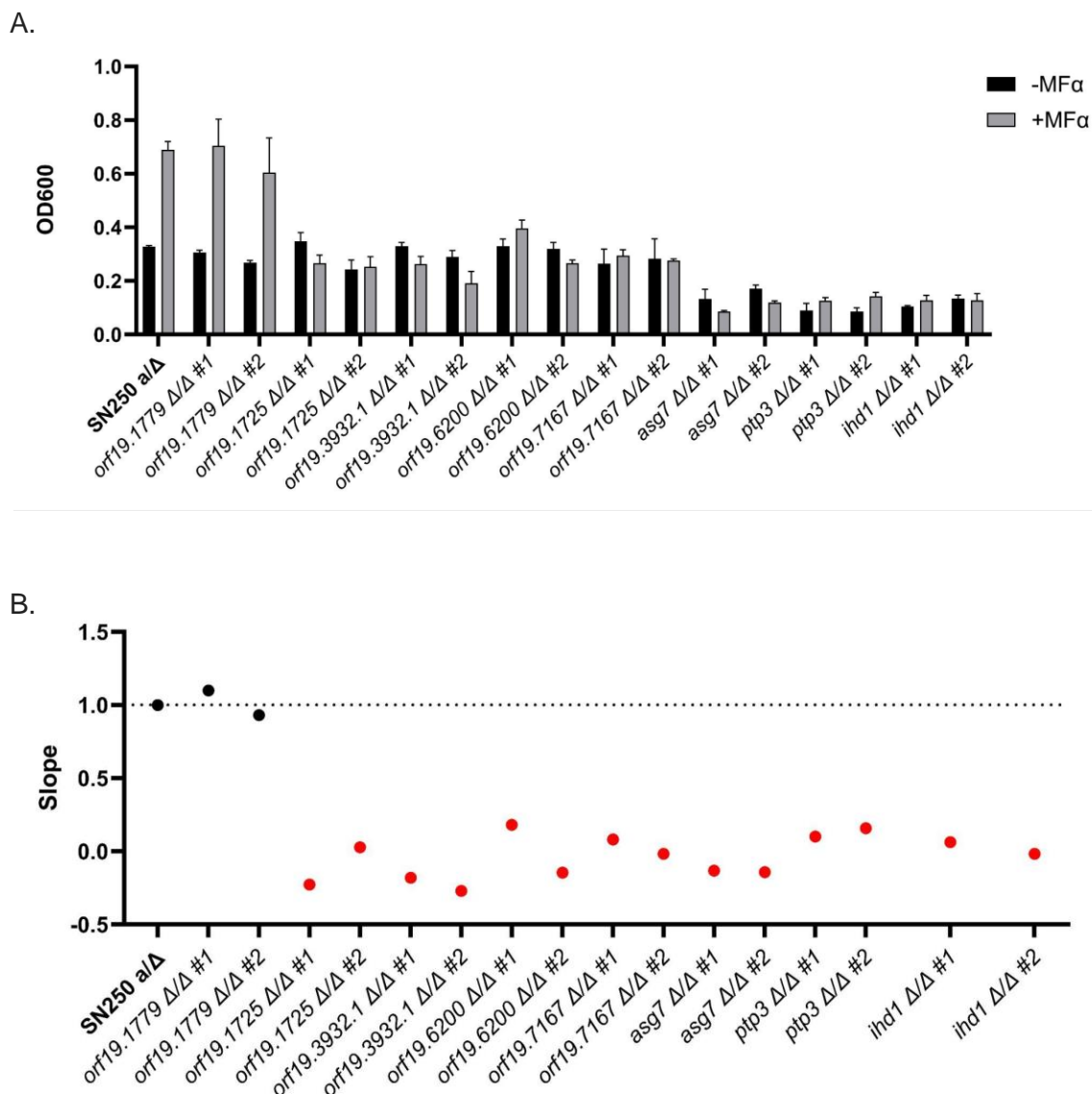


**Figure 2.5 Sexual biofilm formation by gene deletion mutant strains.** (A) Sexual biofilm thickness, as determined by optical density using 600nm light, in Lee's + glucose alone and in the presence of 10  $\mu\text{g/ml}$   $\alpha$ -factor. Averages and standard deviations are taken from one biological replicate and three technical replicates. (B) Each dot represents a normalized value for the difference in  $\text{OD}_{600}$  between treatment conditions of a deletion mutant strain divided by the difference in  $\text{OD}_{600}$  between treatment conditions of the wild-type strain (dotted line). Statistical significance was confirmed using an ANCOVA analysis of each strain normalized to the wildtype ( $p \leq .0001$ ). The wild-type strain and non-significant strains are depicted as black dots. Significant strains are depicted as red dots. Statistics and graph creation were performed in GraphPad Prism.

**Supplemental Table 2.1:** List of strains.

<b>Strain</b>	<b>MTL</b>	<b>Base strain</b>
P78042	a/α	clinical isolate
P78042	a/a	clinical isolate
P78042	α/α	clinical isolate
P37037	a/Δ	clinical isolate
P94015	a/a	clinical isolate
L26	a/a	clinical isolate
12C	a/a	clinical isolate
P37005	a/a	clinical isolate
P60002	a/a	clinical isolate
P87	a/a	clinical isolate
P75063	a/Δ	clinical isolate
P37039	a/Δ	clinical isolate
QMY23	a/α	
QMY23	a/a	QMY23 a/α
QMY23	α/α	QMY23 a/α
APY001	a/Δ	SN250
<i>orf19.1779</i> Δ/Δ #1	a/Δ	APY001
<i>orf19.1779</i> Δ/Δ #2	a/Δ	APY001
<i>orf19.1725</i> Δ/Δ #1	a/Δ	APY001
<i>orf19.1725</i> Δ/Δ #2	a/Δ	APY001
<i>orf19.3932.1</i> Δ/Δ #1	a/Δ	APY001
<i>orf19.3932.1</i> Δ/Δ #2	a/Δ	APY001
<i>orf19.6200</i> Δ/Δ #1	a/Δ	APY001
<i>orf19.6200</i> Δ/Δ #2	a/Δ	APY001
<i>orf19.7167</i> Δ/Δ #1	a/Δ	APY001
<i>orf19.7167</i> Δ/Δ #2	a/Δ	APY001
<i>asg7</i> Δ/Δ #1	a/Δ	APY001
<i>asg7</i> Δ/Δ #2	a/Δ	APY001
<i>ptp3</i> Δ/Δ #1	a/Δ	APY001

<i>ptp3</i> $\Delta/\Delta$ #2	<i>a</i> / $\Delta$	APY001
<i>ihd1</i> $\Delta/\Delta$ #1	<i>a</i> / $\Delta$	APY001
<i>ihd1</i> $\Delta/\Delta$ #2	<i>a</i> / $\Delta$	APY001

**Supplemental Table 2.2:** List of significantly upregulated genes in moderate and strong responders (threshold:  $\log_2 \geq 0.58$ , p-adj. value  $\leq 0.05$ ).

Moderate		Strong	
Gene	$\log_2$ Fold Change	Gene	$\log_2$ Fold Change
<i>AAF1</i>	0.61784942	<i>AAP1</i>	0.811117
<i>AAP1</i>	1.65911357	<i>AAT22</i>	1.216449
<i>ADR1</i>	0.67898399	<i>ACS1</i>	0.721217
<i>AGP2</i>	0.95232622	<i>AGP2</i>	0.755578
<i>ALD5</i>	0.63016453	<i>AHR1</i>	1.186781
<i>ALS1</i>	2.15966846	<i>ALD6</i>	0.808688
<i>ANT1</i>	1.04657093	<i>ARD</i>	1.179718
<i>ARG8</i>	0.64747064	<i>ARO10</i>	0.70596
<i>ASG7</i>	7.87219188	<i>ARP4</i>	0.717597
<i>ATS1</i>	0.68964319	<i>ASG7</i>	6.524768
<i>AXL1</i>	1.8432383	<i>ATO1</i>	3.187456
<i>BRG1</i>	0.82482902	<i>ATO2</i>	1.966835
<i>BUD23</i>	0.63067605	<i>BET2</i>	0.582884
<i>CAN2</i>	0.79100496	<i>calb_CGOB_00013</i>	1.429248
<i>CAR1</i>	1.14084417	<i>calb_CGOB_00017</i>	0.882966
<i>CIS2</i>	0.67959696	<i>CDC5</i>	0.769972
<i>CNT</i>	0.69994749	<i>CDG1</i>	0.906471
<i>CPP1</i>	0.80033551	<i>CFL11</i>	2.816654
<i>CRC1</i>	0.58327233	<i>CHS1</i>	0.983796
<i>CTA8</i>	1.01620816	<i>CHS2</i>	1.215361
<i>CTN1</i>	0.74845819	<i>CHS8</i>	1.24724

<i>CYS3</i>	0.66249868	<i>CHT2</i>	1.147368
<i>CZF1</i>	0.72507257	<i>CIT1</i>	0.59145
<i>DBP3</i>	0.66451628	<i>CRH11</i>	0.86612
<i>DIP2</i>	0.6212683	<i>CSA1</i>	1.731561
<i>DOT6</i>	0.82420971	<i>CSA2</i>	0.630866
<i>DRS1</i>	0.72043225	<i>CYS3</i>	0.699334
<i>ENA2</i>	0.93699831	<i>DAL1</i>	0.673577
<i>FAV1</i>	4.59873562	<i>DBP2</i>	0.678491
<i>FAV2</i>	1.29740503	<i>DEF1</i>	1.012888
<i>FRP3</i>	0.85784524	<i>DES1</i>	0.709538
<i>GAP2</i>	1.028557	<i>DIP5</i>	0.659614
<i>GLY1</i>	0.62456004	<i>DPP3</i>	0.65546
<i>GPX2</i>	1.37462312	<i>ENA2</i>	0.951563
<i>GRF10</i>	0.99025229	<i>ERG10</i>	0.613049
<i>GUT1</i>	0.8825107	<i>FAV1</i>	3.161961
<i>GUT2</i>	0.7029357	<i>FET34</i>	1.103792
<i>HAS1</i>	0.60209975	<i>FRP1</i>	0.697149
<i>HGT10</i>	1.07058411	<i>FRP2</i>	0.801419
<i>ICL1</i>	0.92002861	<i>FRP3</i>	0.98977
<i>IFG3</i>	0.89702422	<i>FTR1</i>	0.642437
<i>LTV1</i>	0.60909048	<i>GAP2</i>	0.666754
<i>MEP1</i>	0.81944898	<i>GCV2</i>	0.648287
<i>MET1</i>	0.72966513	<i>GDH2</i>	0.824702
<i>MET3</i>	1.47497944	<i>GIT1</i>	1.456822



<i>MFA1</i>	8.34363311	<i>GIT2</i>	1.017207
<i>MNN14</i>	0.90279546	<i>GPX2</i>	1.764695
<i>MNN22</i>	0.68589669	<i>GRF10</i>	0.661595
<i>MP65</i>	0.65868849	<i>GUK1</i>	0.686119
<i>MUP1</i>	0.9584603	<i>GUT1</i>	0.653875
<i>NAR1</i>	0.58263823	<i>HGT10</i>	0.995273
<i>NCE103</i>	0.88478917	<i>HGT12</i>	3.977432
<i>NOC4</i>	0.92439451	<i>HGT13</i>	1.414633
<i>NOG2</i>	0.61096679	<i>HGT20</i>	1.222012
<i>NOP4</i>	0.66017471	<i>HHF22</i>	0.662182
<i>NSA1</i>	0.60135263	<i>HMX1</i>	0.941384
<i>NTH1</i>	0.62389569	<i>HPA2</i>	0.840821
<i>ORF19.107</i>	0.64144415	<i>HSP31</i>	1.526229
<i>ORF19.1117</i>	3.89609572	<i>HTS1</i>	0.614222
<i>ORF19.1122</i>	2.56184066	<i>ICL1</i>	0.642721
<i>ORF19.1200</i>	0.58433064	<i>IDI1</i>	0.629351
<i>ORF19.1404</i>	0.62089971	<i>IDP2</i>	1.191898
<i>ORF19.1409.2</i>	1.93786673	<i>IFG3</i>	0.947287
<i>ORF19.1461</i>	0.65751982	<i>IHD1</i>	4.069974
<i>ORF19.1473</i>	1.10594784	<i>IPT1</i>	1.106869
<i>ORF19.1578</i>	0.65244506	<i>LIG4</i>	0.688176
<i>ORF19.1584</i>	0.77913376	<i>MAL2</i>	1.215745
<i>ORF19.1757</i>	0.7362066	<i>MAL31</i>	1.291167
<i>ORF19.1857</i>	0.75889936	<i>MFA1</i>	3.234316

<i>ORF19.2457</i>	2.230223	<i>MNN12</i>	0.599559
<i>ORF19.2529.1</i>	1.2785151	<i>MNN14</i>	0.941827
<i>ORF19.2691</i>	0.65306148	<i>MSB2</i>	0.784864
<i>ORF19.2891</i>	0.67364719	<i>MUM2</i>	0.673241
<i>ORF19.2934</i>	0.79015694	<i>NGT1</i>	1.343053
<i>ORF19.3089</i>	0.65127422	<i>NMA111</i>	0.760564
<i>ORF19.3309</i>	0.58054218	<i>OPT4</i>	1.166104
<i>ORF19.3337</i>	1.16833984	<i>ORF19.1122</i>	1.744799
<i>ORF19.341</i>	0.63291155	<i>ORF19.1124</i>	1.346043
<i>ORF19.3444</i>	1.30543391	<i>ORF19.1394</i>	0.801704
<i>ORF19.3547</i>	0.77667811	<i>ORF19.1403</i>	0.581483
<i>ORF19.3666</i>	0.6431878	<i>ORF19.1414</i>	0.631876
<i>ORF19.3684</i>	1.12314879	<i>ORF19.1473</i>	1.071526
<i>ORF19.3778</i>	0.62645227	<i>ORF19.1584</i>	0.940806
<i>ORF19.3804</i>	0.6198258	<i>ORF19.1626</i>	0.70599
<i>ORF19.3932.1</i>	1.59005944	<i>ORF19.1830</i>	2.14414
<i>ORF19.4241</i>	0.69912288	<i>ORF19.1959</i>	0.660822
<i>ORF19.4273</i>	0.78818379	<i>ORF19.21</i>	0.796631
<i>ORF19.4446</i>	0.67068342	<i>ORF19.2457</i>	2.173177
<i>ORF19.4479</i>	0.75099521	<i>ORF19.2459</i>	0.98259
<i>ORF19.4629</i>	0.68827349	<i>ORF19.2460</i>	2.050484
<i>ORF19.4793</i>	0.64616747	<i>ORF19.2506</i>	1.422538
<i>ORF19.494</i>	0.77909366	<i>ORF19.2638</i>	1.626274
<i>ORF19.5020</i>	0.80896561	<i>ORF19.2653</i>	0.598764

<i>ORF19.5277</i>	0.58963024	<i>ORF19.2671</i>	0.62515
<i>ORF19.5438</i>	0.67656765	<i>ORF19.3110</i>	0.660271
<i>ORF19.6054</i>	0.83922862	<i>ORF19.3309</i>	0.96805
<i>ORF19.6200</i>	4.93107919	<i>ORF19.341</i>	1.135393
<i>ORF19.6234</i>	0.66339624	<i>ORF19.3499</i>	2.496063
<i>ORF19.6484</i>	0.82254978	<i>ORF19.3518</i>	0.762389
<i>ORF19.6660</i>	0.77791635	<i>ORF19.3643</i>	2.265222
<i>ORF19.6713</i>	0.79974663	<i>ORF19.3684</i>	0.666154
<i>ORF19.6754</i>	0.642756	<i>ORF19.3737</i>	0.887839
<i>ORF19.6899</i>	0.65996943	<i>ORF19.376</i>	1.926044
<i>ORF19.6920</i>	0.70488398	<i>ORF19.3932.1</i>	1.241553
<i>ORF19.6983</i>	0.89363733	<i>ORF19.3982</i>	1.316956
<i>ORF19.7020</i>	0.97608898	<i>ORF19.4011</i>	1.430322
<i>ORF19.7167</i>	6.33714305	<i>ORF19.4225.1</i>	0.66697
<i>ORF19.7170</i>	7.14246114	<i>ORF19.4240</i>	0.702782
<i>ORF19.7422</i>	0.64786977	<i>ORF19.4241</i>	0.697426
<i>ORF19.7427</i>	0.67090473	<i>ORF19.4246</i>	0.613437
<i>ORF19.7441</i>	2.48865883	<i>ORF19.4349</i>	1.061943
<i>ORF19.7455</i>	3.68261557	<i>ORF19.4391</i>	0.887858
<i>ORF19.7566</i>	0.59073128	<i>ORF19.4445</i>	0.882785
<i>ORF19.780</i>	0.92018196	<i>ORF19.4735</i>	0.809431
<i>ORF19.787</i>	0.68960368	<i>ORF19.4805</i>	1.319068
<i>ORF19.804</i>	0.69138846	<i>ORF19.5136</i>	0.693853
<i>ORF19.813</i>	0.65072995	<i>ORF19.5288.1</i>	0.973224

<i>OSM2</i>	1.08544491	<i>ORF19.5353</i>	0.60412
<i>PBR1</i>	6.65390669	<i>ORF19.5391</i>	0.590794
<i>PEL1</i>	0.94339599	<i>ORF19.5393</i>	1.610328
<i>PGA18</i>	6.45215482	<i>ORF19.5438</i>	0.648006
<i>PGA42</i>	0.58956582	<i>ORF19.5517</i>	1.459186
<i>PGA61</i>	3.90222813	<i>ORF19.5564</i>	0.902116
<i>PHO89</i>	0.79946435	<i>ORF19.5799</i>	0.659803
<i>PHR1</i>	1.5287977	<i>ORF19.6200</i>	2.635374
<i>POP3</i>	0.58865552	<i>ORF19.6273</i>	1.58199
<i>PRP3</i>	0.88227045	<i>ORF19.6398</i>	1.826375
<i>PTP3</i>	0.93306325	<i>ORF19.6484</i>	1.980731
<i>RAD9</i>	0.70772381	<i>ORF19.6526</i>	0.60589
<i>RAM2</i>	2.36732288	<i>ORF19.670.2</i>	0.60598
<i>RAT1</i>	0.79347682	<i>ORF19.6920</i>	0.718039
<i>RBT4</i>	3.77988093	<i>ORF19.7020</i>	0.991107
<i>RHR2</i>	1.30918913	<i>ORF19.7167</i>	6.21051
<i>RIO2</i>	0.72242824	<i>ORF19.7170</i>	6.1146
<i>ROD1</i>	0.64136384	<i>ORF19.7270</i>	0.693339
<i>RPA34</i>	0.59636528	<i>ORF19.7305</i>	1.556406
<i>RPL7</i>	0.62096639	<i>ORF19.7437</i>	0.618548
<i>RRN11</i>	0.61203709	<i>ORF19.7441</i>	2.428966
<i>RRP15</i>	0.62719527	<i>ORF19.7455</i>	1.742835
<i>RTA2</i>	0.62284639	<i>ORF19.7566</i>	0.743297
<i>SAC7</i>	0.62839376	<i>ORF19.867</i>	0.977941

<i>SAP30</i>	1.71235465	<i>OSM2</i>	0.613788
<i>SAP5</i>	1.33052611	<i>PBR1</i>	2.989606
<i>SDA1</i>	0.601537	<i>PGA18</i>	2.810681
<i>SFC1</i>	0.86731766	<i>PGA23</i>	1.440362
<i>SIT1</i>	0.76903699	<i>PGA31</i>	1.840865
<i>SKN1</i>	0.70830997	<i>PGA61</i>	3.860527
<i>SRP40</i>	1.00788925	<i>PGA7</i>	1.059069
<i>SUL2</i>	0.84907358	<i>PGM2</i>	0.68695
<i>TBF1</i>	0.73285938	<i>PHO84</i>	0.776558
<i>TEC1</i>	1.16514276	<i>PHO88</i>	0.695917
<i>TRY6</i>	0.98442492	<i>PHO89</i>	1.497549
<i>TSR1</i>	0.5863441	<i>PHR1</i>	1.88582
<i>UTP18</i>	0.70754135	<i>PIN3</i>	0.613973
<i>UTP8</i>	0.59128933	<i>PLC2</i>	0.772306
<i>WOR2</i>	0.85180774	<i>PUT2</i>	1.009591
<i>XOG1</i>	2.02889713	<i>RAM2</i>	1.029296
<i>XUT1</i>	0.67791625	<i>RBT1</i>	1.771865
<i>YMX6</i>	1.13472481	<i>RBT4</i>	1.943037
<i>YTA6</i>	0.68688194	<i>RBT5</i>	1.253313
<i>ZCF26</i>	0.92556509	<i>RHD3</i>	0.600417
		<i>SAC7</i>	0.862599
		<i>SAP30</i>	1.364211
		<i>SEF1</i>	0.812683
		<i>SFC1</i>	0.837012

		<i>SOD5</i>	1.514948
		<i>SPE2</i>	0.661154
		<i>SPR28</i>	0.705066
		<i>STE2</i>	1.366076
		<i>SUN41</i>	1.313101
		<i>SUT1</i>	1.761934
		<i>TEC1</i>	1.156822
		<i>TOS1</i>	0.757138
		<i>UAP1</i>	1.354255
		<i>UME6</i>	1.848919
		<i>URA4</i>	0.753118
		<i>WOR3</i>	1.319012
		<i>XOG1</i>	1.130826
		<i>YNK1</i>	0.719182
		<i>ZCF31</i>	0.592108

**Supplemental Table 2.3:** List of significantly downregulated genes in moderate and strong responders (threshold:  $\log_2 \leq -0.58$ , p-adj. value  $\leq 0.05$ ).

Moderate		Strong	
Gene	$\log_2$ Fold Change	Gene	$\log_2$ Fold Change
<i>ORF19.5284</i>	-1.882012397	<i>YWP1</i>	-1.888272769
<i>STF2</i>	-0.9934104121	<i>ORF19.3621</i>	-2.436370811
<i>UCF1</i>	-1.286971366	<i>ORF19.7149</i>	-1.369872978
<i>YTH1</i>	-1.273375352	<i>ORF19.4951</i>	-0.9324194173
<i>PIR1</i>	-1.173474287	<i>ASR2</i>	-1.015000088
<i>ORF19.6554</i>	-1.109292776	<i>ORF19.5621</i>	-0.9539586876
<i>GAL10</i>	-1.004337441	<i>NRG1</i>	-1.066573974
<i>ORF19.5069</i>	-1.293122532	<i>ORF19.2175</i>	-1.357225032
<i>TIM22</i>	-1.337492873	<i>ORF19.3048</i>	-0.7624633521
<i>IFD6</i>	-1.280166331	<i>PGA42</i>	-0.7827013882
<i>RNR1</i>	-1.575514148	<i>BIO32</i>	-1.025287363
<i>ORF19.1052</i>	-1.36122929	<i>IFD6</i>	-1.448876954
<i>HHT21</i>	-1.518700873	<i>ORF19.7285</i>	-0.673161377
<i>ORF19.1691</i>	-1.321231768	<i>NBP35</i>	-0.6810128955
<i>ORF19.3302</i>	-0.9773437333	<i>TRX2</i>	-1.370224
<i>ZRT2</i>	-1.36535158	<i>GPM2</i>	-0.9712438933
<i>ORF19.5626</i>	-0.9085594116	<i>ORF19.3432</i>	-0.8913732325
<i>ORF19.5755</i>	-0.8584521669	<i>IFM3</i>	-0.810107887
<i>GND1</i>	-1.160682599	<i>ORF19.1691</i>	-1.698944999
<i>CDR4</i>	-0.8513361649	<i>CRZ2</i>	-1.786499733

<i>HHT2</i>	-1.386470147	<i>ORF19.50</i>	-0.6190062712
<i>ASR2</i>	-0.8005120484	<i>ORF19.320</i>	-1.583175962
<i>ORF19.2175</i>	-1.073274691	<i>ORF19.4736</i>	-0.9099955232
<i>CSR1</i>	-1.085566438	<i>ORF19.2870</i>	-0.7796719666
<i>LAP3</i>	-1.328332219	<i>ORF19.2686</i>	-0.6161709757
<i>TTR1</i>	-0.8336318552	<i>IFA4</i>	-0.6881687742
<i>ORF19.7283</i>	-0.7567214021	<i>RGS2</i>	-0.8122152997
<i>MAF1</i>	-0.8785092061	<i>ORF19.4550</i>	-0.9185573435
<i>ORF19.3264.1</i>	-0.8309989811	<i>ORF19.6498</i>	-0.827509077
<i>MHP1</i>	-0.9298838812	<i>ORF19.1861</i>	-0.8041598605
<i>ORF19.149</i>	-1.004727779	<i>GAL10</i>	-0.7373897222
<i>POL30</i>	-1.263396524	<i>CDR4</i>	-0.7633205271
<i>MOH1</i>	-0.7832097662	<i>ORF19.1483</i>	-1.46717288
<i>CSP1</i>	-1.606523473	<i>MNN1</i>	-1.021872024
<i>MDM34</i>	-0.9279801793	<i>ORF19.7283</i>	-0.9451771429
<i>CSH1</i>	-0.9295423778	<i>GCY1</i>	-0.6529022684
<i>SOD3</i>	-1.06600548	<i>DAL5</i>	-0.8716741091
<i>HTA2</i>	-1.231269707	<i>ORF19.6350</i>	-1.159476225
<i>ORF19.7296</i>	-0.9927171886	<i>KSP1</i>	-0.7772906829
<i>BMT9</i>	-1.193467062	<i>ORF19.5755</i>	-0.8172953694
<i>ORF19.2414</i>	-0.7254378629	<i>HAP42</i>	-0.9182977627
<i>SRB1</i>	-0.8495950319	<i>TES15</i>	-0.6237749341
<i>GPM2</i>	-0.9807768447	<i>ORF19.5239</i>	-0.9665634323
<i>ORF19.4531</i>	-0.901442797	<i>ORF19.2050</i>	-0.784408317



<i>ORF19.1785</i>	-1.087942811	<i>MDM34</i>	-0.8308684704
<i>ORF19.2371</i>	-0.6569810646	<i>ORF19.2220</i>	-1.401264613
<i>PST1</i>	-0.8260815479	<i>ALK8</i>	-1.046026286
<i>RHD3</i>	-0.8332463392	<i>ORF19.2095</i>	-0.6938643947
<i>RNR21</i>	-1.252625372	<i>ORF19.6688</i>	-0.772557805
<i>PMT2</i>	-1.039778513	<i>ORF19.672</i>	-0.6933353848
<i>GCA1</i>	-1.008251888	<i>ORF19.6821</i>	-0.6529381401
<i>GRE2</i>	-1.026321003	<i>ORF19.1258</i>	-1.128933529
<i>ADH2</i>	-1.112364903	<i>ORF19.3594</i>	-0.6259510995
<i>ORF19.2296</i>	-0.5881062452	<i>ORF19.5070</i>	-0.7586840021
<i>PMT4</i>	-0.8086000712	<i>ORF19.3310</i>	-0.7494905015
<i>HHF1</i>	-0.9278322148	<i>TPO3</i>	-1.004797394
<i>MRF1</i>	-0.9317858255	<i>DBR1</i>	-0.7685652872
<i>ECM21</i>	-0.6548803788	<i>MHP1</i>	-0.6687746886
<i>ORF19.320</i>	-0.9783162443	<i>RME1</i>	-0.9044551519
<i>ORF19.2398</i>	-0.7291899463	<i>FMA1</i>	-0.9322885618
<i>ERG4</i>	-0.8105828039	<i>YTH1</i>	-0.8245005823
<i>SWE1</i>	-0.9232958221	<i>ORF19.4531</i>	-0.6536566845
<i>DYN1</i>	-0.9573166259	<i>ORF19.5284</i>	-1.438165627
<i>ORF19.4370</i>	-0.7589121847	<i>ORF19.11</i>	-0.9060703439
<i>CBK1</i>	-1.118803927	<i>MAF1</i>	-0.8291968006
<i>LSP1</i>	-0.7048418278	<i>FCR1</i>	-0.6344055544
<i>ORF19.399</i>	-0.6760655181	<i>ORF19.149</i>	-1.101849062
<i>TRX2</i>	-1.168880989	<i>GCA1</i>	-1.266921357

<i>NCE102</i>	-0.6215592693	<i>ORF19.173</i>	-0.8359833547
<i>ORF19.2048</i>	-0.6726279367	<i>ALS4</i>	-1.460071321
<i>ORF19.35</i>	-0.6494314872	<i>ORF19.1198</i>	-0.7114633738
<i>PDX3</i>	-0.6967607206	<i>CBK1</i>	-1.133620255
<i>ORF19.7304</i>	-1.002128511	<i>ORF19.281</i>	-0.6348809647
<i>CAT1</i>	-0.8443497935	<i>ORF19.6554</i>	-0.67192574
<i>POL1</i>	-0.8715737635	<i>ARG83</i>	-0.9522014697
<i>ORF19.6225.1</i>	-0.922973512	<i>ORF19.6644</i>	-0.7205543907
<i>ACT1</i>	-1.053581195	<i>ORF19.6557</i>	-0.740130107
<i>ORF19.210</i>	-0.935765748	<i>RBR1</i>	-0.7492106994
<i>HSP70</i>	-0.6411828239	<i>ORF19.4654</i>	-1.160056134
<i>CHT2</i>	-0.8664106466	<i>ORF19.2650</i>	-0.6836248688
<i>CRP1</i>	-0.7143582521	<i>ORF19.1541</i>	-1.013774775
<i>ORF19.6245</i>	-0.6719927984	<i>ORF19.5552</i>	-0.6517720619
<i>ILV5</i>	-0.8193488076	<i>FMP45</i>	-0.9687485972
<i>DPM1</i>	-0.7748834196	<i>HSK3</i>	-0.834649014
<i>HEM13</i>	-0.8109234237	<i>ORF19.6518</i>	-0.6983401289
<i>KSP1</i>	-0.6793915183	<i>ORF19.4952.1</i>	-0.6129285918
<i>NHP6A</i>	-0.7187488851	<i>ORF19.894</i>	-0.5882467189
<i>ORF19.1353</i>	-1.005579797	<i>AQY1</i>	-0.9289291415
<i>ORF19.6084</i>	-0.8446216034	<i>ORF19.4347</i>	-0.6617785101
<i>ERV29</i>	-0.9116729221	<i>ORF19.7596</i>	-0.811694501
<i>ORF19.2769</i>	-0.5852914488	<i>HEM13</i>	-0.6175271915
<i>PGK1</i>	-0.5817984494	<i>RAD7</i>	-0.6872601657

<i>ORF19.3122.2</i>	-0.7277715689	<i>HSM3</i>	-0.8196941251
<i>PST3</i>	-0.8305611508	<i>RGA2</i>	-0.5800611825
<i>ASR1</i>	-0.6636853806	<i>CSP1</i>	-1.913545192
<i>SNZ1</i>	-0.666776876	<i>MOH1</i>	-0.7116186825
<i>GIN4</i>	-0.7829256633	<i>ORF19.2869</i>	-1.276450714
<i>RBP1</i>	-0.5911973208	<i>ORF19.1764</i>	-1.168076108
<i>SFT1</i>	-0.8029382675	<i>CRM1</i>	-0.6338035493
<i>ORF19.4450.1</i>	-0.7946182051	<i>ORF19.210</i>	-0.7259866693
<i>ORF19.7303</i>	-1.431035321	<i>ORF19.4779</i>	-0.5968714951
<i>FMP27</i>	-0.6586098975	<i>ORF19.6802</i>	-0.7049259375
<i>ORF19.5572</i>	-0.6943546222	<i>SAP1</i>	-2.174077291
<i>ATP2</i>	-0.8949182855	<i>ORF19.3302</i>	-0.8312456317
<i>ORF19.1861</i>	-0.5813830663	<i>ORF19.1785</i>	-0.757380307
<i>SUB2</i>	-0.6565755916	<i>ORF19.5076.1</i>	-1.472062759
<i>EGD1</i>	-0.6784955963	<i>ORF19.513</i>	-0.8409126351
<i>ORF19.5267</i>	-2.237707629	<i>ORF19.2068</i>	-0.5970430068
<i>TRA1</i>	-0.6706724532	<i>ORF19.1745</i>	-0.6457691556
<i>IFR2</i>	-0.7962114422	<i>ORF19.4653</i>	-1.157258737
<i>RPM2</i>	-0.69017545	<i>RHD1</i>	-0.6937325076
<i>HSL1</i>	-0.9647782548	<i>ORF19.6810</i>	-0.5949533192
<i>DAK2</i>	-0.7694806091	<i>MNN4-4</i>	-0.6146962602
<i>BUB3</i>	-0.6547994266	<i>ORF19.6267</i>	-0.8741545499
<i>ORF19.5785</i>	-0.9618250187	<i>ORF19.4286</i>	-0.6043246973
<i>PGI1</i>	-0.7235267741	<i>LYS22</i>	-0.6139185755

<i>TAL1</i>	-0.6405584563	<i>ORF19.6475</i>	-1.174525262
<i>RGA2</i>	-0.596478304	<i>ORF19.1369</i>	-0.7804974896
<i>ORF19.5961</i>	-0.5805487513	<i>ORF19.1534</i>	-0.6997212489
<i>ORF19.4347</i>	-0.6063512027	<i>ORF19.2939</i>	-0.6875288264
<i>ORF19.4952.1</i>	-0.8665694224	<i>ORF19.1026.1</i>	-0.9489176865
<i>FGR41</i>	-1.485456195	<i>ORF19.5267</i>	-0.9453454288
<i>CDC54</i>	-0.8705148948		
<i>HOM6</i>	-0.8124401056		
<i>ORF19.449</i>	-0.611201835		
<i>MCM2</i>	-0.7825385441		
<i>ERG13</i>	-1.568826215		
<i>MSH6</i>	-0.7194218201		
<i>VMA10</i>	-0.6157758625		
<i>ORF19.1203.1</i>	-0.6157459575		
<i>TUB1</i>	-1.338454749		
<i>MCM3</i>	-0.6870084794		
<i>ORF19.5394.1</i>	-0.7014130324		
<i>IPP1</i>	-0.6317100601		
<i>RFA1</i>	-0.7193470958		
<i>MTS1</i>	-0.6733652894		
<i>LYS9</i>	-0.6666895448		
<i>TOP2</i>	-0.7244740786		
<i>GAD1</i>	-0.6864358182		
<i>ORF19.2498</i>	-0.6761030381		

<i>CYP1</i>	-0.617409781		
<i>SEC24</i>	-0.6212373698		
<i>ORF19.3100</i>	-0.9564323396		
<i>PFK2</i>	-0.5836756231		
<i>ORF19.86</i>	-0.591125883		
<i>CDC47</i>	-0.6115173708		
<i>SLR1</i>	-0.604579212		
<i>STE23</i>	-0.87778546		
<i>ORF19.7297</i>	-0.6355428543		
<i>YAK1</i>	-0.7182251848		
<i>MIF2</i>	-0.5864196214		
<i>ORF19.6555</i>	-0.5851153369		
<i>PMT1</i>	-0.6568845055		
<i>YVC1</i>	-1.041973331		
<i>MPS1</i>	-1.085946385		
<i>MLC1</i>	-0.9546673834		
<i>ORF19.1562</i>	-0.6440695742		
<i>CDC46</i>	-0.8607273885		
<i>ORF19.4914</i>	-1.64008009		
<i>ORF19.3216</i>	-0.8207596903		
<i>TOS1</i>	-0.5882942336		
<i>ORF19.3373</i>	-0.888048904		
<i>SPF1</i>	-0.6750949118		
<i>SOU1</i>	-0.6310817378		

<i>HAP42</i>	-0.5917663858		
<i>ORF19.5342.2</i>	-0.7004663793		
<i>ORF19.1782</i>	-0.85821347		
<i>VPS70</i>	-0.6218915069		
<i>CDC12</i>	-0.756072907		
<i>HHF22</i>	-0.6113359175		
<i>SUA71</i>	-0.6925630194		
<i>DUT1</i>	-1.509363342		
<i>LSC1</i>	-1.00266385		
<i>PGA53</i>	-0.603869066		
<i>ORF19.5666</i>	-0.6139434971		
<i>SOL1</i>	-1.021508391		
<i>RBR1</i>	-1.144101066		
<i>ACH1</i>	-0.7751338455		
<i>ORF19.4824</i>	-0.7394004281		
<i>LYS12</i>	-0.5867843344		
<i>CHT3</i>	-1.254621989		
<i>RFA2</i>	-0.7270398924		
<i>CHO1</i>	-1.060663777		
<i>ORF19.3475</i>	-0.8865987588		
<i>HHO1</i>	-0.678218317		
<i>ORF19.2770</i>	-0.6195135782		
<i>PDS5</i>	-0.9125107592		
<i>ORF19.4907</i>	-0.6326395762		

<i>HTA1</i>	-0.586763957		
<i>CDC3</i>	-0.5804612955		
<i>ORF19.1258</i>	-0.6157766064		
<i>ORF19.2959.1</i>	-0.6808507285		
<i>HSM3</i>	-0.6569508919		
<i>ORF19.3694</i>	-0.8646322041		
<i>ORF19.547</i>	-0.7508292196		
<i>ERG9</i>	-0.7852398654		
<i>ORF19.200</i>	-0.6845152783		
<i>IDP1</i>	-0.8773653747		
<i>ERP5</i>	-0.7077986482		
<i>RPN6</i>	-0.6002292941		
<i>PTC4</i>	-0.6476700322		
<i>ORF19.6396</i>	-0.6592829958		
<i>ORF19.1664</i>	-0.5804647099		
<i>ASF1</i>	-0.8369516041		
<i>ORF19.4030</i>	-0.6897239354		
<i>ORF19.6267</i>	-0.6531259355		
<i>CWH8</i>	-0.7308160627		
<i>ORF19.6869</i>	-0.6490603161		
<i>ATP14</i>	-0.7308479242		
<i>ORF19.6592</i>	-0.6115202375		
<i>FMP45</i>	-0.7621265175		
<i>ORF19.2739</i>	-0.6333583441		

<i>MYO1</i>	-0.6431637013		
<i>YWP1</i>	-0.6893176752		



**Supplemental Table 2.4:** List of primers.

CJNO4774	<i>MTLa1</i> _cPCR_FWD_Miller	CATACCCAAACTCTTATTTGGG
CJNO4775	<i>MTLa1</i> _cPCR_REV_Miller	CACCTTCAACCTCCTCGTTTTTCC
CJNO4776	<i>MTLalpha2</i> _cPCR_FWD_Miller	GGTCTTTTTGCAGATACGGA
CJNO4777	<i>MTLalpha2</i> _cPCR_REV_Miller	CACATCTGGAGGCACTCTTTG
CJNO5299	<i>OBPa</i> cPCR forward	CCTTCAATTGCATCGTAAGTACC
CJNO5300	<i>OBPa</i> cPCR reverse	GAAGATGACTCAGGTCATGC
CJNO5301	<i>OBPa</i> cPCR forward	GTGGTCAATGGAGCTGATAC
CJNO5302	<i>OBPa</i> cPCR reverse	ACATGTGGTCGCCCAACTCC
CJNO5303	<i>PAPa</i> cPCR forward	CTGGCATTTCGATGAAGTCTA
CJNO5304	<i>PAPa</i> cPCR reverse	CATGTCCGATTCAATGGCCC
CJNO5305	<i>PAPa</i> cPCR forward	GGAATTGAATTGATGAATGAC
CJNO5306	<i>PAPa</i> cPCR reverse	CAGCCCTCTTCCTTTTCGCA
CJNO5951	ASG7_KO_gRNA_1	CGTAAACTATTTTTAATTTG AAAAATTTGAAGGTAAGCC GGTTTTAGAGCTAGAAATAGC
CJNO5952	ASG7_KO_gRNA_2	CGTAAACTATTTTTAATTTG AATAAACTGCTTGATTGACT GTTTTAGAGCTAGAAATAGC
CJNO5953	ASG7_KO_AddTag_dDNA_FWD	GAAATTCCAAAATAATCCTC TCAAGCAATTAACAAAACCT ATTAACTTTCTCAGTGGG GGAATAACAATTGTCAAGC GAGACGAGTGCTCGACAT Gagg
CJNO5954	ASG7_KO_AddTag_dDNA_REV	TTTTTGACTTCTACAAGACT TAACTCAATTGCTTTTCA TTATATAAATCAATTCTCTC

		CTATTTAATACACATATcctC ATGTCGAGCACTCGTCTCG
CJNO5955	ASG7_KO_cPCR_FWD	TACTCCGAGACCAATAGAG C
CJNO5958	ASG7_KO_cPCR_REV	AATTCTATGTGAGCTTCAT GC
CJNO5968	IHD1_KO_gRNA_2	CGTAAACTATTTTTAATTTG AATGGTAACGATGGTGCTA GGTTTTAGAGCTAGAAATA GC
CJNO5969	IHD1_KO_AddTag_dDNA_FWD	AACTAGGAATTTAGCCAAA AAAGCTGTAAAACCTTTCTT TTCAAATACTAAACCAAAC CTTTACCACACAGTCATCC GAGACGAGTGCTCGACAT Gagg
CJNO5970	IHD1_KO_AddTag_dDNA_REV	ATATTAACGTACAAACAA GAATTTAAAACCGAAAATAT GTAAAACACACAACGAAGC ACTGGTTTCAACTTAGACTc ctCATGTGCGAGCACTCGTCT CG
CJNO5971	IHD1_KO_cPCR_FWD	GTATAAATACCACCAAAGT CC
CJNO5974	IHD1_KO_cPCR_REV	TTAGTCTCTACAACACCATT AC
CJNO6217	PTP3_KO_gRNA_1	CGTAAACTATTTTTAATTTG TAACTGATGATGGACTTGG CGTTTTAGAGCTAGAAATA GC
CJNO6218	PTP3_KO_gRNA_2	CGTAAACTATTTTTAATTTG AACTAACGATGCAAACAAC AGTTTTAGAGCTAGAAATA GC
CJNO6219	PTP3_KO_AddTag_dDNA_FWD	ATTTTTCAATTGTTAATTTAC TTTCTTAGTTTAGGTATATA TATATACAAATTTGCACCAA TACTGTTAACACCCCCACG AGACGAGTGCTCGACATGa gg
CJNO6220	PTP3_KO_AddTag_dDNA_REV	ATAGCCAAAGCTACAACAA CTAACCAAAGAAAAACATTT GTCTATATTATAAAGTCCAT CATAATCGTCCGTGAAAAcc

		tCATGTCGAGCACTCGTCT CG
CJNO6221	<i>PTP3_KO_cPCR_FWD</i>	TCCTAATATTTCTCCCTCC
CJNO6222	<i>PTP3_KO_cPCR_REV</i>	AAAGTCCATCATAATCGTC C
CJNO5981	<i>orf19.1725_KO_gRNA_1</i>	CGTAAACTATTTTTAATTTG ACTATTCCTCCAAGTCCAT GGTTTTAGAGCTAGAAATA GC
CJNO5982	<i>orf19.1725_KO_gRNA_2</i>	CGTAAACTATTTTTAATTTG ACTGGTCCATCTAGTCCAG GGTTTTAGAGCTAGAAATA GC
CJNO5983	<i>orf19.1725_KO_AddTag_dDNA_F WD</i>	TTTTGTTTTAGTTCAAGTTT TTTCAACATCATCAAATAAA GAACTTCTTCTTCTTACC CACTCCATCACTGAAACG AGACGAGTGCTCGACATGa gg
CJNO5984	<i>orf19.1725_KO_AddTag_dDNA_RE V</i>	AATAAAACATGGAAACAATT AAATTTCAAACCGAAATAA TTAACAAAATAAAAATGAAA ACAATTTATAATTAAGTcctC ATGTCGAGCACTCGTCTCG
CJNO5985	<i>orf19.1725_KO_cPCR_FWD</i>	AAACTTCTTCTTCTTACCC
CJNO5986	<i>orf19.1725_KO_cPCR_REV</i>	CTTATAGTTTTGATGCCAC C
CJNO5987	<i>orf19.1779_KO_gRNA_1</i>	CGTAAACTATTTTTAATTTG TCTCCATACAGTGACAATG GGTTTTAGAGCTAGAAATA GC
CJNO5988	<i>orf19.1779_KO_gRNA_2</i>	CGTAAACTATTTTTAATTTG TCTCCATACAGTGACAATG GGTTTTAGAGCTAGAAATA GC
CJNO5989	<i>orf19.1779_KO_AddTag_dDNA_F WD</i>	TATCAGTCTTTCCTTACAAT CCTTTAGAAGTAACTTTATT CGTTCTTTTTTATATAACA TAATACCCAACCTAATACGA GACGAGTGCTCGACATGag g
CJNO5990	<i>orf19.1779_KO_AddTag_dDNA_RE V</i>	TAATTGTTATTTTTAAAAAA TAAAAAGGATTCACCGGA TATATAATGAAAAATAAAC

		TAAAGCCAATTAATGTGCcc tCATGTCGAGCACTCGTCT CG
CJNO5991	<i>orf19.1779_KO_cPCR_FWD</i>	TCAGTCTTTCCTTACAATCC
CJNO5992	<i>orf19.1779_KO_cPCR_REV</i>	CTTCTTCTTCTTCTTCTTCG
CJNO5993	<i>ORF19.3932.1_KO_gRNA_1</i>	CGTAAACTATTTTTAATTTG GAATTGACTGATGGTCAAG TGTTTTAGAGCTAGAAATA GC
CJNO5994	<i>ORF19.3932.1_KO_gRNA_2</i>	CGTAAACTATTTTTAATTTG GAAGTTCCAGAATTGACTG AGTTTTAGAGCTAGAAATA GC
CJNO5995	<i>ORF19.3932.1_KO_AddTag_dDNA_FWD</i>	CAAAGTATGATCAGTTCTCT CATTAAATTTTTAGTTCACT AAGTTCCTCATTCAATACTC TATATTACCCACTAACACG AGACGAGTGCTCGACATGa gg
CJNO5996	<i>ORF19.3932.1_KO_AddTag_dDNA_REV</i>	CACCACAATTAATATGCTTT AAAATATAAAAATTTTCTAAA CAAAGTGTATGAACTATTT CTAGCTAATATTTTCAAcctC ATGTCGAGCACTCGTCTCG
CJNO5997	<i>ORF19.3932.1_KO_cPCR_FWD</i>	GATGTTGATGCTATTGACC C
CJNO5998	<i>ORF19.3932.1_KO_cPCR_REV</i>	ACAACATTTCCACCCTATTG G
CJNO5999	<i>ORF19.6200_KO_gRNA_1</i>	CGTAAACTATTTTTAATTTG ACTAACAGCATTAGCCCCT GGTTTTAGAGCTAGAAATA GC
CJNO6000	<i>ORF19.6200_KO_gRNA_2</i>	CGTAAACTATTTTTAATTTG TGATGTGTGAGCAATAACC GGTTTTAGAGCTAGAAATA GC
CJNO6001	<i>ORF19.6200_KO_AddTag_dDNA_FWD</i>	CTCTTTATAAACACAATTGT TGAATTAACAAAACTATTA AGTGGATAAAAGAGATAAA AGCAAAGAAGAAGACTGTCC GAGACGAGTGCTCGACAT Gagg
CJNO6002	<i>ORF19.6200_KO_AddTag_dDNA_REV</i>	CAATGGAACAAAAACAACA AGCAGCTCTAGAAACAATT

		TCATCTCTCCACCATCCAT CTCCTCTCCTTCGTAACCA AcctCATGTCGAGCACTCGT CTCG
CJNO6003	<i>ORF19.6200_KO_cPCR_FWD</i>	TCATAAAAACGATATTCCC C
CJNO6004	<i>ORF19.6200_KO_cPCR_REV</i>	AGAAACAATTTTCATCTCTCC
CJNO6005	<i>ORF19.7167_KO_gRNA_1</i>	CGTAAACTATTTTTAATTTG CCAACTTAGACAAGAGAG GGTTTTAGAGCTAGAAATA GC
CJNO6006	<i>ORF19.7167_KO_gRNA_2</i>	CGTAAACTATTTTTAATTTG TGGAGTAGTTGTAGGAACT GGTTTTAGAGCTAGAAATA GC
CJNO6007	<i>ORF19.7167_KO_AddTag_dDNA_FWD</i>	GGGACAACATTTCCAATT TCTGATCATTTCGAAACGTT CAATAACCAACAAACATTAT AGTTTAATCTACAACAAAAC GAGACGAGTGCTCGACAT Gagg
CJNO6008	<i>ORF19.7167_KO_AddTag_dDNA_REV</i>	GGTATTACAAAAACAGAAA ACATAAAAAGAGCTAAACT AAAAAATAAGCAAATTATT CAGAAAGACTGGTAAATAC cctCATGTCGAGCACTCGTC TCG
CJNO6009	<i>ORF19.7167_KO_cPCR_FWD</i>	CTGATTCTTTCAACCCTAG C
CJNO6010	<i>ORF19.7167_KO_cPCR_REV</i>	GCAACAATCAGATCAACTA CC

## Chapter 3

### **A systematic genetic screen for transcriptional regulators of *Candida albicans* sexual biofilms**

*Austin M. Perry, Deepika Gunasekaran, Clarissa J. Nobile*  
*In preparation for submission*

#### **3.1 Abstract**

Transcription networks lie at the regulatory heart of nearly every biological process on our planet. A transcription network consists of a series of positive and negative feedback loops between transcription factors, proteins that bind DNA in a sequence-specific manner, and the genes they regulate. These are complex systems that only become more entangled in higher organisms. Thus, studying transcription networks in simpler organisms provides a useful foundation on which to build our understanding of higher organisms. *Candida albicans* is an opportunistic pathogenic yeast that serves as a model organism for studying transcription networks. Several have been illuminated in the species so far, regulating diverse phenotypes from cell-type regulation to the switch between commensal and pathogenic lifestyles, and biofilm formation. Interestingly, *C. albicans* can form two distinct types of biofilms, regulated by distinct signaling pathways and transcription factors; referred to as sexual and conventional. Previous work elucidated the complete transcription network regulating conventional biofilm formation. Here, we combine genetic screens and genome-wide approaches to describe a limited set of transcription factors involved in the regulation of sexual biofilms. Several of the transcription factors involved in the conventional biofilm network also regulate sexual biofilms, though each system contains unique transcription factors. Interestingly, some transcription factors appear to have flipped regulatory roles. This work provides a vital basis on which additional studies can fully uncover the complete sexual biofilm transcriptional network.

#### **3.2 Introduction**

A transcription network is the summation of the complete set of genetic regulatory information required for an organism to adopt or maintain a particular phenotype<sup>1</sup>. Although there are many components of these gene expression networks, at the heart of them all lie transcription factors and the genes they regulate. We define a transcription factor as sequence-specific DNA-binding proteins that control the transcription of specific genes by binding to *cis*-regulatory sequences (i.e. short, typically 6-15 base pair, DNA sequences)<sup>1</sup>. Transcription networks can be found in nearly all life on earth from simple microorganisms to humans. The complexity of transcription networks generally escalates with the complexity of the organism it regulates, making those in higher eukaryotes difficult to understand. In addition, investigation of transcription networks relies heavily on genetic manipulation, something that can be difficult to achieve in more complex organisms. Thus, many researchers use simpler organisms, such as yeasts, to study the nebulous nature of transcription networks.

*Candida albicans* is a model yeast and is widely used for understanding transcription networks<sup>2-5</sup>. Even in this simple yeast, TNs are complex and intricate; involving multiple transcription factors and vast numbers of downstream genes, usually as much as 20% of the genome, if not more<sup>2-5</sup>. There are even interactions between transcription networks<sup>4</sup>. Thus, as a genetically tractable and medically relevant

microorganism, *C. albicans* is a prime candidate for research into TNs. To date, complete transcription networks have been identified in *C. albicans* that regulate a diverse array of phenotypes such as the switch from a commensal lifestyle to a pathogenic, the white-opaque switch, and biofilm formation<sup>2,3,5</sup>.

*C. albicans* can form various types of biofilms depending on the genotype of the cells within, conventional and sexual, each regulated by a unique transcription network. Conventional biofilms have been the predominant focus in the field as they are formed by the vast majority (~97%) of *C. albicans* clinical isolates due to their genetic status as mating type-like heterozygotes (**a/α**)<sup>6,7</sup>. These biofilms are formed in response to a variety of environmental factors, which, through the Ras1/cAMP signaling pathway, activate a core network of 9 transcription factors (i.e. Efg1, Bcr1, Brg1, Tec1, Ndt80, Rob1, Gal4, Flo8, and Rfx2), regulate each other and over 1,000 downstream genes to give rise to conventional biofilms<sup>2,8,9</sup>. Alternatively, *MTL*-homozygous or –hemizygous cells (**a/a**, **a/Δ**, **α/α**, or **α/Δ**) only make up a small subset of the global population (~3%)<sup>6,7</sup>. These cells form a unique and specialized “sexual” biofilm, requiring mating pheromone of the opposite mating type to do so<sup>10–12</sup>. The mating pheromone signal is transduced through the MAPK pathway to activate Cph1, a transcription factor only peripherally involved in conventional biofilm formation, along with a subset of the transcription factors involved in conventional biofilm formation (i.e. Rob1, Brg1, Bcr1, and Tec1)<sup>13–15</sup>. Many more regulators are likely involved in sexual biofilm formation, though what they are and how all of these transcription factors impact sexual biofilms is unknown.

Identifying the underlying transcriptional mechanisms that govern these two similar yet distinct systems will provide a deeper understanding of the lifestyle of *C. albicans* and provide a unique model from which we can better understand the evolution of biofilm formation in *C. albicans* and eukaryotic transcription networks. Here, we combine a classical forward genetics approach and transcriptional profiling to produce a comprehensive set of transcription factors involved in the regulation of sexual biofilm formation in *C. albicans* and the genes they directly or indirectly regulate. I screened a library of 207 strains, each with a single gene encoding a transcription factor deleted from their genome, for their abilities to form sexual biofilms as a way of identifying exactly which transcription factors may be involved in regulating this structure. Transcriptomic analyses were used to further identify the sets of genes directly or indirectly controlled by each TF, allowing us to begin to understand the role of each transcription factor in regulating sexual biofilms.

### 3.3 Results

#### 3.3.1 Identification of sexual biofilm regulators in vitro

Transcription factors are proteins that bind DNA in a sequence specific manner and regulate the expression of nearby target genes<sup>1</sup>. These proteins are crucial to the regulation of all biological systems in response to external stimuli and maintaining homeostasis. In order to identify the transcription factors involved in sexual biofilm formation, we screened an existing library of 207 TF deletion mutant strains to identify which were most severely affected in their abilities to form sexual biofilms when compared to a wild-type reference strain (APY001)<sup>16</sup>. Strains that exhibited defective growth behaviors were excluded. A true white version of the *efg1* Δ/Δ mutant strain was unable to be obtained and was excluded from these assays<sup>17</sup>. Of the 207 deletion mutant strains, 30 were severely defective in sexual biofilm formation compared to the reference strain, hardly reacting at all when exposed to a synthetic α-factor in sexual biofilm-inducing

conditions. In addition, 2 deletion mutant strains, *rfx2*  $\Delta/\Delta$  and *ndt80*  $\Delta/\Delta$ , formed more robust sexual biofilms compared to the reference strain (Figure 3.1). The screen was performed blindly and identification of previously identified deletion mutant strains like *cph1*  $\Delta/\Delta$ , *bcr1*  $\Delta/\Delta$ , *rob1*  $\Delta/\Delta$ , *bcr1*  $\Delta/\Delta$ , *ndt80*  $\Delta/\Delta$ , and *brg1*  $\Delta/\Delta$  served as an internal control for the screen<sup>14</sup>. All 32 TF deletion mutant strains exhibited a statistically significant difference in their abilities to form sexual biofilms compared to the wildtype. Statistical significance was determined using an ANCOVA analysis of each strain normalized to the wildtype ( $p \leq .0001$ ). Of these deletion mutant strains it has been proposed that deletion of *ndt80*  $\Delta/\Delta$  does not have a direct impact on sexual biofilm formation, but rather indirectly increases the thickness of sexual biofilms by causing the misregulation of two genes involved in cell-separation<sup>14</sup>. Interestingly, deletion of *GAL4* appears to have the opposite regulatory function for sexual biofilms as it does for conventional biofilms<sup>9</sup>. Indeed, the *gal4*  $\Delta/\Delta$   $\alpha/\alpha$  strain displays enhanced conventional biofilm formation whereas white *gal4*  $\Delta/\Delta$  mutant  $\alpha$  strains form weaker sexual biofilms upon pheromone stimulation as compared to wildtype strains<sup>9</sup>.

### 3.3.2 Genome wide differential gene expression patterns of sexual biofilm regulators

Understanding the regulatory relationships that a particular transcription factor has with its downstream genes is paramount in explaining their role in various biological and developmental processes. Here we performed RNA-sequencing on TF deletion mutants treated with synthetic alpha-pheromone to identify the target genes differentially expressed in the transcription factor deletion mutants when forming sexual biofilms. Identical conditions were maintained between the screen and the growth of each of the 32 TF mutants for cell harvesting. Total RNA was extracted from sexual biofilm harvested cells after 24-hours of biofilm growth. Sequencing ready libraries were then prepared, with Lexogen's 3' Quant-seq kit, and sequenced on the Illumina Next-seq platform.

To identify the specific impact of transcription factor deletion on sexual biofilms, we compared gene counts between our isogenic wild-type strain treated with a .01% DMSO vehicle and the wild-type versus TF deletion mutant strains treated with synthetic mating-pheromone. Using a threshold of  $\log_2 \geq 0.58$  and  $\log_2 \leq -0.58$  and a p-adj. value of  $\leq 0.05$ , we found 133 genes to be upregulated and 217 genes to be downregulated in our isogenic wild-type when treated with a synthetic alpha-pheromone as compared to treatment with the vehicle. 371 genes were upregulated and 595 genes were downregulated in *cph1*  $\Delta/\Delta$  deletion mutant strains. 175 genes were upregulated and 109 genes were downregulated in *bcr1*  $\Delta/\Delta$  deletion mutant strains. 378 genes were upregulated and 315 genes were downregulated in *zcf21*  $\Delta/\Delta$  deletion mutant strains. 459 genes were upregulated and 485 genes were downregulated in *leu3*  $\Delta/\Delta$  deletion mutant strains. 432 genes were upregulated and 508 genes were downregulated in *orf19.5026*  $\Delta/\Delta$  deletion mutant strains. 199 genes were upregulated and 314 genes were downregulated in *gal4*  $\Delta/\Delta$  deletion mutant strains. 381 genes were upregulated and 510 genes were downregulated in *lys14*  $\Delta/\Delta$  deletion mutant strains. 390 genes were upregulated and 529 genes were downregulated in *sko1*  $\Delta/\Delta$  deletion mutant strains. 411 genes were upregulated and 401 genes were downregulated in *ndt80*  $\Delta/\Delta$  deletion mutant strains. 517 genes were upregulated and 432 genes were downregulated in *orf19.3625* deletion  $\Delta/\Delta$  mutant strains. 409 genes were upregulated and 603 genes were downregulated in *mig1*  $\Delta/\Delta$  deletion mutant strains. 937 genes were upregulated and 1092 genes were downregulated in *rob1*  $\Delta/\Delta$  deletion mutant strains. 293 genes were upregulated and 325 genes were downregulated in *ash1*  $\Delta/\Delta$  deletion mutant strains. 260 genes were upregulated and 394 genes were downregulated in *tec1*  $\Delta/\Delta$  deletion mutant



strains. 769 genes were upregulated and 705 genes were downregulated in *orf19.5910*  $\Delta/\Delta$  deletion mutant strainw. 496 genes were upregulated and 507 genes were downregulated in *aaf1*  $\Delta/\Delta$  deletion mutant strains. 246 genes were upregulated and 234 genes were downregulated in *ahr1*  $\Delta/\Delta$  deletion mutant strains. 680 genes were upregulated and 803 genes were downregulated in *bcr1*  $\Delta/\Delta$  deletion mutant strains. 117 genes were upregulated and 217 genes were downregulated in *orf19.173*  $\Delta/\Delta$  deletion mutant strains. 474 genes were upregulated and 595 genes were downregulated in *cph2*  $\Delta/\Delta$  deletion mutant strains. 448 genes were upregulated and 536 genes were downregulated in *cap1*  $\Delta/\Delta$  deletion mutant strains. 375 genes were upregulated and 440 genes were downregulated in *gis2*  $\Delta/\Delta$  deletion mutant strains. 484 genes were upregulated and 629 genes were downregulated in *rfg1*  $\Delta/\Delta$  deletion mutant strains. 574 genes were upregulated and 502 genes were downregulated in *wor3*  $\Delta/\Delta$  deletion mutant strains. 895 genes were upregulated and 828 genes were downregulated in *flo8*  $\Delta/\Delta$  deletion mutant strains. 984 genes were upregulated and 1034 genes were downregulated in *fgr3*  $\Delta/\Delta$  deletion mutant strains. 1170 genes were upregulated and 1343 genes were downregulated in *hfl3*  $\Delta/\Delta$  deletion mutant strains. 38 genes were upregulated and 71 genes were downregulated in *zcf5*  $\Delta/\Delta$  deletion mutant strains. 651 genes were upregulated and 645 genes were downregulated in *ctf1*  $\Delta/\Delta$  deletion mutant strains. 549 genes were upregulated and 649 genes were downregulated in *rxf2*  $\Delta/\Delta$  deletion mutant strains.

### 3.3.3 Gene ontology analyses of transcription factor deletion mutant strains

By analyzing the significantly differentially expressed biological processes produced from gene ontology analyses one may infer the categories of genes whose expression is impacted by the deletion of a given TF. *rxf2*  $\Delta/\Delta$  deletion mutant strains formed much more robust sexual biofilms than our wild-type strain (Figure 3.1) and we see many biological processes related to biofilm formation being upregulated, such as “cell adhesion” (p-adj. = .013073), cell-cell adhesion (p-adj. = .031025), “single-species biofilm formation in or on host organism” (p-adj. = .006487) and “single-species biofilm formation on inanimate substrate” (p-adj. = .00089) (Figure 3.2A). We also find that the genes that fill out these categories are more dramatically upregulated in *rxf2*  $\Delta/\Delta$  deletion mutant strains upon pheromone stimulation as compared to the wild-type strain. Interestingly, we find that many of these same biological processes that are upregulated in *rxf2*  $\Delta/\Delta$  deletion mutant strains are downregulated in many transcription factor deletion mutant strains (e.g. *cph1*  $\Delta/\Delta$ , *rob1*  $\Delta/\Delta$ , *brg1*  $\Delta/\Delta$ ) that formed weaker sexual biofilms than the wild-type (Figure 3.2B & 3.2C). For example, when comparing the “cell adhesion” biological process between *cph1*  $\Delta/\Delta$  deletion mutant strains and *rxf2*  $\Delta/\Delta$  deletion mutant strains, we found *cph1*  $\Delta/\Delta$  deletion mutant strains to have a Normalized Enrichment Score (NES) of -2.11 (p-adj. = .000075), whereas the *rxf2*  $\Delta/\Delta$  deletion mutant strains have an NES of 1.8 (p-adj. = .01). Interestingly, some TF mutants that formed weaker sexual biofilms than the wild-type still depicted a slight upregulation of key biological processes involved in biofilm formation and a downregulation of other key biological processes. For example, the gene ontology analysis of *bcr1*  $\Delta/\Delta$  deletion mutant strains showed an upregulation of “filamentous growth of a population of unicellular organisms in response to biotic stimulus” (NES = 1.414, p-adj. = .0316) and “cellular response to biotic stimulus” (NES = 1.376, p-adj. = .0405) yet lacked any annotation relating to “adhesion” (Figure 3.2C). This may mean that *bcr1* deletion mutant strains are able to sense and respond to mating-pheromone by filamenting, yet are unable to translate that into increased adhesion. We

see this in the fact that genes such as *STE4* (subunit of heterotrimeric G-protein of mating signal transduction pathway) and *CST5* (scaffolding protein for the mating signal transduction pathway) are significantly upregulated yet some adhesion genes known to be involved in sexual biofilm formation (e.g. *orf19.1725*) are not differentially expressed in *bcr1*  $\Delta/\Delta$  deletion mutant strains responding to pheromone. This fits with existing knowledge of the role of Bcr1 in conventional biofilms, where Bcr1 is primarily responsible for the expression of adhesins on hyphal cells, rather than the formation of the hyphae itself<sup>18</sup>.

### 3.4 Discussion

Identification of the transcription network that governs conventional biofilm formation has provided great insight into the molecular mechanisms and biological processes that enable *a/α C. albicans* to form such a complicated structure<sup>2,9</sup>. However very little was known about how these mechanisms translate to sexual biofilm formation in *a* or *α C. albicans* cells. In this work, we screened a pre-existing library of strains, each with a single gene encoding a transcription factor deleted from its genome, to determine which transcription factors impact sexual biofilm formation. From this screen, we identified 30 strains that formed much weaker sexual biofilms and 2 strains that formed more robust sexual biofilms as compared to the isogenic wild-type strain. Among these, several of the canonical conventional biofilm regulators were found to also impact sexual biofilm formation. Some of these dual biofilm regulators were identified previously (i.e. *BRG1*, *ROB1*, *TEC1*, *BCR1*)<sup>2,14,19</sup> however we have found many additional dual biofilm regulators (e.g. *AHR1*, *FGR3*, *FLO8*, *GAL4*, *LEU3*, *RFG1*, etc.)<sup>2,9,19</sup>. Each system still contains many regulators that are unique to that system which may explain the phenotypic differences between sexual and conventional biofilms. And interestingly some regulators even appear to switch roles between each system. Previous research has shown this phenomenon for *NDT80*, however we have shown that *GAL4* also appears to switch from a negative regulator of conventional biofilm formation to a positive regulator of sexual biofilm formation. That is to say that deletion of *gal4* results in weaker sexual biofilms but more robust conventional biofilms. Further research will need to be performed to understand this phenomenon.

To begin to understand the role of each transcription factor in sexual biofilm formation, we performed RNA-sequencing across all strains after exposure to mating pheromone or the vehicle. These data shows which sets of downstream genes each transcription factor is responsible for. We found that the deletion of some transcription factors had minimal impact on differential expression patterns (e.g. *zcf5*  $\Delta/\Delta$ ) while others resulted in the differential expression of over a thousand genes (e.g. *hfl3*  $\Delta/\Delta$ ). There could be many explanations for this including the direct and indirect nature of genetic regulation by transcription factors. That is to say that transcription factors can either directly regulate a downstream gene by binding to the *cis*-regulatory region of that downstream gene or by regulating another transcription factor that subsequently regulates that downstream gene, potentially resulting in the misregulation of large numbers of genes<sup>1</sup>. Unfortunately, RNA-sequencing alone cannot differentiate between indirect and direct regulatory relationships, but only their end product. Additional experiments such as CUT&RUN or ChIP-sequencing will need to be performed to demonstrate the binding locations of each transcription factor along the genome. By comparing the binding locations of a transcription factor with the differential gene expression patterns of a deletion mutant for that transcription factor, which we have generated in this work, one can determine whether each gene is under

direct or indirect regulation by that transcription factor. In addition, a previous collaborator from the Hernday lab has published a method to infer gene regulatory networks from transcriptional profiling data<sup>20</sup>. This can be applied to the transcriptional profiling presented in this work to give us an idea of what the sexual biofilm transcriptional network looks like prior to the completion of CUT&RUN or ChIP-sequencing.

### 3.5 Methods and Materials

#### 3.5.1 Strains and media

*C. albicans* strains were cultured at 25°C in YPD (2% Bacto peptone, 2% dextrose, 1% yeast extract, pH 6.8). Biofilms were grown in Lee's Medium supplemented with 1.25% glucose. The previously described *C. albicans* reference strain SN250 (His+Leu+Arg-background), a derivative of the clinical isolate strain SC5314 was used throughout the study as the wildtype reference strain. However, as this strain is naturally *a/α*, it was converted to the pheromone-responsive *a/Δ* background using pJD1<sup>16</sup>. Mating types of the resulting strains were verified by colony PCR against both the *a* and *α* *MTL* loci. The previously described 207 *C. albicans* transcription factor deletion mutant strain library was used to screen for sexual biofilm formation<sup>16</sup> (Supplemental Table 1). All strains were converted to the white state prior to subjection to the pheromone-stimulated biofilm assay.

#### 3.5.2 Pheromone-stimulated biofilm assay

The sexual biofilm assay was performed as previously described (Chapter 2). Briefly, each well of a 12-well plate was inoculated with  $5 \times 10^7$  cells ( $OD_{600} = 2.5$ ) of an overnight culture grown in Spider to 1,000  $\mu$ L of Lee's media. Synthetic *C. albicans*  $\alpha$ -pheromone (GFRLTNFGYFEPG) -- diluted in pure DMSO to 100 mg/mL and subsequently diluted to 10 mg/mL in sterile water before addition to wells -- was added to each well at a final concentration of 10  $\mu$ g/ml (6.6  $\mu$ M). Control wells were treated with .01% DMSO. Biofilms were incubated at 25°C in Elmi plate incubators for 24 hours. Spent media was aspirated and biofilms were washed with 1,000  $\mu$ L of 1xPBS. After removal of the 1xPBS wash and unadhered cells, biofilm thickness was quantified via  $OD_{600}$  using a BioTek Epoch 2 plate reader.

#### 3.5.3 RNA-seq cell harvesting and library preparation

Growth of pheromone-stimulated biofilms was performed as described above. However, after the 1xPBS wash and removal of unadhered cells, fresh 1000  $\mu$ L of 1xPBS was used to resuspend the remaining adhered cells. Each sample was pooled from five wells of a 12-well plate into a 50 mL Falcon centrifuge tube. Two biological replicates were collected for each strain and condition. Samples were centrifuged at 4000 rpm for five minutes at ambient temperature. The supernatant was decanted under sterile conditions and the pellets were frozen in a -80°C freezer until their RNA was extracted. RNA was extracted using the RiboPure RNA Purification Kit for yeast (Invitrogen). 500 ng total RNA was prepared for mature poly(A) RNA selection for 100 bp single-end sequencing using QuantSeq 3' mRNA-seq Library Prep Kit FWD (Lexogen).

#### 3.5.4 Differential expression and gene enrichment analysis

Transcriptomic data was generated using 3' Tag-Seq and sequenced using Illumina NextSeq or HiSeq platforms. The data was mapped to *Candida albicans* SC5314

reference genome and transcript abundance was retrieved for the *C. albicans* genes using the computational workflow published by Paropkari *et al.*, 2023<sup>21</sup>. Briefly, single-end reads were trimmed using BBDuk (BBMap version 38.18)<sup>22</sup>, aligned to the reference genome and transcript abundance was estimated using STAR (version 2.7.10a)<sup>23</sup> as mentioned in Paropkari *et al.*, 2023<sup>21</sup>. *C. albicans* SC5314 reference genome, coding sequence annotations and Gene Ontology (GO) annotations were retrieved from the *Candida* Genome Database (CGD)<sup>24</sup>. All statistical analyses such as identifying differentially expressed genes, estimating log<sub>2</sub> fold change values, adjusting p-values for multiple hypothesis testing and functional enrichment analysis and plots were generated using custom scripts in R (version 4.1.2). Differentially expressed genes were identified using DESeq2<sup>25</sup> and log<sub>2</sub> fold change values were estimated using the Approximate Posterior Estimation for the GLM (apeglm) method<sup>26</sup>. Statistical significance of the log<sub>2</sub> fold change of genes between conditions was estimated by adjusting p-values for multiple hypothesis testing using Independent Hypothesis Weighting (IHW)<sup>27</sup>. Genes were considered significantly differentially expressed if the IHW adjusted p-value is less than 0.05 and absolute log<sub>2</sub> fold change is greater than 0.58. Gene Set Enrichment Analysis (GSEA) was used to identify significantly differentially expressed GO functional categories<sup>28</sup>.

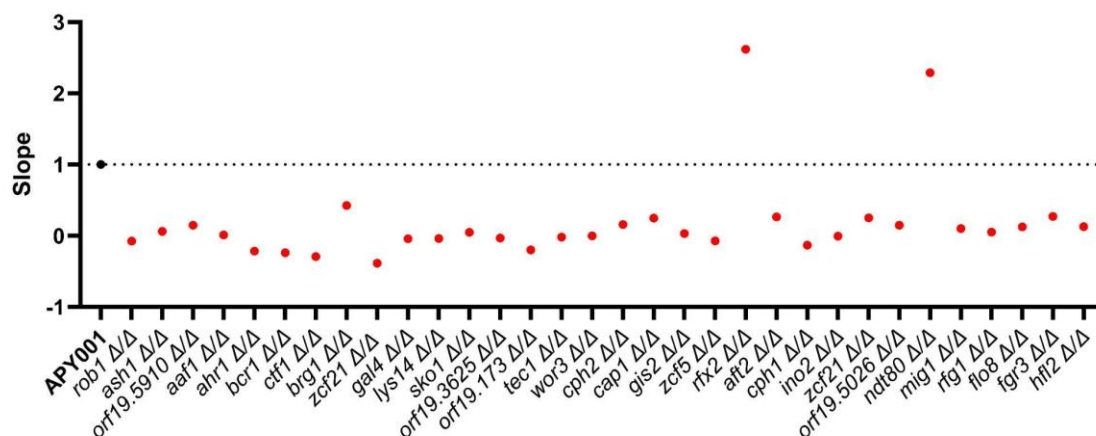
### 3.6 References

1. Sorrells, T. R. & Johnson, A. D. Making Sense of Transcription Networks. *Cell* **161**, 714–723 (2015).
2. Nobile, C. J. *et al.* A Recently Evolved Transcriptional Network Controls Biofilm Development in *Candida albicans*. *Cell* **148**, 126–138 (2012).
3. Hernday, A. D. *et al.* Structure of the transcriptional network controlling white-opaque switching in *Candida albicans*. *Mol. Microbiol.* **90**, 22–35 (2013).
4. Rodriguez, D. L., Quail, M. M., Hernday, A. D. & Nobile, C. J. Transcriptional Circuits Regulating Developmental Processes in *Candida albicans*. *Front. Cell. Infect. Microbiol.* **10**, (2020).
5. Pérez, J. C., Kumamoto, C. A. & Johnson, A. D. *Candida albicans* Commensalism and Pathogenicity Are Intertwined Traits Directed by a Tightly Knit Transcriptional Regulatory Circuit. *PLoS Biol.* **11**, e1001510 (2013).
6. Yi, S. *et al.* Alternative Mating Type Configurations (*a/a* versus *α/a* or *a/α*) of *Candida albicans* Result in Alternative Biofilms Regulated by Different Pathways. *PLoS Biol.* **9**, e1001117 (2011).
7. Lockhart, S. R. *et al.* In *Candida albicans*, White-Opaque Switchers Are Homozygous for Mating Type. *Genetics* **162**, 737–745 (2002).
8. Inglis, D. O. & Sherlock, G. Ras Signaling Gets Fine-Tuned: Regulation of Multiple Pathogenic Traits of *Candida albicans*. *Eukaryot. Cell* **12**, 1316–1325 (2013).
9. Fox, E. P. *et al.* An expanded regulatory network temporally controls *Candida albicans* biofilm formation. *Mol. Microbiol.* **96**, 1226–1239 (2015).
10. Daniels, K. J., Srikantha, T., Lockhart, S. R., Pujol, C. & Soll, D. R. Opaque cells signal white cells to form biofilms in *Candida albicans*. *EMBO J.* **25**, 2240–2252 (2006).
11. Perry, A. M., Hernday, A. D. & Nobile, C. J. Unraveling How *Candida albicans* Forms Sexual Biofilms. *J. Fungi* **6**, 14 (2020).
12. Sahni, N. *et al.* Tec1 Mediates the Pheromone Response of the White Phenotype of *Candida albicans*: Insights into the Evolution of New Signal Transduction Pathways. *PLoS Biol.* **8**, e1000363 (2010).
13. Yi, S. *et al.* The Same Receptor, G Protein, and Mitogen-activated Protein Kinase

- Pathway Activate Different Downstream Regulators in the Alternative White and Opaque Pheromone Responses of *Candida albicans*. *Mol. Biol. Cell* **19**, 957–970 (2008).
14. Lin, C.-H. *et al.* Genetic Control of Conventional and Pheromone-Stimulated Biofilm Formation in *Candida albicans*. *PLoS Pathog.* **9**, e1003305 (2013).
  15. Chen, J., Chen, J., Lane, S. & Liu, H. A conserved mitogen-activated protein kinase pathway is required for mating in *Candida albicans*. *Mol. Microbiol.* **46**, 1335–1344 (2002).
  16. Lohse, M. B. *et al.* Systematic Genetic Screen for Transcriptional Regulators of the *Candida albicans* White-Opaque Switch. *Genetics* **203**, 1679–1692 (2016).
  17. Tao, L. *et al.* Discovery of a “White-Gray-Opaque” Tristable Phenotypic Switching System in *Candida albicans*: Roles of Non-genetic Diversity in Host Adaptation. *PLoS Biol.* **12**, e1001830 (2014).
  18. Pannanusorn, S. *et al.* Characterization of Biofilm Formation and the Role of BCR1 in Clinical Isolates of *Candida parapsilosis*. *Eukaryot. Cell* **13**, 438–451 (2014).
  19. Lohse, M. B., Gulati, M., Johnson, A. D. & Nobile, C. J. Development and regulation of single- and multi-species *Candida albicans* biofilms. *Nat. Rev. Microbiol.* **16**, 19–31 (2018).
  20. Li, R. Inferring gene regulatory networks using transcriptional profiles as attractors and its application on the white-opaque switch in *Candida albicans*. (UC Merced, 2023).
  21. Paropkari, A. D., Bapat, P. S., Sindi, S. S. & Nobile, C. J. A Computational Workflow for Analysis of 3' Tag-Seq Data. *Curr. Protoc.* **3**, e664 (2023).
  22. Bushnell, B. *BBMap: A Fast, Accurate, Splice-Aware Aligner*. <https://www.osti.gov/biblio/1241166> (2014).
  23. Dobin, A. *et al.* STAR: ultrafast universal RNA-seq aligner. *Bioinformatics* **29**, 15–21 (2013).
  24. Skrzypek, M. S. *et al.* The *Candida* Genome Database (CGD): incorporation of Assembly 22, systematic identifiers and visualization of high throughput sequencing data. *Nucleic Acids Res.* **45**, D592–D596 (2017).
  25. Love, M. I., Huber, W. & Anders, S. Moderated estimation of fold change and dispersion for RNA-seq data with DESeq2. *Genome Biol.* **15**, 550 (2014).
  26. Zhu, A., Ibrahim, J. G. & Love, M. I. Heavy-tailed prior distributions for sequence count data: removing the noise and preserving large differences. *Bioinformatics* **35**, 2084–2092 (2019).
  27. Ignatiadis, N., Klaus, B., Zaugg, J. B. & Huber, W. Data-driven hypothesis weighting increases detection power in genome-scale multiple testing. *Nat. Methods* **13**, 577–580 (2016).
  28. Subramanian, A. *et al.* Gene set enrichment analysis: A knowledge-based approach for interpreting genome-wide expression profiles. *Proc. Natl. Acad. Sci.* **102**, 15545–15550 (2005).

## 3.7 Figures

A.



B.

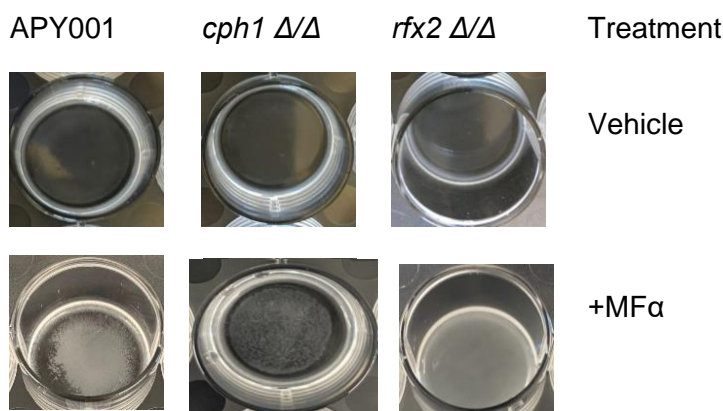
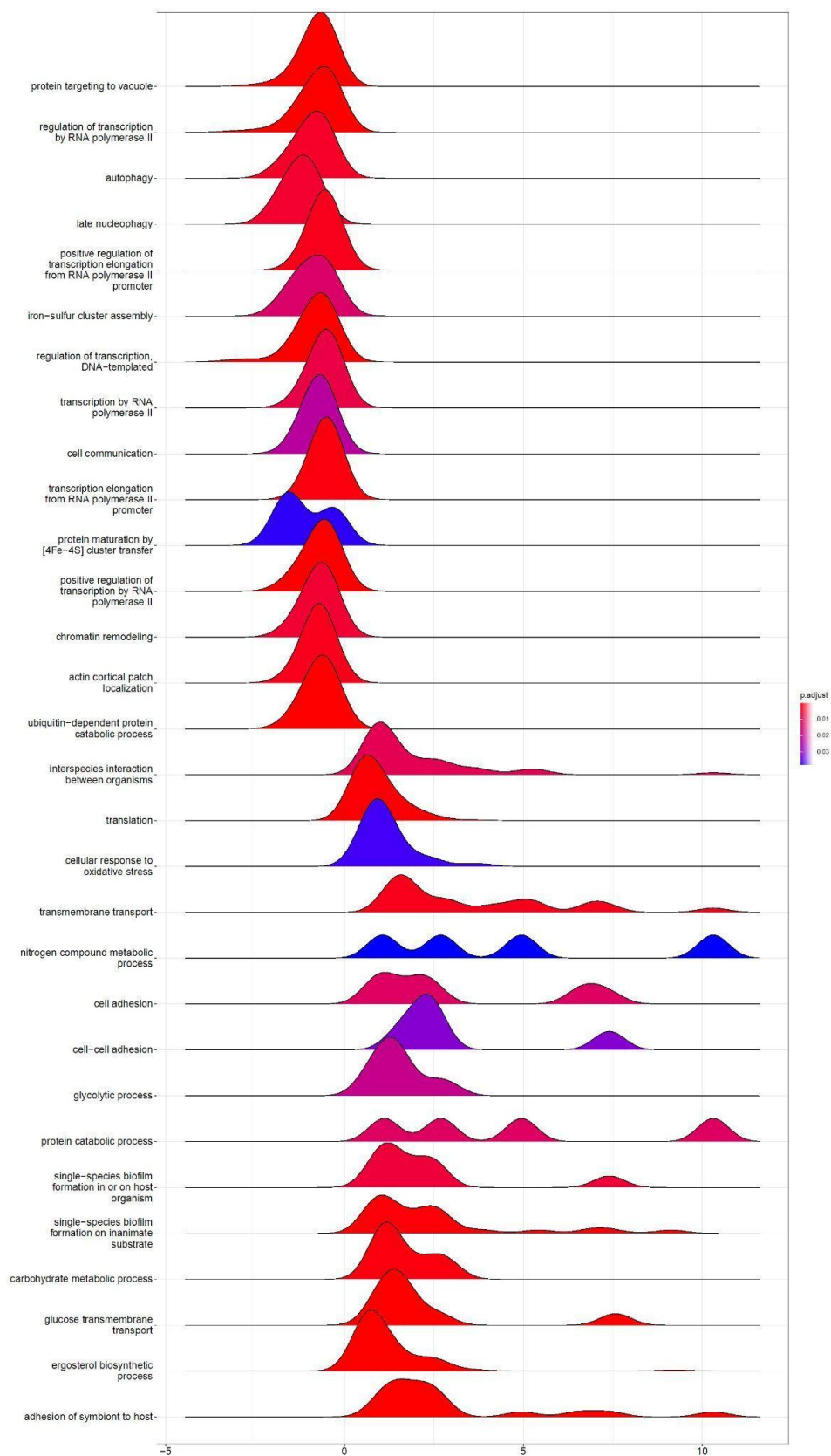
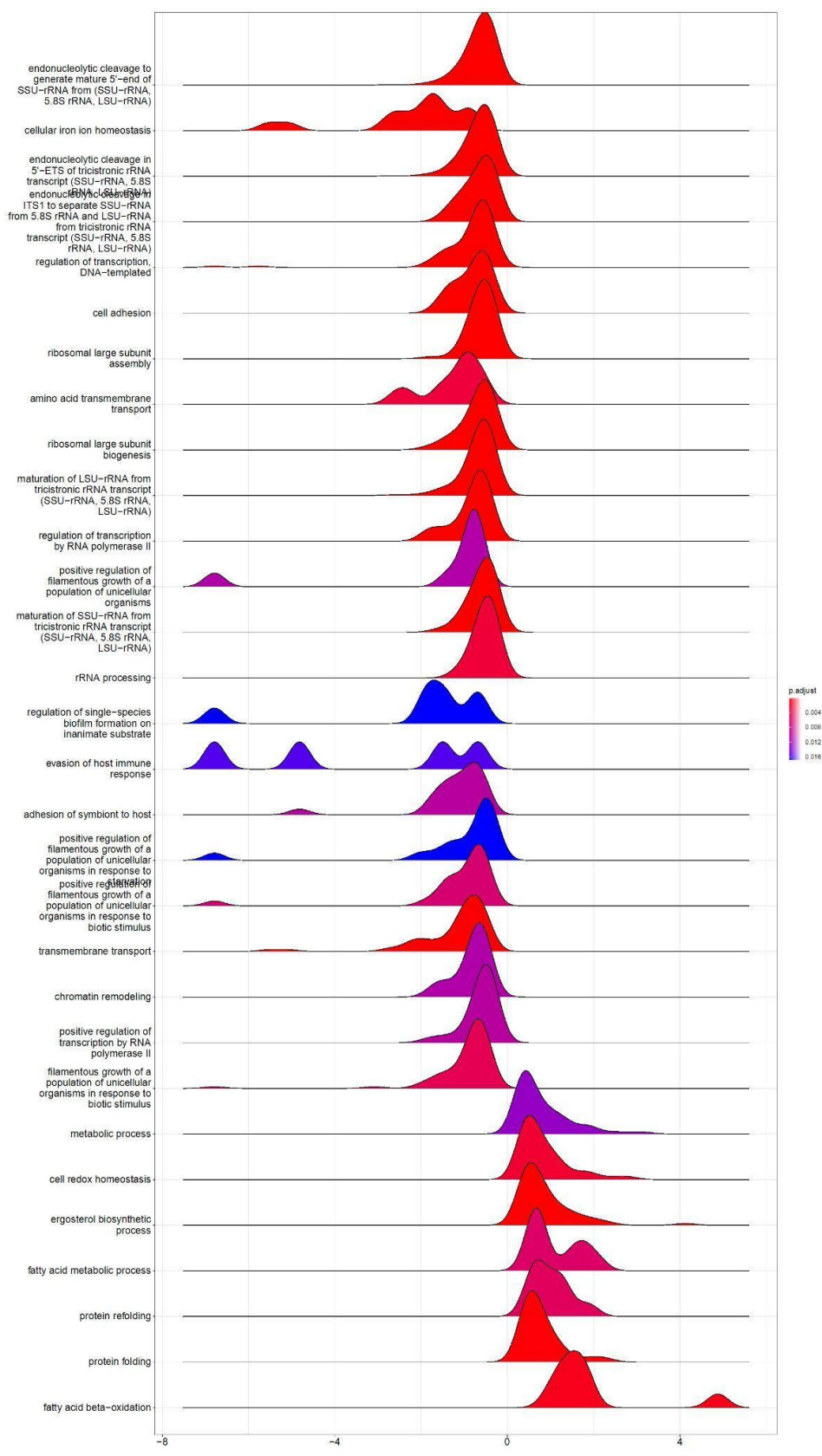


**Figure 3.1 Screening and characterization of transcription factors involved in sexual biofilm formation.** (A) Scatter plot depicting the transcription factor deletion mutant strain library screen for sexual biofilm formation. Each dot is a normalized value representing the difference in OD<sub>600</sub> between treatment conditions of a TF deletion mutant strain divided by the difference in OD<sub>600</sub> between treatment conditions of the wild-type strain (dotted line). For ease of visualization, of the 207 TF deletion mutant strains, only those which formed significantly thinner or thicker biofilms as compared to the wildtype reference strain are depicted and are colored red. Statistical significance was determined using an ANCOVA analysis of each strain normalized to the wildtype ( $p \leq .0001$ ). Statistics and graph creation were performed in GraphPad Prism. Three technical replicates were used for each strain and condition. (B) Representative images of transcription factor deletion mutant strains that form weaker or more robust sexual biofilms as compared to the wildtype reference strain.

A)



B)





C)

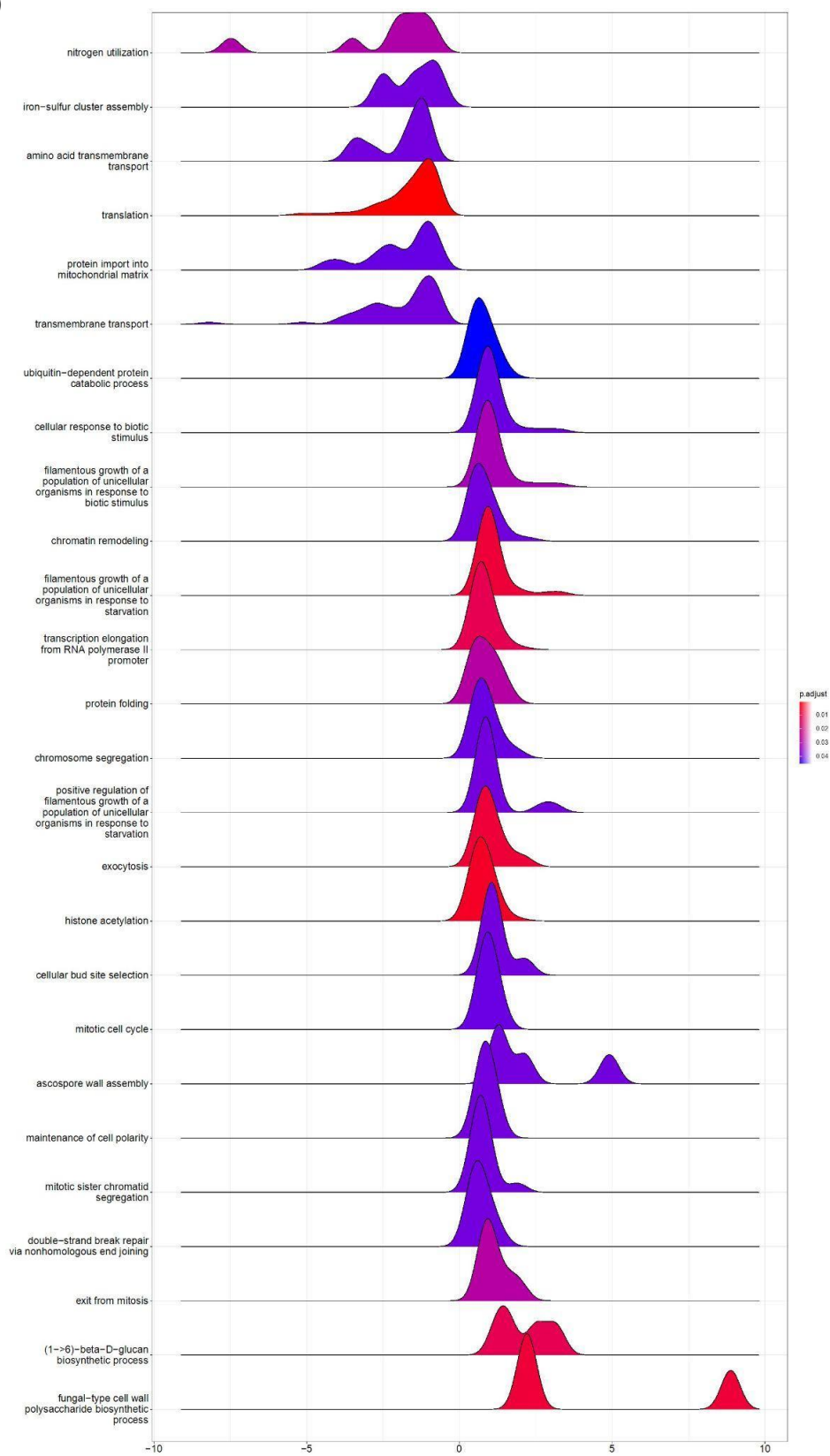


**Figure 3.2 Gene ontology analyses of transcription factor deletion mutants forming sexual biofilms.** Each of the following comparisons is between the isogenic wild-type strain treated with a vehicle versus a transcription factor deletion mutant strain treated with  $\alpha$ -factor. (A) Gene ontology ridgeplot from *rfx2*  $\Delta/\Delta$  deletion mutant strain. (B) Gene ontology ridgeplot from *cph1*  $\Delta/\Delta$  deletion mutant strain. (C) Gene ontology ridgeplot from *bcr1*  $\Delta/\Delta$  deletion mutant strain.

**Supplemental Table 3.1: List of strains**

APY001	White SN250, <i>MTL-a</i> /Δ	TF105	<i>orf19.3625</i> Δ/Δ
TF001	<i>sfl1</i> Δ/Δ	TF106	<i>csr1</i> Δ/Δ
TF002	<i>hms2</i> Δ/Δ	TF107	<i>mig1</i> Δ/Δ
TF003	<i>rpn4</i> Δ/Δ	TF108	<i>hap3</i> Δ/Δ
TF004	<i>pho4</i> Δ/Δ	TF109	<i>msn4</i> Δ/Δ
TF005	<i>ctf1</i> Δ/Δ	TF110	<i>rob1</i> Δ/Δ
TF006	<i>zcf13</i> Δ/Δ	TF111	<i>orf19.5249</i> Δ/Δ
TF007	<i>zcf14</i> Δ/Δ	TF112	<i>ash1</i> Δ/Δ
TF008	<i>orf19.2730</i> Δ/Δ	TF113	<i>rbf1</i> Δ/Δ
TF009	<i>arg83</i> Δ/Δ	TF114	<i>fgr17</i> Δ/Δ
TF010	<i>tac1</i> Δ/Δ	TF115	<i>tec1</i> Δ/Δ
TF011	<i>hal9</i> Δ/Δ	TF116	<i>orf19.5910</i> Δ/Δ
TF012	<i>zcf17</i> Δ/Δ	TF117	<i>tup1</i> Δ/Δ
TF013	<i>stb5</i> Δ/Δ	TF118	<i>mnl1</i> Δ/Δ
TF014	<i>try5</i> Δ/Δ	TF119	<i>fgr27</i> Δ/Δ
TF015	<i>sef1</i> Δ/Δ	TF120	<i>zfu2</i> Δ/Δ
TF016	<i>bas1</i> Δ/Δ	TF121	<i>ssn6</i> Δ/Δ
TF017	<i>zcf19</i> Δ/Δ	TF122	<i>fcr1</i> Δ/Δ
TF018	<i>gln3</i> Δ/Δ	TF123	<i>orf19.6888</i> Δ/Δ
TF019	<i>orf19.3928</i> Δ/Δ	TF124	<i>tea1</i> Δ/Δ
TF020	<i>sfl2</i> Δ/Δ	TF125	<i>nrg1</i> Δ/Δ
TF021	<i>grf10</i> Δ/Δ	TF126	<i>rim101</i> Δ/Δ
TF022	<i>brg1</i> Δ/Δ	TF127	<i>isw2</i> Δ/Δ
TF023	<i>zcf20</i> Δ/Δ	TF128	<i>aaf1</i> Δ/Δ
TF024	<i>zcf21</i> Δ/Δ	TF129	<i>fcr3</i> Δ/Δ

TF025	<i>leu3</i> $\Delta/\Delta$	TF130	<i>arg81</i> $\Delta/\Delta$
TF026	<i>zcf22</i> $\Delta/\Delta$	TF131	<i>zcf35</i> $\Delta/\Delta$
TF027	<i>cta7</i> $\Delta/\Delta$	TF132	<i>ahr1</i> $\Delta/\Delta$
TF028	<i>rme1</i> $\Delta/\Delta$	TF133	<i>znc1</i> $\Delta/\Delta$
TF029	<i>zcf23</i> $\Delta/\Delta$	TF134	<i>swi4</i> $\Delta/\Delta$
TF030	<i>zcf24</i> $\Delta/\Delta$	TF135	<i>zcf26</i> $\Delta/\Delta$
TF031	<i>zcf25</i> $\Delta/\Delta$	TF136	<i>orf19.173</i> $\Delta/\Delta$
TF032	<i>rlm1</i> $\Delta/\Delta$	TF137	<i>bcr11</i> $\Delta/\Delta$
TF033	<i>cas5</i> $\Delta/\Delta$	TF138	<i>cph22</i> $\Delta/\Delta$
TF034	<i>rtg1</i> $\Delta/\Delta$	TF139	<i>gat1</i> $\Delta/\Delta$
TF035	<i>lyz142</i> $\Delta/\Delta$	TF140	<i>cap1</i> $\Delta/\Delta$
TF036	<i>hcm1</i> $\Delta/\Delta$	TF141	<i>zcf8</i> $\Delta/\Delta$
TF037	<i>tye7</i> $\Delta/\Delta$	TF142	<i>rtg3</i> $\Delta/\Delta$
TF038	<i>ofl1</i> $\Delta/\Delta$	TF143	<i>orf19.2612</i> $\Delta/\Delta$
TF039	<i>cup2</i> $\Delta/\Delta$	TF144	<i>gis2</i> $\Delta/\Delta$
TF040	<i>orf19.5026</i> $\Delta/\Delta$	TF145	<i>kar4</i> $\Delta/\Delta$
TF041	<i>cat8</i> $\Delta/\Delta$	TF146	<i>zcf28</i> $\Delta/\Delta$
TF042	<i>zcf29</i> $\Delta/\Delta$	TF147	<i>sfu1</i> $\Delta/\Delta$
TF043	<i>zcf30</i> $\Delta/\Delta$	TF148	<i>zcf4</i> $\Delta/\Delta$
TF044	<i>mig2</i> $\Delta/\Delta$	TF149	<i>zcf5</i> $\Delta/\Delta$
TF045	<i>gal4</i> $\Delta/\Delta$	TF150	<i>zcf6</i> $\Delta/\Delta$
TF046	<i>lys144</i> $\Delta/\Delta$	TF151	<i>orf19.1577</i> $\Delta/\Delta$
TF047	<i>efh1</i> $\Delta/\Delta$	TF152	<i>fgr15</i> $\Delta/\Delta$
TF048	<i>lys14</i> $\Delta/\Delta$	TF153	<i>aro80</i> $\Delta/\Delta$
TF049	<i>orf19.5651</i> $\Delta/\Delta$	TF154	<i>zcf27</i> $\Delta/\Delta$

TF050	<i>cwt1</i> $\Delta/\Delta$	TF155	<i>dal81</i> $\Delta/\Delta$
TF051	<i>mbp1</i> $\Delta/\Delta$	TF156	<i>efg1</i> $\Delta/\Delta$
TF052	<i>stp3</i> $\Delta/\Delta$	TF157	<i>orf19.1150</i> $\Delta/\Delta$
TF053	<i>zcf31</i> $\Delta/\Delta$	TF158	<i>rap1</i> $\Delta/\Delta$
TF054	<i>zcf32</i> $\Delta/\Delta$	TF159	<i>orf19.1757</i> $\Delta/\Delta$
TF055	<i>try4</i> $\Delta/\Delta$	TF160	<i>orf19.2743</i> $\Delta/\Delta$
TF056	<i>wor2</i> $\Delta/\Delta$	TF161	<i>lys143</i> $\Delta/\Delta$
TF057	<i>uga32</i> $\Delta/\Delta$	TF162	<i>stp2</i> $\Delta/\Delta$
TF058	<i>rca1</i> $\Delta/\Delta$	TF163	<i>rfx1</i> $\Delta/\Delta$
TF059	<i>ace2</i> $\Delta/\Delta$	TF164	<i>rgt1</i> $\Delta/\Delta$
TF060	<i>zcf34</i> $\Delta/\Delta$	TF165	<i>ppr1</i> $\Delta/\Delta$
TF061	<i>cup9</i> $\Delta/\Delta$	TF166	<i>rfg1</i> $\Delta/\Delta$
TF062	<i>try6</i> $\Delta/\Delta$	TF167	<i>rep1</i> $\Delta/\Delta$
TF063	<i>orf19.6874</i> $\Delta/\Delta$	TF168	<i>orf19.5210</i> $\Delta/\Delta$
TF064	<i>yox1</i> $\Delta/\Delta$	TF169	<i>orf19.4342</i> $\Delta/\Delta$
TF065	<i>mac1</i> $\Delta/\Delta$	TF170	<i>wor3</i> $\Delta/\Delta$
TF066	<i>uga33</i> $\Delta/\Delta$	TF171	<i>ecm22</i> $\Delta/\Delta$
TF067	<i>suc1</i> $\Delta/\Delta$	TF172	<i>orf19.1604</i> $\Delta/\Delta$
TF068	<i>crz1</i> $\Delta/\Delta$	TF173	<i>rfx2</i> $\Delta/\Delta$
TF069	<i>mrr1</i> $\Delta/\Delta$	TF174	<i>pth2</i> $\Delta/\Delta$
TF070	<i>cta4</i> $\Delta/\Delta$	TF175	<i>flo8</i> $\Delta/\Delta$
TF071	<i>zcf38</i> $\Delta/\Delta$	TF176	<i>wor11</i> $\Delta/\Delta$
TF072	<i>uga3</i> $\Delta/\Delta$	TF177	<i>orf19.3048</i> $\Delta/\Delta$
TF073	<i>zcf39</i> $\Delta/\Delta$	TF178	<i>ndt80A</i> $\Delta/\Delta$
TF074	<i>asg1</i> $\Delta/\Delta$	TF179	<i>ume6</i> $\Delta/\Delta$

TF075	<i>orf19.217</i> $\Delta/\Delta$	TF180	<i>aft2</i> $\Delta/\Delta$
TF076	<i>zcf1</i> $\Delta/\Delta$	TF181	<i>wor4</i> $\Delta/\Delta$
TF077	<i>upc2</i> $\Delta/\Delta$	TF182H	<i>cbf1</i> heterozygous $\Delta/\Delta$
TF078	<i>zcf2</i> $\Delta/\Delta$	TF183	<i>cph1</i> $\Delta/\Delta$
TF079	<i>hap31</i> $\Delta/\Delta$	TF184	<i>gcn4</i> $\Delta/\Delta$
TF080	<i>hap43</i> $\Delta/\Delta$	TF185	<i>ino2</i> $\Delta/\Delta$
TF081	<i>ino4</i> $\Delta/\Delta$	TF186	<i>orf19.2064</i> $\Delta/\Delta$
TF082	<i>stp4</i> $\Delta/\Delta$	TF187	<i>fgr3</i> $\Delta/\Delta$
TF083	<i>skn7</i> $\Delta/\Delta$	TF188	<i>adr1</i> $\Delta/\Delta$
TF084	<i>sko1</i> $\Delta/\Delta$	TF189	<i>orf19.7397</i> $\Delta/\Delta$
TF085	<i>war1</i> $\Delta/\Delta$	TF190	<i>orf19.7098</i> $\Delta/\Delta$
TF086	<i>zcf3</i> $\Delta/\Delta$	TF191	<i>orf19.3722</i> $\Delta/\Delta$
TF087	<i>hap2</i> $\Delta/\Delta$	TF192	<i>orf19.4195</i> $\Delta/\Delta$
TF088	<i>orf19.1274</i> $\Delta/\Delta$	TF193	<i>std1</i> $\Delta/\Delta$
TF089	<i>orf19.1496</i> $\Delta/\Delta$	TF194	<i>hap42</i> $\Delta/\Delta$
TF090	<i>opi1</i> $\Delta/\Delta$	TF195	<i>iro1</i> $\Delta/\Delta$
TF091	<i>zcf7</i> $\Delta/\Delta$	TF196	<i>hap41</i> $\Delta/\Delta$
TF092	<i>sef2</i> $\Delta/\Delta$	TF197	<i>hac1</i> $\Delta/\Delta$
TF093	<i>hap5</i> $\Delta/\Delta$	TF198	<i>orf19.6626</i> $\Delta/\Delta$
TF094	<i>dpb4</i> $\Delta/\Delta$	TF199	<i>zcf9</i> $\Delta/\Delta$
TF095	<i>ndt80</i> $\Delta/\Delta$	TF200	<i>orf19.3088</i> $\Delta/\Delta$
TF096	<i>crz2</i> $\Delta/\Delta$	TF201	<i>orf19.2674</i> $\Delta/\Delta$
TF097	<i>orf19.2476</i> $\Delta/\Delta$	TF202	<i>hfl2</i> $\Delta/\Delta$
TF098	<i>ume7</i> $\Delta/\Delta$	TF203	<i>orf19.7301</i> $\Delta/\Delta$
TF099	<i>zcf15</i> $\Delta/\Delta$	TF204	<i>cas4</i> $\Delta/\Delta$

TF100	<i>zcf16</i> $\Delta/\Delta$	TF205	<i>sip5</i> $\Delta/\Delta$
TF101	<i>gzf3</i> $\Delta/\Delta$	TF206	<i>orf19.1178</i> $\Delta/\Delta$
TF102	<i>orf19.2961</i> $\Delta/\Delta$	TF207	<i>orf19.6845</i> $\Delta/\Delta$
TF103	<i>hfl1</i> $\Delta/\Delta$		
TF104	<i>czf1</i> $\Delta/\Delta$		

## Chapter 4

### Conclusion and Future Directions

Austin M. Perry, Clarissa J. Nobile

#### 4.1 Conclusions

The opportunistic human fungal pathogen, *C. albicans*, is highly relevant for human health and serves as a genetically tractable model organism used to study genetic regulation. Of particular interest is *C. albicans*' ability to form biofilms, a major virulence factor that is tightly coordinated by transcription networks<sup>1-5</sup>. As described previously (Chapter 1), *C. albicans* can form various types of biofilms<sup>3,3,6-8</sup>. Here, we focus on sexual biofilms formed by *MTL*-homozygous or -hemizygous *C. albicans* cells. Identifying the molecular mechanisms by which sexual biofilms are formed will advance our understanding of the evolution of transcription networks and genetic regulation, interactions of fungal cells in a community and perhaps lead to improvements in antifungal therapeutics for use in hospitals. This dissertation sheds new light on the genes that govern sexual biofilm formation and the transcriptional regulation underlying this biological process.

In chapter one, we reviewed certain aspects of *C. albicans* lifestyle as they pertain to sexual biofilms, the unique characteristics of sexual and conventional biofilms and the mechanisms by which these structures are formed. We discussed the cryptic parasexual life cycle of *C. albicans* and roles that white and opaque cells play in it. Of particular interest was how these cell types come together to create sexual biofilms, a structure formed by white cells in order to increase the mating frequency of opaque cells. From there, we discussed the molecular mechanisms (e.g. signaling pathways, transcription factors) *C. albicans* employs to form sexual biofilms and how these compare and contrast with that of conventional biofilms. Unlike conventional biofilms, there have been no attempts to demonstrate *C. albicans* ability to form sexual biofilms *in vivo*. Thus, we include a discussion of the potential niches in which sexual biofilms may form; predominantly those that induce loss of heterozygosity and white-opaque switching.

Chapter two provides a look at the transcriptomes of white cells as they form sexual biofilms and identifies genes that are functionally relevant to biofilm formation. We look at white cells stimulated with synthetic alpha mating pheromone to get a pure transcriptomic profile of white cells as they are induced to form sexual biofilms. These strains were isolated from both healthy and diseased individuals, and from a variety of regions around the body. These features did not correlate with biofilm thickness, confirming that sexual biofilm formation is a generalized feature of *C. albicans* strains<sup>9</sup>. Additionally, we co-culture white and opaque cells to investigate sexual biofilm formation in a more natural environment, relying on mating pheromone and possible other signals from opaque cells to stimulate sexual biofilm formation. From these data we identified a list of genes which, upon deletion, inhibit *C. albicans* ability to form sexual biofilms. These results indicate that *ORF19.1725*, *ORF19.3932.1*, *ORF19.6200* and *ORF19.7167* are required for sexual biofilm formation *in vitro*.

In chapter three, we present the results from a systematic screen of transcriptional regulators of *C. albicans* sexual biofilm formation. By screening a library of 207 transcription factors<sup>10</sup> through a sexual biofilm assay, we identified 30 transcription factors which, when deleted, inhibited sexual biofilm formation in *C. albicans*. Additionally, we identified 2 transcription factors which, when deleted, bolstered sexual biofilm formation. By performing RNA-sequencing on these 32 mutant strains and an isogenic wild type



strain, we determined which genes each transcription factor directly or indirectly controlled. Overall these findings suggest that a number of transcription factors are required for both conventional and sexual biofilm formation (e.g. Bcr1, Brg1, Tec1, Rfx2, Rob1). However, each system has some transcription factors that are unique (e.g. Efg1, Cph1). Interestingly, some transcription factors appear to have flipped regulatory roles depending on the system in question (e.g. Ndt80, Gal4)<sup>4,5</sup>.

## 4.2 Future directions

In this dissertation, I characterized the sexual biofilm forming abilities of white *C. albicans* cells and identified 7 genes involved in sexual biofilm formation (Chapter 2). I subsequently identified 32 transcription factors that are involved in the regulation of sexual biofilms in *C. albicans* (Chapter 3). As enlightening as these experiments are, much work remains to complete our understanding of sexual biofilms. We still don't understand the role of sexual biofilms *in vivo* – and thus their clinical relevance – and their contribution to the *C. albicans* parasexual mating cycle. In addition, we lack a complete understanding of the evolutionary histories and regulatory differences between sexual and conventional biofilms.

To dissect the evolutionary and regulatory differences between conventional and sexual biofilms, the complete transcriptional network underlying sexual biofilm formation must be resolved. In this work, we identified a number of transcription factors that are involved in sexual biofilm formation. However, these transcription factors may be directly (transcription factor regulates a gene by binding to the *cis*-regulatory region of a gene) or indirectly (transcription factor regulates a gene by means of controlling another gene) regulating the other transcription factors and genes involved in sexual biofilm formation. To determine the regulatory relationships between transcription factors and their regulons, a form of chromatin-immunoprecipitation known as CUT & RUN (cleavage under targets & release using nuclease) needs to be performed on each of the transcription factors identified in this dissertation. These experiments will show us exactly where in the genome each transcription factor is binding. By combining these data with the expression profiles of each transcription factor deletion mutant strain, we can determine whether a transcription factor elicits its regulatory effects in a direct or indirect manner. By finding out where transcription factors directly bind, we can also determine the average length of the intergenic regions of *cis*-regulated genes. This can provide information on the approximate age of the sexual biofilm network. The oldest genes can be found in nearly all distantly related yeast species, whereas the youngest genes are found only in *C. albicans*. Previously, Nobile et al. discovered that the conventional biofilm network is enriched for recently evolved genes, indicating that biofilm formation is a relatively “new” phenomenon in the yeast world<sup>4</sup>. Interestingly, many of these intergenic regions were even longer than the average “young” gene. By uncovering the complete transcription network regulating sexual biofilms, we may be able to determine the relative age of that network as compared to the transcription network regulating conventional biofilms. In addition, we may be able to learn the evolutionary history of Cph1, the transcription factor canonically known to regulate mating in yeast species, and how it became involved in regulating genes involved in biofilm formation. Additionally, a time-course based approach to understanding how the chromatin landscapes of sexual and conventional biofilms become established would aid in our understanding of how certain genes are regulated within each system. A number of techniques may be employed to dissect this aspect of biofilm regulation, such as MNase-seq (micrococcal nuclease) or ATAC-seq (assay for transposase-accessible chromatin) among others. The snapshot of genomic architecture these methods yield provides an

essential understanding of the relationship between chromatin structure and gene regulation which, when combined with transcription factor binding maps produced by CUT & RUN and transcriptional profiling, would provide a unique and valuable insight into the subtle differences between sexual and conventional biofilms, and possibly aid in our understanding of how transcription factors and chromatin interact to yield a highly specialized phenotypic output. Finally, other *Candida* species (e.g. *Candida dubliniensis*) form sexual biofilms as well, it would be interesting to determine whether the same transcription factors that regulate sexual biofilms in *C. albicans* regulate sexual biofilm formation in these other species and what their binding patterns look like along the genome. This would provide further information on the evolutionary history of sexual biofilms in ascomycetes.

The role of sexual biofilms in the life cycle of *C. albicans* remains elusive. Preliminary studies demonstrate that opaque cells are better able to navigate toward cells of the opposite mating type in the interior of a biofilm as pheromone gradients have been stabilized by the architecture of the biofilm as compared to those on the periphery, where the pheromone gradient gets disrupted by environmental forces<sup>6,11</sup>. In addition, the white cells themselves secrete pheromone that promotes mating between opaque cells<sup>12</sup>. These results indicate that the presence of a majority white cell population in which fecund opaque cells are embedded may boost their mating frequency. However, these studies were performed under controlled conditions *in vitro*. We still need to determine whether this phenomenon holds true *in vivo*. While it would be bittersweet from a clinical perspective if researchers could prove that sexual biofilms form on implanted medical devices, such as by culturing white and opaque cells separately and together in catheter model of infection, this may not be the natural niche for which sexual biofilms formed. It is hypothesized that environments which promote loss of heterozygosity, or white-opaque switching are likely the natural niches of sexual biofilms (e.g. high levels of CO<sub>2</sub> or N-acetylglucosamine, or treatment with antifungal drugs)<sup>13</sup>. Interestingly, glucose-deprivation can stimulate the expression of mating and sexual biofilm associated genes in white cells, even causing normally sterile white cells to mate<sup>14</sup>. Before approaching sexual biofilm formation in a mammalian host, it would be helpful to determine whether sexual biofilms can form in the presence of an innate immune system. This could be done, for example, cheaply and easily by using an invertebrate infection model, such as the *Schmidtea mediterranea* model developed here in the Nobile lab<sup>15</sup>. These worms can be cultured at a wide range of temperatures, including 25°C, enabling opaque cells to be easily included in an infection study. For investigation of sexual biofilms in this model, one would have to culture white and opaque cells of opposite mating types together and alone to determine if white cells can be induced to form a biofilm if they're in the presence of opaque cells. One could even imagine mating experiments being done in this model by culturing auxotrophic opaque-locked cells with and without white cells to determine whether their presence can boost the mating frequency between opaque cells. This would be an ideal model for analyzing how sexual biofilms stabilize pheromone-gradients as the worms are able to move about while submerged in a liquid, thereby providing a near-constant and light shear flow condition to cells bound to the exterior of the worm. Uncovering the real evolutionary benefit that sexual biofilms provide for *C. albicans* will greatly improve our understanding of the cryptic mating lifecycle of *C. albicans* and provide an understanding of the role of sexual biofilms in the host.

### 4.3 References

1. Nobile, C. J. & Johnson, A. D. *Candida albicans* Biofilms and Human Disease. *Annu. Rev. Microbiol.* **69**, 71–92 (2015).
2. Gulati, M. & Nobile, C. J. *Candida albicans* biofilms: development, regulation, and molecular mechanisms. *Microbes Infect.* **18**, 310–321 (2016).
3. Lohse, M. B., Gulati, M., Johnson, A. D. & Nobile, C. J. Development and regulation of single- and multi-species *Candida albicans* biofilms. *Nat. Rev. Microbiol.* **16**, 19–31 (2018).
4. Nobile, C. J. *et al.* A Recently Evolved Transcriptional Network Controls Biofilm Development in *Candida albicans*. *Cell* **148**, 126–138 (2012).
5. Fox, E. P. *et al.* An expanded regulatory network temporally controls *Candida albicans* biofilm formation. *Mol. Microbiol.* **96**, 1226–1239 (2015).
6. Yi, S. *et al.* Alternative Mating Type Configurations ( $a/a$  versus  $α/a$  or  $a/α$ ) of *Candida albicans* Result in Alternative Biofilms Regulated by Different Pathways. *PLOS Biol.* **9**, e1001117 (2011).
7. Yi, S. *et al.* The Same Receptor, G Protein, and Mitogen-activated Protein Kinase Pathway Activate Different Downstream Regulators in the Alternative White and Opaque Pheromone Responses of *Candida albicans*. *Mol. Biol. Cell* **19**, 957–970 (2008).
8. Daniels, K. J., Srikantha, T., Lockhart, S. R., Pujol, C. & Soll, D. R. Opaque cells signal white cells to form biofilms in *Candida albicans*. *EMBO J.* **25**, 2240–2252 (2006).
9. Sahni, N., Yi, S., Pujol, C. & Soll, D. R. The White Cell Response to Pheromone Is a General Characteristic of *Candida albicans* Strains. *Eukaryot. Cell* **8**, 251–256 (2009).
10. Lohse, M. B. *et al.* Systematic Genetic Screen for Transcriptional Regulators of the *Candida albicans* White-Opaque Switch. *Genetics* **203**, 1679–1692 (2016).
11. Park, Y.-N., Daniels, K. J., Pujol, C., Srikantha, T. & Soll, D. R. *Candida albicans* Forms a Specialized “Sexual” as Well as “Pathogenic” Biofilm. *Eukaryot. Cell* **12**, 1120–1131 (2013).
12. Tao, L. *et al.* White Cells Facilitate Opposite- and Same-Sex Mating of Opaque Cells in *Candida albicans*. *PLOS Genet.* **10**, e1004737 (2014).
13. Huang, G. *et al.* N-Acetylglucosamine Induces White to Opaque Switching, a Mating Prerequisite in *Candida albicans*. *PLOS Pathog.* **6**, e1000806 (2010).
14. Guan, G. *et al.* Glucose depletion enables *Candida albicans* mating independently of the epigenetic white-opaque switch. *Nat. Commun.* **14**, 2067 (2023).
15. Maciel, E. I., Valle Arevalo, A., Ziman, B., Nobile, C. J. & Oviedo, N. J. Epithelial Infection With *Candida albicans* Elicits a Multi-System Response in Planarians. *Front. Microbiol.* **11**, 629526 (2021).